Final report

General information

*Depending of project type, project size and project complexity the **number of pages** in the final report may vary. For smaller **development and demonstration** projects, the final report normally should not be more than 20 pages plus possible relevant appendices. For larger **research, development and demonstration** projects, the final report should not be more than 50 pages.*

The final report will be used for dissemination purposes and the information stated in the final report should be suitable for dissemination. The final report will be published at www.eudp.dk.

Please attach relevant pictures from the project as a separate file (.png or .jpeg/.jpg).

*The guidance text (in italic) should be deleted, so the application form **only** contains numbered headings as well as relevant text from the applicant.*

1. Project details

Project title	Towards H2-driven business model: Portfolio management of a multi-energy system under uncertainty (HOMEY)
File no.	64021-7010
Name of the funding scheme	EUDP
Project managing company / institution	Siemens Gamesa Renewable Energy
CVR number (central business register)	76486212
Project partners	DTU Electrical Engineering/ DTU WIND
Submission date	26 April 2024

2. Summary

Describe the objectives of the project, the obtained results and how they will be utilized in the future, both in English and in Danish. The summary will be published on www.eudp.dk and www.energiforskning.dk.

Project summary:

- **The purpose of the project**

HOMEY aimed at the development of a first of its kind portfolio management software (RHYPE) for hybrid hydrogen - renewable power plants, optimizing operations and planning for bids into different markets (i.e., day-ahead, ancillary services markets) under uncertainty. Optimizing under forecast uncertainty was the key innovation besides added value to renewable energy power plants.

- **Results, conclusions, and perspective**

Main results:
- A stochastic approach was added to the energy management system (EMS) for hybrid renewable (RE) power plants, to make informed uncertainty-aware decisions on the operation as well as planning for bidding into different electricity markets.
- The software was designed flexible to accommodate for varying asset configurations (wind, battery storage, electrolyzer, …) as well as electricity markets (Day-Ahead, FCR, mFRR, …).
- Key parameters for a tested hybrid renewable power plant (over one year):
  - Income increased by ~ 10% compared to a wind-only power plant (revenue increase by ~ 15%).
  - Added flexibility by 11%.
  - 48 tons of green hydrogen (GH2) production.

Future use:
- Under the current circumstances at SGRE, the new solution will not immediately be exploited as a product. It can be expected that the topic of “hybrid renewable power plants” will be picked up in few years when the marked situation improves, and the developed solution will be deployed to the market in the future.
- A non-uncertainty aware version is currently implemented for one commercial project with wind and battery storage, optimizing bids into day-ahead and ancillary market (Kragerup Gods, Denmark).

Besides adding value to hybrid RE power plants, increasing profitability, and aiding the cost-efficient production of GH2, it is expected that this solution also plays a role in improved grid stability with an increased number of renewables.

Projektresumé:

- **Formålet med projektet**

HOMEY sigtede mod udvikling af en første af sin slags porteføljestyringssoftware (RHYPE) til hybridbrint - vedvarende kraftværker, optimering af drift og planlægning af bud på forskellige markeder (dvs. day-ahead, balancemarkedet) under usikkerhed. Optimering under prognoseusikkerhed var den vigtigste innovation ud over merværdi til vedvarende energikraftværker.

- **Resultater, konklusioner og perspektiv**

Vigtigste resultater:
- Der blev tilføjet en stokastisk tilgang til energistyringssystemet (EMS) for hybride vedvarende kraftværker (VE) for at træffe informerede usikkerhedsbevidste beslutninger om driften samt planlægge bud på forskellige el markeder.
- Softwaren blev designet fleksibelt til at rumme forskellige aktivkonfigurationer (vind, batterilagring, elektrolysator, ...) samt el markeder (day-ahead, FCR, mFRR, ...).
- Nøgleparametre for et testet hybridt vedvarende kraftværk (over et år):
  - Indkomsten steg med ~ 10% sammenlignet med et kraftværk kun med vind (omsætningen stiger med ~ 15%).
  - Øget fleksibilitet med 11%.
  - 48 tons grøn brint (GH2) produktion.

Fremtidig brug:

- Under de nuværende omstændigheder hos SGRE vil den nye løsning ikke umiddelbart blive udnyttet som produkt. Det kan forventes, at emnet "hybride vedvarende kraftværker" vil blive afhentet om få år, når den markante situation forbedres, og den udviklede løsning vil blive implementeret på markedet i fremtiden.
- En usikkerhedsbevidst version implementeres i øjeblikket til et kommercielt projekt med vind- og batterilagring, der optimerer bud til day-ahead og accessoriske marked (Kragerup Gods, Danmark).

Ud over at tilføre værdi til hybride VE-kraftværker, øge rentabiliteten og bidrage til en omkostningseffektiv produktion af GH2, forventes det, at denne løsning også spiller en rolle i forbedret net stabilitet med en øget mængde vedvarende energi.

3. Project objectives

The focus of the “Towards H2-driven business model: Portfolio management of a multi-energy system under uncertainty” (HOMEY) project was to develop and test a first of its kind portfolio management software (RHYPE) for hybrid hydrogen (H2) - renewable (RE) power plants. RHYPE shall support and optimize operations across planning, forecasting, and trading of various energy vectors (i.e., electricity, H2 and power reserve) into different markets (i.e., day-ahead, ancillary services markets) under uncertainty. RHYPE shall increase the flexibility capacity of hybrid RE power plants, making them a viable option for frequency support in the electrical power system while mitigating the RE volatility. Leveraging on electrolyzer (ELH2) capacity, RHYPE aims at optimizing power-to-grid (P2G), power-to-hydrogen (P2H) and provisioning of various ancillary services in a probabilistic framework to deal with the intrinsic uncertainty of stochastic variables like energy prices and RE production. Such comprehensive data gathering, and handling input has never been implemented in multi-energy management systems before. The main objectives of RHYPE were:

- to steadily reduce CO2 gas emission by promoting the production of green H2 (GH2) as a viable alternative to grey/blue hydrogen options.
- to increase the sources of flexibility in the electrical power system – primarily for transmission system operators (TSOs) – through optimized management and increased flexibility of RE hybrid power plants.
- to optimize the profits of the bids of hybrid RE power plants to be submitted to the day-ahead (e.g., Nord Pool) and to the frequency-supporting ancillary services markets, namely frequency containment reserve (FCR), automatic frequency restoration reserve (aFRR), and manual frequency restoration reserve (mFRR) markets.
- to decrease the production cost of GH2 and to increase availability by making it a more competitive and versatile option for hybrid RE power plants to use.
- to provide hybrid RE power plants with a new business model based on GH2 as a source of flexibility and a product to sell directly.

RHYPE was supposed to be integrated with an existing hybrid RE power plant control tool currently under development by Siemens Gamesa Renewable Energy (SGRE), to provide a unique multi-energy management system (EMS) that optimally manages several energy assets and provides the power system with more flexibility sources. The sketch of the hybrid RE power plant to be considered in HOMEY is portrayed in Figure 1 with input of wind-speed and price forecasts.

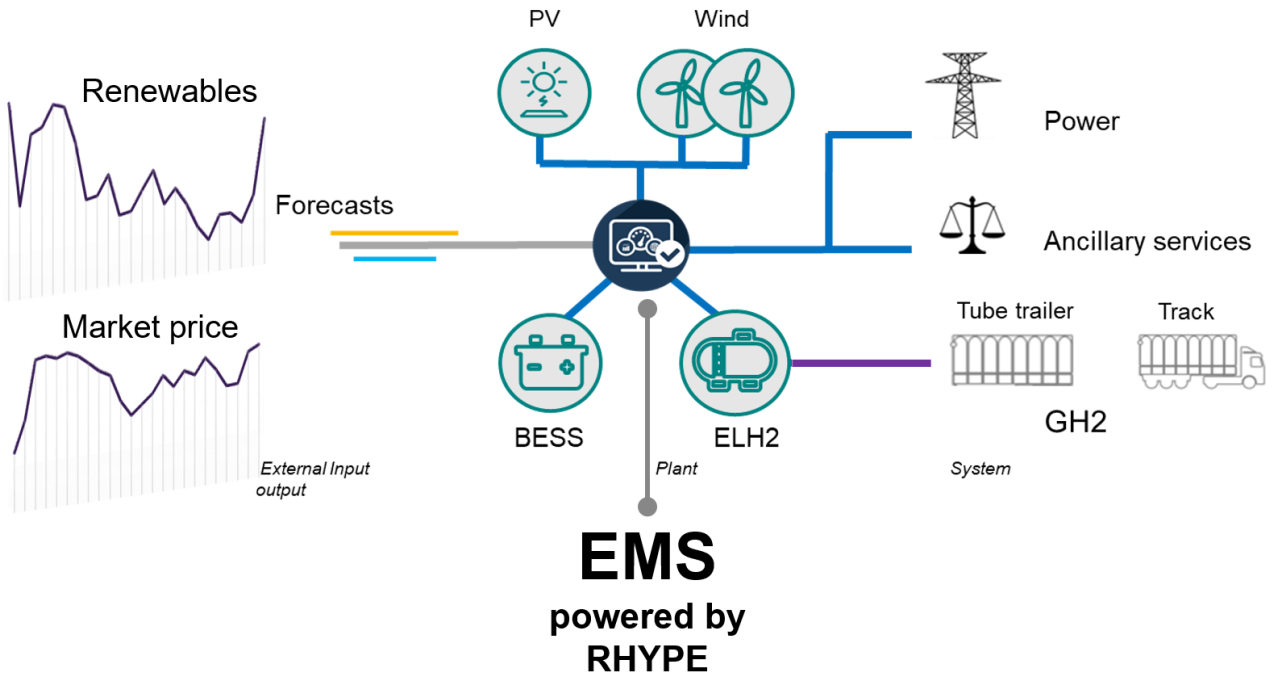

Figure 1 Schema of potential hybrid renewable energy power plant operated by the developed EMS solution.

4. Project implementation

The project evolved as expected and nearly without any delays, especially during the first year. The first activity T2.1 regarding development of a deterministic model without ancillary services has been completed swiftly. This was achieved through research on operational model for electrolyzers, after which several model formulations were developed and evaluated, and feedback was given by the SGRE team, in particular by the lead engineer of Power-to-X at SGRE. Further, work on the addition of ancillary services and stochastic input to the model has been initiated.

In parallel, the software architecture for the energy management system was successfully designed (T3.1) and the prototype code deployed (T3.2) on a demonstration site to manage and accommodate for the new additional features needed by hybrid-site energy managers such as energy bidding under uncertainty. Back/front-end software development were ongoing. The optimization unit was designed for easy integration of new mathematical problem formulations, which was also an advantage throughout the project. The design allows for flexible, easy, and modular model integration for new assets or different model types and selection between those. As a result, the integration of new models can be achieved with minimum efforts. Data Management unit for collecting field measurements as well as forecast data was implemented, likewise the Communication module to link the EMS with the power plant controller. And finally, for the user interface (UI) a draft developed within Grafana was extended to its final state for the project.

After the first year, the developments of the deterministic portfolio management problem both without (T2.1) and with (T2.2) ancillary services have been completed and were ready for integration and testing in the operational environment. Another focus on the models lay on approximating non-linearities of the electrolyzer for integration in a linear program, and on the implications of an electrolyzer delivering ancillary services on the upstream components. Further work started on exploring the potential benefit of applying ambiguity-aware

Distributionally Robust Optimization (DRO) compared “conventional” uncertainty-aware methods such as stochastic optimization (T2.3). This led to the development of a DRO model (T2.4), which showed promising preliminary results.

Meanwhile also the deterministic model was integrated into RHYPE (T.3.3), however, with a small delay of one month. To compensate for the delay with implementation, activities started with designing an effective test plan and preparation on the test site, to prove the reliability and effectiveness of the devised operation and control strategies as well as identifying necessary signals (actual measurements) from deployed assets to be read by the EMS to improve the simulation accuracy. Further progress was the introduction of methods to select arbitrary forecast providers.

By end of two thirds of the project, the development and first application of Distributionally Robust Optimization (DRO) model, which considers uncertainty of the wind-forecast and spot-market prices, was completed (T2.4). This model was further extended to include ancillary services (T2.5), building on the developments from (T2.2) and (T2.4). The integration of the RHYPE stochastic model (T3.4) was started at that time, but not yet concluded and meant an additional small delay. This delay was compensated for with ongoing and past data collection at the test site as well as a detailed testing and evaluation module. Changes within the team and the business unit at SGRE meant a small risk to the project, which however, did not cause further impact to the project execution.

During the last few months of the project, the required software module for the evaluation of historic forecast errors (needed for T3.4) as part of the stochastic model was finalise in RHYPE. Testing and analyzing results and the performance for both models as part of (T4.2) and (T4.3) were finally concluded (T4.4). Overall, only small delays of about one month occurred towards the end of the project and the risks mitigated successfully.

One Objective and deliverable was not fulfilled: *D4.1: Commissioning of RHYPE for use*. The reason is SGRE stopping all activities for further development of hybrid RE power plants as well as solutions for optimized operation due to the company’s known constraint financial situation. Further, all hybrid RE power plants (in operation, currently in development or future) are sold to external investors and not available for further activities. However, all projects with a near due date were being finished to benefit from the findings and experience in a later stage. The findings and the technical solution will be available for offering of solutions to the market by SGRE’s mother company Siemens Energy.

Already during the project’s timeline, some results were disseminated successfully: A paper based on the developments of (T2.2), regarding an electrolyzer operating in ancillary service markets, has been submitted to the PSCC conference (PSCC2024 – Power Systems Computation Conference) to be held in Paris, June 4-7, 2024. Further, work related to (T2.4), a DRO model, was presented at the INFORMS Annual Meeting held in Phoenix, Arizona in October 2023.

5. Project results

5.1 Summary

The project HOMEY was contributing to SGRE’s RHYPE solution, with the following goals in mind:

- *to steadily reduce CO2 gas emission by promoting the production of green H2 (GH2) as a viable alternative to grey/blue hydrogen options.*

- *to increase the sources of flexibility in the electrical power system – primarily for transmission system operators (TSOs) – through optimized management and increased flexibility of RE (renewable energy) hybrid power plants.*
- *to optimize the profits of the bids of hybrid RE power plants to be submitted to the day-ahead (e.g., Nord Pool) and to the frequency-supporting ancillary services markets, namely frequency containment reserve (FCR), automatic frequency restoration reserve (aFRR), and manual frequency restoration reserve (mFRR) markets. Given the growth in H2 demand, we expected RHYPE to become a key enabler to optimize profit of bids in an established H2 marketplace as well.*
- *to decrease the production cost of GH2 and to increase availability by making it a more competitive and versatile option for hybrid RE power plants to use.*
- *to provide hybrid RE power plants with a new business model based on GH2 as a source of flexibility and a product to sell directly.*

HOMEY's objective was to develop the following modules/microservices to be integrated with the control tool software:

(a) *Stochastic optimizer module that formulates and solves predictive stochastic optimization problems under uncertainty. The core engine of the stochastic optimizer was developed at DTU Wind and Energy Systems (section: Energy Markets & Analytics).* ***This is one of the key features of HOMEY.***
(b) *Data management module that was updated to collect, aggregate, interpolate, filter and store data (e.g., wind and electricity price forecasts, field measurements, optimizer output, among others). Our data management module is robust enough to support several components (i.e., WTG, BESS, ELH2, H_2 storage tank), products (i.e., P2G, P2H, ancillary services, GH_2), time-series forecasts (i.e., wind generation, electricity price forecast, H_2 price forecast, etc.) and their uncertain parameters.*
(c) *Connectivity module that was updated to manage communication with the different energy flexibility sources and third-party systems (e.g., forecast providers such as Wattsight-VolueInsight, or SGRE's WEF).*
(d) *User interface, which was updated to enable granular visualization of optimizations input/outputs and to provide energy insights through customizable dashboards. The user interface is the interaction point with site operators and is paired with the control tool software to provide with input data and actionable dashboard where site operators can engage/disengage the relevant action.*
(e) *Orchestrator module which was updated to accommodate RHYPEs input. The orchestrator module coordinates and automates all facets and decision of energy management, from forecast data collection to the optimization's results exposure.*

All these modules were successfully implemented. The developed solution allows for absolute flexibility regarding support of number of components as well as combination of those. Likewise, key parameters for assets and participation in different markets with arbitrary requirements is adjustable, i.e., participation in different ancillary service markets, e.g., FCR, FCR-D and -N, mFRR, …, with or without symmetry requirements. As planned, the choice of forecast providers is adjustable. Figure 2 illustrates the main work done during HOMEY and the services that RHYPE will provide. Figure 3 depicts the EMS with its input (forecasts, plant status, …), basic objective (revenue maximization, curtailment minimization, imbalance mitigation, …), output (site optimization, KPIs) and decision-making stages (portfolio management, intraday control).

One technological key feature is the stochastic model, which allows dealing with forecast uncertainty. During pre-tests and after fine-tuning parameters at DTU, the stochastic model performed significantly better than the deterministic version. However, during the final analysis for SGRE's test site FIø, the stochastic model was slightly more conservative with proposed bids compared to the deterministic model. It is believed that the method for estimating uncertainty is crucial for its performance. There are numerous ways of implementing forecast error analysis, and SGRE did decide for a simple method for this project. It must be noted, that at the final stage of the project, a new wind-forecast model became available (developed at SGRE in parallel to this project). The newer forecast WEF included a "probabilistic" forecast, i.e., not only the most likely wind speeds,

but also forecasts at different probabilities, e.g., 90%ile, 10%ile, which may significantly improve the performance and the bids with the stochastic model.

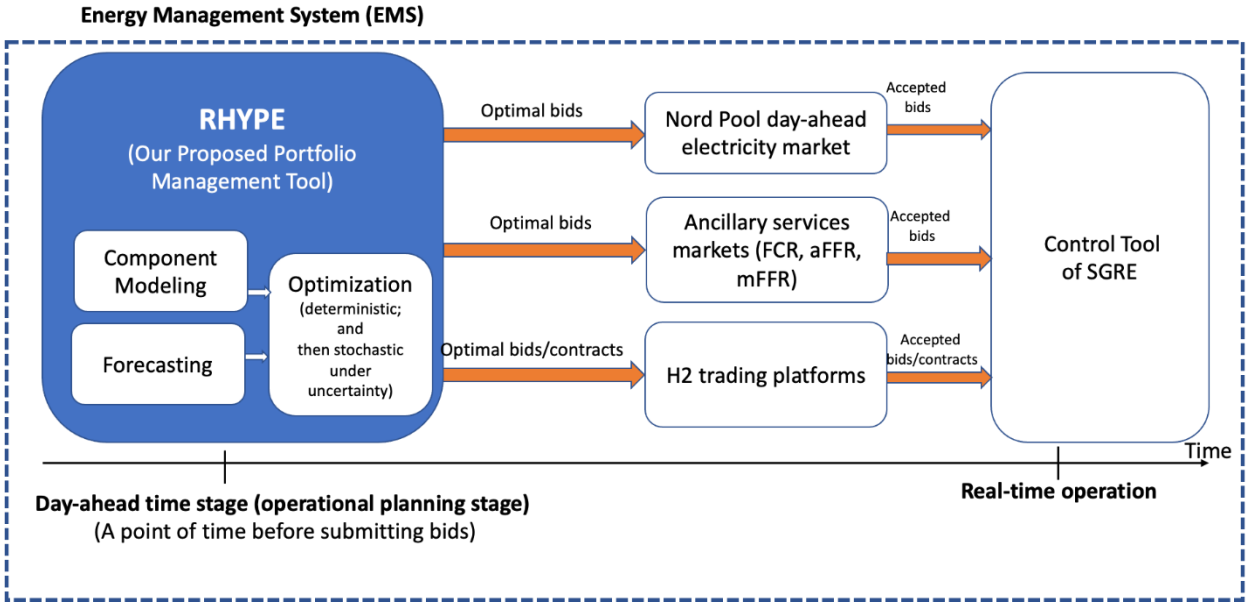

Figure *2* RHYPE after integration with SGRE´s existing control tool for optimized hybrid RE power plant management and the first EMS under uncertainty.

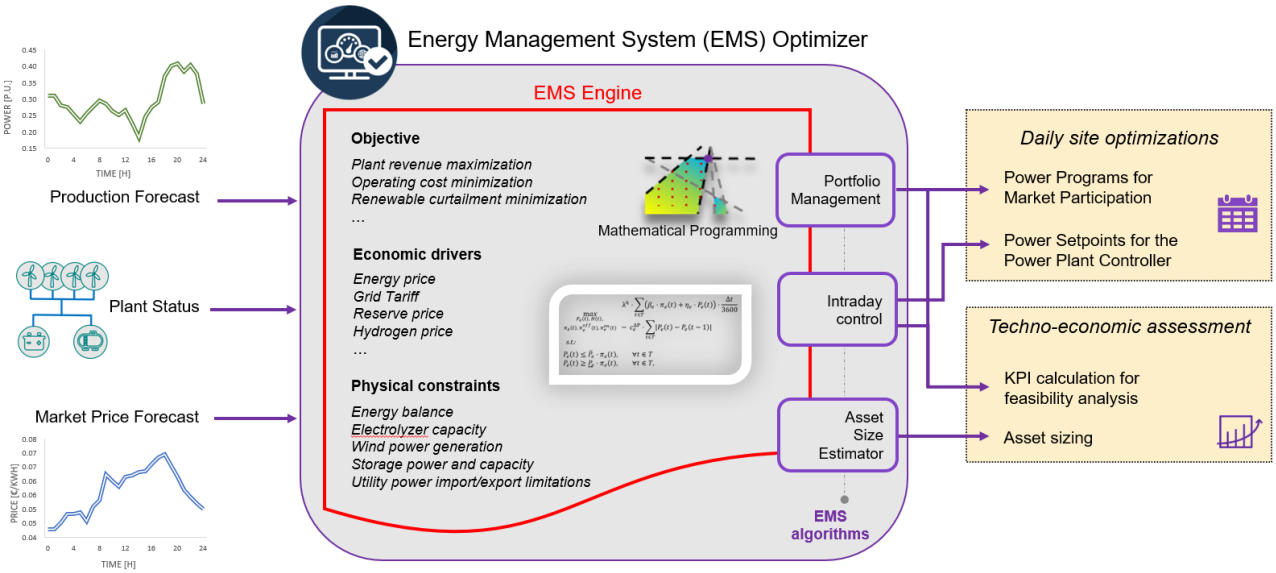

Figure 3 EMS functionality: input (forecasts, plant status, …), basic objective (revenue maximization, curtailment minimization, imbalance mitigation, …), output (site optimization, KPIs) and decision-making stages (portfolio management, intraday control).

As mentioned in the previous section, RHYPE was not commissioned for use in product quality, only used as prototype for test-purposes. The reason is SGRE stopping all activities for further development of hybrid RE power plants as well as solutions for optimized operation. Further, all hybrid RE power plants (in operation, currently in development or future) are sold to external investors and not available for further activities.

5.2 Commercial outcome for SGRE's test site Flø

The performance of the EMS and its optimization algorithm was tested with the historical data SGRE's Floe site in Brande for about 9 months. The test site has the following characteristics:

Table 1 Key characteristics for SGRE's test site near Flø (Denmark)

Characteristic	Value	Measurement unit
Wind power capacity	12	MW
Electrolyzer capacity	0.43	MW
Electrolyzer efficiency	75	%
H2 storage tank	1.00	ton
BESS capacity	0.5	MWh

For the demonstrator site Flø, SGRE implemented FCR from wind-power and the battery storage system, and mFRR provided by the electrolyser. Optimized market bids were calculated for all markets (day ahead, ancillary, H2 demand) based on market price forecast (only on Day-Ahead market) and wind speed forecast. While serving the market, operation-setpoints were calculated every 10 minutes. Intra-day adjustments of power-setpoints were calculated based on the accepted bids and deviation of realized market prices as well as true wind-speed from their respective forecasts.

Overall, this solution has successfully:

- provided additional flexibility (via ancillary markets **and** H2 production).
- produced GH2, while reducing production cost.
- optimised and increased profits by serving additional markets.
- reduced CO2 gas emission by production of green H2, in contrast to grey hydrogen.

Selected technical and commercial results are shown in Table 2 below, alongside the estimates provided before the project. The further commercial results are shown in Table 3 (KPIs that are considered key where RHYPE can make ans impact). **Overall, the project confirms and exceeds expectations from a commercial perspective.** Except for the total hydrogen production, which is significantly lower than expected. However, it is believed that with an improved strategy for estimating and quantifying uncertainty for the wind-power forecast the production of GH2 can be increased significantly.

Table 2 BaU vs RHYPE scenario within a 1-year timeline (2020 historical data), and test results with new RHYPE implementation (extrapolated to 1 year, with data from June 2023 to January 2024).

	H_2 production (ton)	Average Capacity Flexibility (MW)	H_2 prod.cost (DKK/ton)	Site income (1000x DKK)
BaU Scenario (2020)	64.31	0.81	10,863	7,084
RHYPE Scenario (2020)	64.31	0.88	9,942	7,492
HOMEY Results (2023/24)	48.03	1.38	26,748 (vs. BaU: 31,429)	8,887 (vs. BaU: 8,097)

Table 3 KPIs for RHYPEs operational performance (Results from HOMEY project versus values stated in the proposal)

KPI	HOMEY result (proposal)	Unit	Explanation

H2 production (capacity factor-CF)	68.26 (89.45[1])	[%]	The capacity factor is the measure of how often a given asset runs for a specific period of time. It's expressed as a percentage and calculated by dividing the actual output by the maximum possible output. This is a % of the amount of time the ELH2 is operated for the given time. Using the ELH2 gives us H2 for selling. The higher the increase in the utilization of the asset, the higher its ROI which is a considerable metric when deciding to purchase an ELH2 (approx. DKK 13 MN for 0,43 MW unit).
H2 production cost reduction	+14.6 (+8.48)	[%]	This is a % decrease in production cost for H2 due to operational efficiencies and improved decision making vis-à-vis H2 price and electricity price.
Site income increase	+9.8 (+5.77)	[%]	This is % increase in site bottom line income due to the optimal decision-making surrounding selling electricity, GH2 or ancillary services (i.e., FCR, aFRR, mFRR). The incorporation of DTU Energy Markets & Analytics to model the forecast with extreme limited amount of information with regards to H2 prices is crucial addition to HOMEY.
Site flexibility increase	+11.5 (+9.02)	[%]	This is a % increase in site flexibility (i.e., power reserve). More flexibility is achieved by incorporating better planning in the day-ahead market and for ancillary services. Flexibility in RE is a challenge since their source of power is inherently uncertain and thus are unable to provide a lot of flexibility to TSOs.
CO2 emission reduction	-325 (–)	[ton]	CO2 reduction by optimized planning to produce green hydrogen (GH2) in comparison to the production of hydrogen 100% from grid at the current energy mix in Denmark's electricity grid.
	– (-21.17)	[ton]	We simulated potential effects of wrong planning that could cause ELH2 unavailability due downstream bottleneck (e.g., GH2 tank filled). This is CO2 reduction due to an improved planning of ELH2 operations, where we avoid ELH2 shutdown due to no H2 storage tank capacity, avoid waiting times for tube-trailer trucks due to non-available GH2, which in turns decrease GH2 production.
Grid dependency reduction (to supply ELH2)	-100.0 [0.05 MWh/kg] (-50.79)	[%]	This is measured as a % of the energy from the electrical grid used to power the ELH2. Decreased grid dependency (i.e., hybrid RE power plant having more control on deciding whether to use the local generation when convenient) is key to the successful portfolio management of the hybrid RE power plant. Notwithstanding the occasional beneficial price, grid electricity

[1] This metric is highly dependent on H2 prices and electricity prices – 2020 was an outlier year for electricity, as it was very cheap. A successful KPI for this metric should by between 20-50% increase in H2 production (capacity factor-CF).

			has been **Error! Reference source not found.** to be a more expensive way to produce H2. As an example, on top of the energy price, we are subject to a power tariff (approx. DKK 145.03/MWh), that affects our production cost.

5.3 RHYPE interfaces

Within HOMEY the following modules were developed for the solution (see Figure 4):

- Modular EMS system, allowing flexible configuration of different assets.
- Communication interface with forecast providers (configurable).
- Communication interface with power plant controller
- Data management module
- Dashboard (Grafana)

Additional development was a stochastic model handling forecast uncertainty for improved planning, bidding, and intra-day operation strategies.

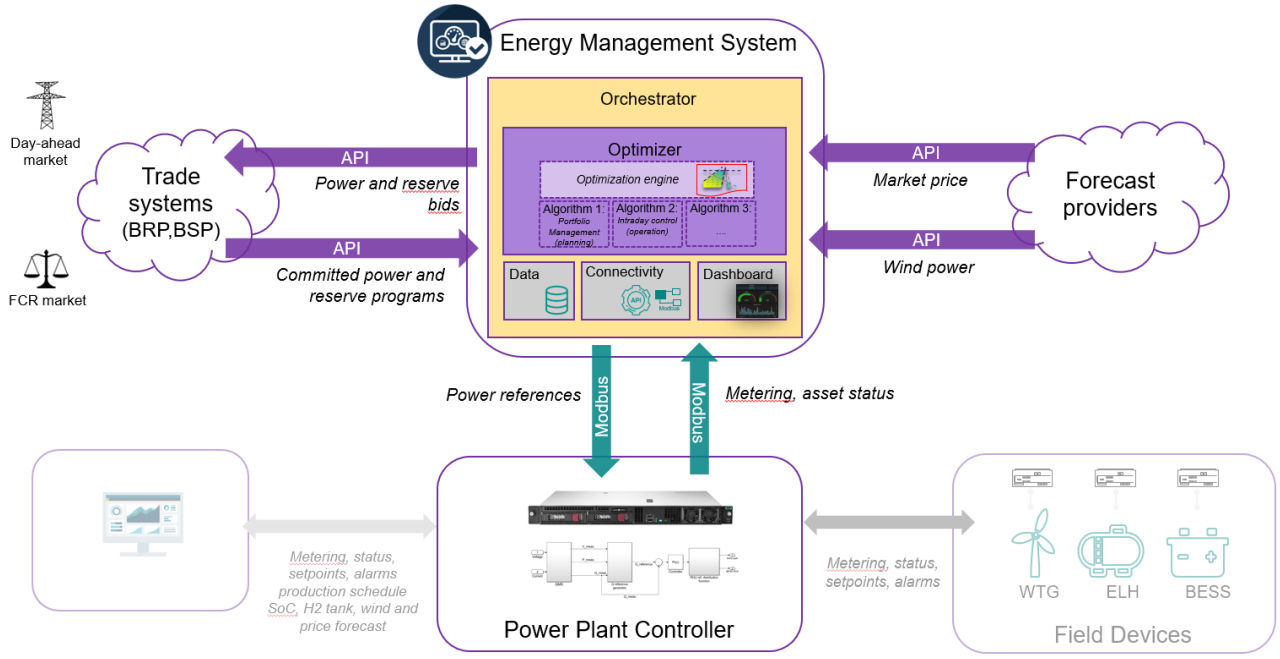

Figure 4 Interfaces and modules in the EMS further developed within the project.

5.4 Advanced model development

The two key developments were made to achieve advanced modelling: (a) investigation of a non-linear electrolyzer model and its impact for decision making, (b) stochastic model, to account for forecast uncertainty. In the following the two developments are summarized and details shown in the appendix.

5.4.1 Electrolyzer modelling

Initially, only a linear efficiency model was used, which can be implemented easily into a linear optimization problem. However, implementation of a non-linear efficiency was found to result in higher flexibility for the

decision making, as it seems that more intermediate power steps become available to the solution space. This is not intuitive and is explained in the literature in the appendix. Figure 5 shows the difference between different modelling approaches. Within the project tests of the non-linear electrolyzer model were conducted, but this model was not used for the final test at Flø site, to reduce model complexity and computational efforts. Nevertheless, this may change again for a final product, to gain profit from the found benefits.

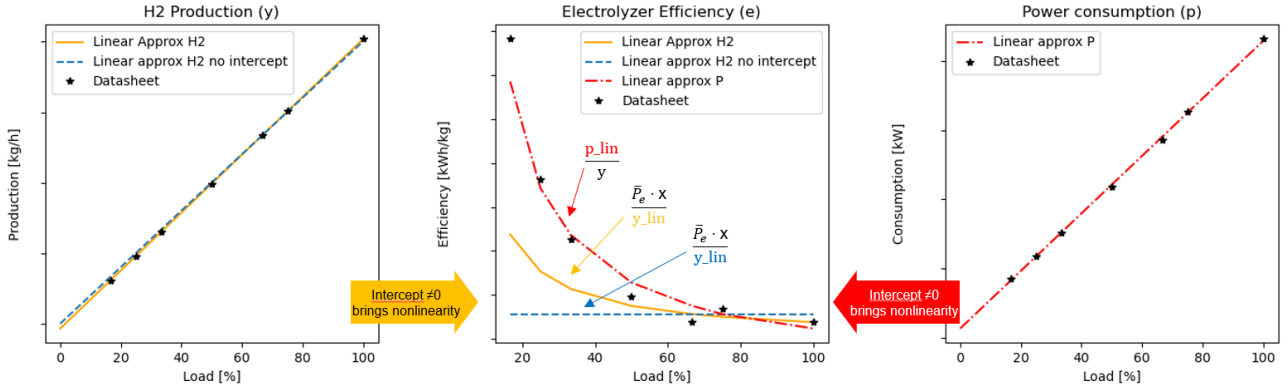

Figure 5 Linearity versus non-linearity in electrolyzer efficiency (values removed for confidentiality).

5.4.2 Stochastic model

Initial investigations of historical data saw a great potential in improving the decision performance in terms of increased profits through incorporating both uncertainty and ambiguity (Figure 6). The model is exposed to uncertainty in the forecasts for wind production and Day-Ahead clearing prices. Furthermore, due to insufficient historical data and a non-stationary environment, the underlying distributions might also be exposed to ambiguity. To tackle this, we formulate a Distributionally Robust Optimization model, where one can adjust the level of conservativeness with a single parameter, the Wasserstein radius. When this radius is set to zero, the model is equivalent to a sample average approximation model (or scenario-based optimization), not taking ambiguity into account. We place the uncertainty on the *forecast error* of wind production and DA price, leveraging historical data for the specific forecasts we have available.

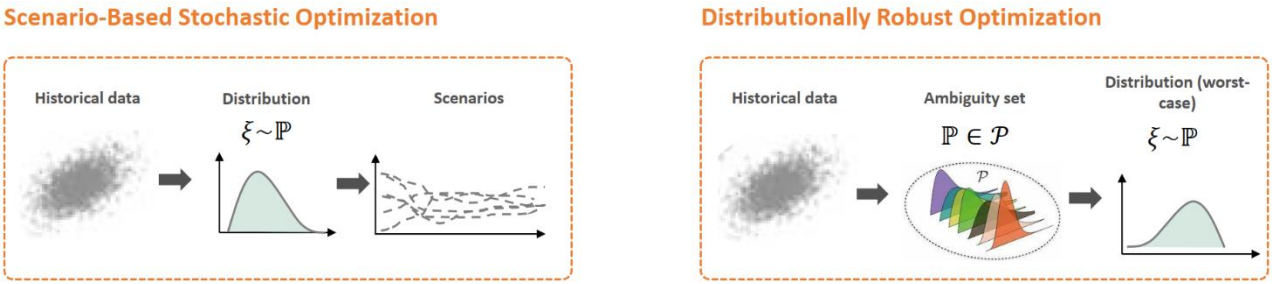

Figure 6 Basic idea behind Stochastic and Distributionally Robust Optimization: Utilizing information on statistical distribution of forecast versus measured/realized quantities.

5.5 Solution target group

The energy management solution RHYPE by SGRE is thought as a service product, that can be sold as upgrade to existing renewable power plants or for newly developed hybrid RE power plants. As such, potential customers are RE power plant owners and/or operators.

5.6 Dissemination

The project has resulted in three publications, one of which is still under review. One paper was submitted and accepted to the 15th IEEE PES PowerTech Conference of 2023. The work was presented at the conference and published in its proceedings. Another paper was also accepted to the 23rd Power Systems Computations Conference 2024, which proceedings are published Electric Power Systems Research journal. This work will also be presented at the conference in early June 2024. The project results were also presented at the 2023 INFORMS annual meeting.

6. Utilisation of project results

Currently, SGRE's activities for further development of hybrid RE power plants as well as solutions for optimized operation are on hold due to the company's known constraint financial situation. However, all projects with a near due date were being finished to benefit from the findings and experience in a later stage. The findings and the technical solution will be available for offering of solutions to the market by SGRE's mother company Siemens Energy.

One market obstacle was identified during the last year within other projects at SGRE, that slow commercialisation of the solution:
Due to a lack of H2 off-takers and the perceived long distance between production site and H2 consumers, the market was found in other projects to still decide against the production of GH2. This market situation may change in the future with increasing demand for GH2, or increased density of H2 production sites and/or off-taker locations.

Another critical point for the future of GH2 production is the way GH2 is sold on the market. Currently, Hydrogen Purchase Agreements are negotiated individually with off-takers. If the negotiated price is too low, this may make it less profitable for the operator of hybrid RE power plants to even offer or invest in the infrastructure for GH2 production.

If RHYPE is available on the market, then it can help increasing available flexibility on the electricity market. That means also improved grid stability and increased capacity of renewable electricity sources to be added to the electricity grid. Further, the production of green hydrogen (GH2) reduces CO2 emissions compared to alternative production methods. In addition, the potential of GH2 production lies at replacing fossil fuels used in transportation or generating heat for district heating systems as well as in electricity production (as last resort). Finally, RHYPE add value to e.g., wing power plants by adding further markets to their portfolios and reducing curtailment.

Since Ph.D.s have been part of the project, the project results have been utilized in teaching activities, both in supervision, lectures, and class assignments. Electrolyzer modelling was part of a grade-forming assignment in the DTU course "Renewables in Electricity Markets" of fall 2023, completed by more than 100 students. Further, the Ph.D. student has directly supervised three master students based on and contributing to the project results. This included work on formulating DRO models and risk mitigation in a Hybrid Power Plant set-up. One additional master thesis was supervised based on the early project results. A special course was also arranged for a master student who showed particular interest in this project work of electrolyzer modelling. The projects work on modelling of ancillary services and uncertainty for a hybrid power plant was used to give a lecture in the PhD course "Planning Under Uncertainty in Energy Markets" hosted by the Norwegian University of Science and Technology. Finally, a one-day seminar was given at the Smart Energy and Stochastic Optimization Workshop 2023, hosted by Ecole du Ponts ParisTech, where the Ph.D. student was directly involved in teaching.

7. Project conclusion and perspective

The developed energy management system (EMS) solution RHYPE and decision-making algorithms reveal a promising potential for hybrid RE power plants. The income gains and reduction in curtailment can become a game-changer for these power plants and potentially increase the market for hybrid RE power plants. RHYPE is significantly adding flexibility that helps stabilizing the electricity grid, whilst also allowing to add more renewable energy powerplant capacity. In addition, RHYPE supports efforts in reducing CO2 emissions by production of green hydrogen, which reduced emissions during production as well as by replacing fossil fuels with hydrogen.

Next development steps would include refinement of the algorithms to improve estimation of forecast uncertainty. This will improve both the amount of flexibility and the amount of imbalance realized in the operation. Otherwise, the solution is ready for integration into products. Due to SGRE's financial situation, further development is expected to be delayed, but the potential is perceived.

However, the current market situation still limits acceptance amongst project developers and potential power plant owners. The demand for hydrogen appears currently too low for investors to add hydrogen production. The investment risks seem still too high, but it is believed to lower significantly within the next years.

8. Appendices

8.1 Deterministic model – Improved modelling of hydrogen efficiency

See following pages, at sections:

- When is a Detailed Electrolyzer Model Necessary?
- The Value of Ancillary Services for Electrolyzers

8.2 Stochastic model – Need for dealing with forecast uncertainty

See following pages, at section:

- Stochastic Model for Trading Wind Power and Hydrogen

When is a Detailed Electrolyzer Model Necessary?

1 Introduction

1.1 Background

In order to limit global warming to a maximum of 1.5 °C, greenhouse gas emissions must be reduced to net zero by 2050, as called for in the European Green Deal 2019 [1]. Renewable hydrogen produced through electrolysis could aid in two major challenges on the path towards the net zero goal. First, electrolyzers can act as flexible loads and therefore potential frequency restoration ancillary service providers, contributing to maintaining the power balance in power systems with increased penetration of renewable energy sources. Second, renewable hydrogen can be further synthesized into other green fuels, eventually enabling decarbonization in the hard-to-abate sectors, such as heavy transport and industry.

Hybrid power plants comprising of renewable power sources (wind and/or solar) and electrolyzers are the key components to accelerate the current energy transition through hydrogen [2]. Nonetheless, uncertainties in terms of the cost-benefit of electrolyzers in the long run have challenged the widespread investment in said technologies and thereby large-scale production of renewable-based green hydrogen [3]. In Denmark, there is currently a special focus on green hydrogen at the governmental level and also, among the regulator, system operator, and many industry stakeholders, envisioning a large deployment of electrolyzers and other power-to-X facilities in the coming years. In 2021 the Danish government published a strategy for the national power-to-X development, aiming to build 4 to 6 GW of electrolysis capacity by 2030, doubling the current Danish peak demand [4]. This emerging trend is not limited to Denmark, and many other countries both in Europe and globally see hydrogen as a key solution for the realization of green societies of the future [2, 5].

1.2 Aim and Literature Review

It is a common practice in the current literature to use a simplified operational model for electrolyzers e.g., by using a constant power-to-hydrogen conversion ratio irrespective of whether the electrolyzer operates in full capacity or not [6–9]. In addition, some papers do not consider operational states of the electrolyzer [6, 9]. This paper challenges these simplification practices. While a simplified model works satisfactorily under certain operational circumstances, there are several other circumstances under which a simplified one yields a sub-optimal operation of electrolyzers, underestimating their value. This paper answers when a detailed operational model should be applied, and to what extent the profit and hydrogen production can be increased by using a detailed model. We will also discuss to what extent a detailed model brings additional computational burden.

In general, two main physical aspects of electrolyzers need to be modeled for operation in the day-ahead time stage:

1. *Electrolyzer efficiency*: The power-to-hydrogen conversion efficiency is a function of the power consumption of the electrolyzer. To accurately model the hydrogen production of the electrolyzer, the varying efficiency should be captured, which introduces non-linearities to the model. The simple models usually use a constant efficiency, while more accurate modeling incorporates the non-linearities, which can be later linearized.

2. *Number of operating states*: Proper operational modeling of electrolyzers may require introducing three states, namely on, off, and standby, to ensure no hydrogen production below a given minimum allowed partial loading, for which additional binary variables are needed. Many papers in the literature do not even model states, thus assuming the electrolyzer is always on, or model two states only, i.e., on and off, similar to conventional power generators[1].

Various studies have incorporated different levels of operational details of the electrolyzer into their optimization problems. In [7] and [8], a constant efficiency is applied but two and three states are modeled, respectively, by adding binary variables. In [10], three states are modeled, while assuming a linear hydrogen production curve, despite showing that the production curve is not well approximated by a first-order interpolation. A hybrid power plant including an electrolyzer is modeled in [11], where the non-linear hydrogen production is linearized between two points, with a single binary variable representing the on/off state of the electrolyzer. In [12] a quadratic production curve is applied and the resulting non-linear program is eventually solved by a heuristic. In [13], three states are included, and differently from the other papers, the operating temperature is considered as a variable, providing an extra degree of freedom in the electrolyzer operation. This model allows to take into account the temperature impact on the conversion efficiency and the quality of the generated heat. The non-linear hydrogen production is then linearized around a fixed reference operating point to formulate the problem as a mixed-integer linear programming (MILP) problem.

1.3 Contributions and Paper Organization

To the best of our knowledge, there is a lack of a comprehensive analysis in the current literature, identifying the operational circumstances under which a simple model ends up in a sub-optimal operation of electrolyzers, resulting in a reduced profit and hydrogen production[2]. This paper bridges such a gap through the following contributions:

- To embed constraints describing the physics of electrolyzers while keeping the final model as a MILP,
- To thoroughly investigate ex-post the impact of the inclusion of different operational details on the final profit of the hybrid power plant and the amount of hydrogen produced,
- and finally, to provide a set of recommendations in terms of including operational details of electrolyzers, depending on the application, the range of electricity prices, and the hydrogen price.

[1] We will discuss later in Section 4 that under some operational conditions, a two-state model including on and standby states works well too.

[2] Reference [13] provides a similar analysis, however, the Faraday efficiency is assumed to be one. The consequences of this assumption will be further discussed in Section 2.2.

Without loss of generality, this paper focuses on alkaline electrolyzers, as they are currently the most mature technology [14]. The proposed model can be extended to other low-temperature electrolyzers, such as polymer electrolyte membrane (PEM). More operational characteristics may be necessary for modeling solid-oxide electrolyzers (SOEC).

The rest of the paper is organized as follows. Section 2 describes the electrolyzer physics, focusing on the operating states and the hydrogen production curve. Section 3 provides the proposed MILP, representing all three states of the electrolyzer. Section 4 discusses the impact of the electrolyzer modeling choices by means of a test case and a thorough sensitivity analysis. Section 5 concludes the paper. In the Appendix, the day-ahead price range where electrolyzer details matter is analytically formulated. Finally, the Online Companion [15] provide two MILPs (simpler than the one proposed in Section 3), both representing two states of the electrolyzer only, where one is a model with on-off states, and the other one is a model with on-standby states.

2 Electrolyzer physics

The core of the renewable-hydrogen hybrid power plant is the electrolyzer, where water is decomposed into hydrogen and oxygen by means of electrical power. The physics and operating characteristics of alkaline electrolyzers are described in this section and will be formulated as a set of mixed-integer linear constraints in Section 3.

2.1 States

To describe and model the real operation of an alkaline electrolyzer, it is necessary to distinguish three different states:

On state

the electrolyzer operates within its feasible load range, consuming power and producing hydrogen with a conversion efficiency that depends on the partial load, which will be explained in Section 2.2. The minimum operating power for alkaline electrolyzers is around 15-20% of the nominal power, below which the electrolyzer must go into standby or off.

Standby state

the electrolyzer does not produce any hydrogen but consumes the power needed to maintain the system temperature and pressure so that it can rapidly resume production. The value of the standby power consumption is not usually disclosed by manufacturers, but values between 1-5% of the electrolyzer full load capacity have been adopted in the literature [7, 8, 10]. The time needed to switch from standby to on, i.e., a warm start-up is of the order of 30 seconds [8].

Off state

the electrolyzer is shut down completely and does not consume any power nor produce any hydrogen. However, to switch back to on, a significant amount of electricity is needed, corresponding to a cold start-up cost. Moreover, at least 20 minutes are necessary before resuming hydrogen production [8]. Apart from the introduced cold start-up cost and start-up time, the frequent shut down of the electrolyzer may have a negative impact on the device degradation and lifetime [16].

2.2 Efficiency and Production Curve

The conversion efficiency of electricity into hydrogen is not constant but depends on the *partial load*, i.e., the ratio between power consumption at a specific time and the nominal power of the electrolyzer. The variation of the efficiency based on the operating set-point is mainly due to two phenomena: (i) the current-voltage relationship, also called the polarization curve, and (ii) the Faraday efficiency. We explain both phenomena in the following.

The current-voltage relationship describes the voltage increase (also called over-voltage or over-potential) with increasing current density, due to different losses, as explained in [17] and [13]. Ulleberg [18] introduced a widely adopted empirical formulation that describes the relationships between voltage, current density, and electrolyzer operating temperature. To further take into account the operating pressure, this formulation was modified by Sanchez et al. [19]. For a given temperature and pressure, this can be formulated as

$$U^{\text{cell}}(i) = U^{\text{rev}} + K_1 i + K_2 \log(K_3 i + 1), \tag{1}$$

where $U^{\text{cell}}(i)$ is the cell voltage as a function of the current density i. In addition, U^{rev} is the open-circuit voltage (i.e., voltage corresponding to current density equal to zero). The parameters K_1, K_2, K_3 are constants obtained from experimental data and can be found in [19]. Voltage U^{rev} can be calculated for a specific operating temperature according to an empirical equation that can be found in [19]. The power consumed by the electrolyzer $p^{\text{e}}(i)$ can be calculated as

$$p^{\text{e}}(i) = U^{\text{cell}}(i) i A, \tag{2}$$

where A is the total area of the cells composing the electrolyzer. The Faraday law calculates the hydrogen production $h(i)$ of the electrolyzer as

$$h(i) = 3600 \cdot \frac{\eta^{\text{F}}(i) M^{\text{H}_2} i A}{2F}, \tag{3}$$

where $h(i)$ is the hydrogen production rate in kg/h, M^{H_2} is the molar mass of hydrogen in kg/mol, F is the Faraday constant, and $\eta^{\text{F}}(i)$ is the Faraday efficiency as a function of current density. The latter is defined as the ratio between the actual and the theoretical maximum amount of hydrogen produced. The difference between actual and theoretical output is explained in [18], and it increases significantly when the electrolyzer is working at low-current densities. In [19], an empirical expression that captures the relationship between the Faraday efficiency and the current density at a given temperature is provided: $\eta^{\text{F}}(i)$ is close to one for higher current densities, and it drops to zero when reducing the current. The electrolyzer efficiency is defined as

$$\eta(i) = \frac{h(i)}{p^{\text{e}}(i)}, \tag{4}$$

where generally $\eta(i)$ is expressed in kg/MWh. For different values of i, the black curve in Fig. 1(a) shows efficiency $\eta(i)$ versus power consumption $p^{\text{e}}(i)$. In addition, the black curve in Fig. 1(b) shows the hydrogen production $h(i)$ versus power consumption $p^{\text{e}}(i)$. For notational clarity, we drop (i) in the rest of the paper. The black curves in Fig. 1 show that the model is non-linear. The efficiency has a peak at around 30% of the load. This characteristic peak in the efficiency curve is not captured when a constant conversion efficiency is used, as done in [6, 8, 10], or when the Faraday efficiency is assumed to be equal to one in the entire feasible operating range, as done in [13].

To keep the final problem a MILP, but describe the hydrogen production with more details, we use a piecewise linearization of the hydrogen production curve as shown by the red curve in Fig. 1(b),

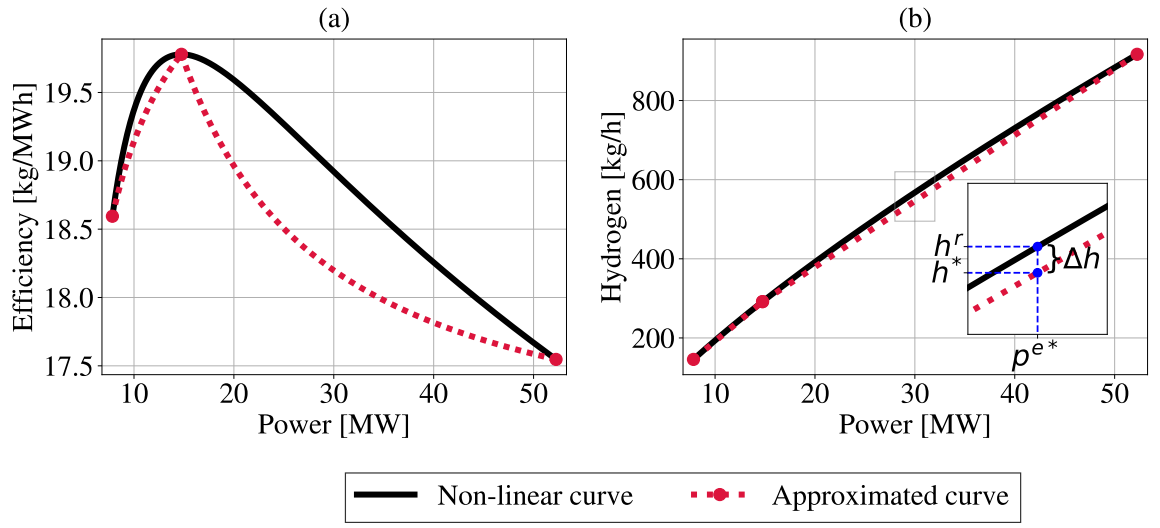

Figure 1: Plot (a): the efficiency curve, and plot (b): the hydrogen production curve of a 52.25-MW alkaline electrolyzer, as a function of the electric power consumption, working at 90 °C and 30 bar. The black curves represent the original non-linear curves. Approximated by two segments, the red curve in plot (b) is the piecewise linearized hydrogen production curve. The non-linear efficiency curve corresponding to this piecewise linearization is represented by the red curve in plot (a). In our formulation, we will only use the red piecewise linear production curve in plot (b). The inner plot of (b) shows the hydrogen production discrepancy Δh between original and approximated curves, for a given power consumption level.

for two linearization segments. For each segment $s \in \mathcal{S}$, the A_s (slope) and B_s (intercept) coefficients of the line can be calculated such that the approximated hydrogen production is $A_s p^{\mathrm{e}} + B_s$. Later we will define a binary variable indicating which segment is active. The proposed approximation is exact only at the segment endpoints (i.e., linearization points), otherwise, it is an underestimation of the original non-linear curve. For example, the optimal power set-point p^{e^*} in the inset of Fig. 1(b) corresponds to the hydrogen production h^* according to the proposed piecewise linear model with two segments[3]. However, the actual hydrogen realization based on the electrolyzer physics is h^{r}. The hydrogen production difference Δh is reduced by increasing the number of segments, and the effect of the hydrogen surplus obtained when choosing only one segment, as done in [10], is discussed in Section 4.

According to this piecewise linear formulation for the hydrogen production curve, the efficiency η for segment s can be calculated based on (4), resulting in $\eta = A_s + \frac{B_s}{p^{\mathrm{e}}}$. This is depicted by the red dotted curve in Fig. 1(a), given two linearization segments used. Note that it does not present a linear behavior. However, this non-linear efficiency curve does not appear in our optimization problem. The hydrogen production curve is used instead, which is linearized through segments, as illustrated by the red dotted curve in Fig. 1(b).

[3]Symbol * refers to the optimal value.

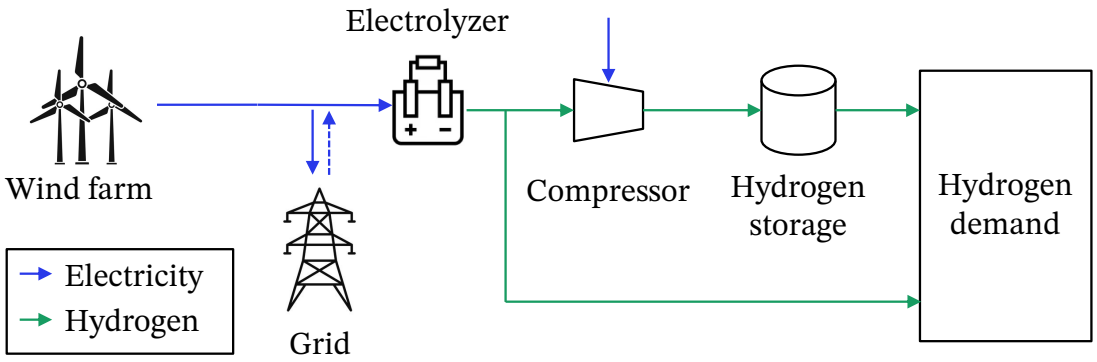

Figure 2: Schematic representation of a hybrid power plant.

3 Problem formulation

We consider a hybrid power plant, as depicted in Fig. 2, consisting of a wind farm, an electrolyzer, a hydrogen compressor, and a hydrogen storage. The generated wind power can be either sold to the grid at the electricity market price, or consumed by the electrolyzer to produce 100% renewable-based green hydrogen. The hydrogen produced can either be directly delivered to the demand or temporarily stored in an on-site hydrogen storage, with an associated cost for compressing the gas. The dashed blue line in Fig. 2 represents the option to buy electricity from the grid only to supply the electrolyzer's standby power when there is no wind power.

The hydrogen price is assumed to be a single-value constant, and the hybrid power plant serves a minimum daily hydrogen demand. We assume the plant has perfect foresight of future wind power production and electricity price. Given the 1-hour time resolution in our model, we neglect the ramping limitation which are typically around ±20% of the nominal power per second [10], as well as the warm and cold start-up times of the electrolyzer.

For the optimal operation of the hybrid power plant, we develop a complete MILP in Section 3.1 accounting for three states of the electrolyzer and then provide two simplified counterparts in Section 3.2, each with two states of the electrolyzer.

Notation: All parameters are upper-case or Greek letters, whereas all variables are lower-case letters. All binary variables are noted by z.

3.1 Three-state Model

The most complete MILP includes the objective function (5) constrained by (6)-(28).

Objective function

Over the set of hours $t \in \mathcal{T}$, the objective function (5) maximizes the total profit of the hybrid power plant as

$$\max_{\mathbf{x}} \sum_{t \in \mathcal{T}} p_t \lambda_t^{\mathrm{DA}} + d_t \lambda^{\mathrm{h}} - p_t^{\mathrm{in}} \lambda_t^{\mathrm{in}} - z_t^{\mathrm{su}} \lambda^{\mathrm{su}}, \tag{5}$$

where the variable set $\mathbf{x}$ will be defined later. The first term corresponds to selling power p_t to the grid at the day-ahead electricity market price λ_t^{DA}. The second term pertains to delivered hydrogen

d_t at a fixed price λ^{h}. The third term represents the cost for purchasing standby power p_t^{in} to support the electrolyzer's standby state in case the wind power is insufficient. The corresponding price is $\lambda_t^{\mathrm{in}} = \lambda_t^{\mathrm{DA}} + \lambda^{\mathrm{TSO}}$, where λ^{TSO} is the grid tariff imposed by the Transmission System Operator (TSO). Finally, the fourth term corresponds to the cold start-up cost of the electrolyzer, where the binary variable z_t^{su} indicates the start-up at hour t, associated with the cost per startup λ^{su}.

Power balance

In every hour t, the power p_t sold in the day-ahead market is equal to the wind farm power production P_t^{w} plus power p_t^{in} bought from the grid to support the standby state of the electrolyzer, subtracted by the power consumption p_t^{e} of the electrolyzer and the power consumption p_t^{c} of the compressor, such that

$$p_t = P_t^{\mathrm{w}} + p_t^{\mathrm{in}} - p_t^{\mathrm{e}} - p_t^{\mathrm{c}} \qquad \forall\, t \in \mathcal{T}. \tag{6}$$

Limit on p_t^{in}

The input power p_t^{in} is limited by the standby state consumption of the electrolyzer, implying that power cannot be bought from the grid to produce hydrogen:

$$p_t^{\mathrm{in}} \leq P^{\mathrm{sb}} z_t^{\mathrm{sb}} \qquad \forall\, t \in \mathcal{T}, \tag{7}$$

where the parameter P^{sb} is the standby consumption, and the binary variable z_t^{sb} indicates whether the electrolyzer is in the standby mode in hour t.

Electrolyzer operational states

Constraint (8) ensures that the electrolyzer can take only one out of three states at any hour t, namely online, standby, or off:

$$z_t^{\mathrm{on}} + z_t^{\mathrm{off}} + z_t^{\mathrm{sb}} = 1 \qquad \forall\, t \in \mathcal{T}, \tag{8}$$

where similar to z_t^{sb}, binary variables z_t^{on} and z_t^{off} indicate whether in hour t the electrolyzer is on and off, respectively. The states are activated based on the electricity consumption of the electrolyzer. In the online state, the electricity consumption p_t^{e} of the electrolyzer can neither exceed the capacity C^{e} nor go below a minimum load limit P^{min}. In the standby state, the electricity consumption must be equal to the standby power consumption P^{sb}. These constraints are enforced by

$$p_t^{\mathrm{e}} \leq C^{\mathrm{e}} z_t^{\mathrm{on}} + P^{\mathrm{sb}} z_t^{\mathrm{sb}} \qquad \forall\, t \in \mathcal{T}, \tag{9}$$

$$p_t^{\mathrm{e}} \geq P^{\mathrm{min}} z_t^{\mathrm{on}} + P^{\mathrm{sb}} z_t^{\mathrm{sb}} \qquad \forall\, t \in \mathcal{T}. \tag{10}$$

To represent the cold start-up of the electrolyzer, the binary variable z_t^{su} is defined, taking the value 1 in the case of a transition from off to on state in hour t, as enforces by constraints (11) and (12). Further, constraint (13) ensures that the transition from an off-state to a standby-state is not allowed, to avoid bypassing of the start-up cost.

$$z_t^{\mathrm{su}} \geq z_t^{\mathrm{on}} - z_{t-1}^{\mathrm{on}} - z_{t-1}^{\mathrm{sb}} \qquad \forall\, t \in \mathcal{T} \setminus \{1\}, \tag{11}$$

$$z_{t=1}^{\mathrm{su}} = 0, \tag{12}$$

$$z_{t-1}^{\mathrm{off}} + z_t^{\mathrm{sb}} \leq 1 \qquad \forall\, t \in \mathcal{T} \setminus \{1\}. \tag{13}$$

Electrolyzer hydrogen production

The hydrogen production h_t is a function of the electricity consumption of the electrolyzer. As explained in Section 2.2, for each segment $s \in \mathcal{S}$, a linear function of the segment power consumption $\hat{p}^{\mathrm{e}}_{ts}$ with slope A_s and intercept B_s is defined, such that

$$h_t = \sum_{s \in \mathcal{S}} (A_s \hat{p}^{\mathrm{e}}_{ts} + B_s z^{\mathrm{h}}_{ts}) \qquad \forall\, t \in \mathcal{T}, \tag{14}$$

where the binary variable z^{h}_{ts} defines which segment s is active in hour t. Each segment is valid within a pre-defined interval of upper $\overline{P}_s$ and lower $\underline{P}_s$ power consumption levels, i.e.,

$$\underline{P}_s z^{\mathrm{h}}_{ts} \leq \hat{p}^{\mathrm{e}}_{ts} \leq \overline{P}_s z^{\mathrm{h}}_{ts} \qquad \forall\, t \in \mathcal{T}, s \in \mathcal{S}. \tag{15}$$

Constraint (16) ensures that hydrogen production happens in the online state only, while one segment only can be active at any hour t. In addition, (17) computes the total power consumption of the electrolyzer:

$$z^{\mathrm{on}}_t = \sum_{s \in \mathcal{S}} z^{\mathrm{h}}_{ts} \qquad \forall\, t \in \mathcal{T}, \tag{16}$$

$$p^{\mathrm{e}}_t = \sum_{s \in \mathcal{S}} \hat{p}^{\mathrm{e}}_{ts} + P^{\mathrm{sb}} z^{\mathrm{sb}}_t \qquad \forall\, t \in \mathcal{T}. \tag{17}$$

Hydrogen storage

Constraints (18)-(24) represent the storage operation:

$$h_t = h^{\mathrm{d}}_t + s^{\mathrm{in}}_t \qquad \forall\, t \in \mathcal{T}, \tag{18}$$

$$d_t = h^{\mathrm{d}}_t + s^{\mathrm{out}}_t \qquad \forall\, t \in \mathcal{T}, \tag{19}$$

$$s^{\mathrm{out}}_t \leq S^{\mathrm{out}} \qquad \forall\, t \in \mathcal{T}, \tag{20}$$

$$p^{\mathrm{c}}_t = K^{\mathrm{c}} s^{\mathrm{in}}_t \qquad \forall\, t \in \mathcal{T}, \tag{21}$$

$$s_{t=1} = S^{\mathrm{ini}} + s^{\mathrm{in}}_{t=1} - s^{\mathrm{out}}_{t=1} \tag{22}$$

$$s_t = s_{t-1} + s^{\mathrm{in}}_t - s^{\mathrm{out}}_t \qquad \forall\, t \in \mathcal{T} \setminus \{1\}, \tag{23}$$

$$s_t \leq C^{\mathrm{s}} \qquad \forall\, t \in \mathcal{T}. \tag{24}$$

The hydrogen produced h_t can either go directly to the demand h^{d}_t or be injected into the hydrogen storage s^{in}_t, as enforced by (18). The total hydrogen d_t delivered to the demand is equal to the sum of hydrogen directly from the electrolyzer and that from the storage s^{out}_t, as per (19). The storage output of every hour is limited by the output flow capacity S^{out} in (20). Further, the compressor consumes power p^{c} to compress the hydrogen injected into the storage. Assuming adiabatic compression, the compression coefficient K^{c} can be calculated, as proposed by [13]. The power consumption for compression is then (21). The state of charge of the hydrogen storage in the initial and following hours is calculated by (22) and (23), where S^{ini} is the hydrogen initially stored in the storage at the beginning of time horizon $\mathcal{T}$. The storage hydrogen mass capacity C^{s} is enforced by (24). Note that we do not impose any constraint for the energy stored at the end of time horizon $\mathcal{T}$. Therefore, pursuing profit maximization in this time horizon, the hybrid power plant will leave the storage empty in the last hour[4].

[4] One can enforce a constraint on the minimum stored hydrogen at the end of the time horizon, or add a value for this stored energy to the objective function.

Hydrogen demand

Imagine within the underlying time horizon $\mathcal{T}$, which could be, for example, a year, there are N number of time subsets, e.g., 365 days, indexed by n, such that there is a minimum hydrogen demand for each n:

$$\sum_{t \in \mathcal{H}_n} d_t \geq D_n^{\min} \qquad \forall\, n \in \{1, ..., N\}, \tag{25}$$

where $\mathcal{H}_n$ is the set of hours within time subset n.

Variable declaration

Constraint (26) declares the non-negativity conditions:

$$d_t, h_t, h_t^{\mathrm{d}}, p_t, p_t^{\mathrm{c}}, p_t^{\mathrm{in}}, \hat{p}_{ts}^{\mathrm{e}}, s_t, s_t^{\mathrm{in}}, s_t^{\mathrm{out}} \in \mathbb{R}^+. \tag{26}$$

Constraint (27) lists binary variables:

$$z_t^{\mathrm{su}}, z_{ts}^{\mathrm{h}}, z_t^{\mathrm{on}}, z_t^{\mathrm{off}}, z_t^{\mathrm{sb}} \in \{0, 1\}. \tag{27}$$

Therefore, the total number of binary variables is $|\mathcal{T}|(4 + |\mathcal{S}|)$ binaries, where $|\mathcal{T}|$ and $|\mathcal{S}|$, respectively, are the number of hours and the number of segments used to linearize the hydrogen production curve. Finally, the variable set $\mathbf{x}$ is defined as

$$\begin{aligned}\mathbf{x} = \{&d_t, h_t, h_t^{\mathrm{d}}, p_t, p_t^{\mathrm{c}}, p_t^{\mathrm{in}}, \hat{p}_{ts}^{\mathrm{e}}, \\ &s_t^{\mathrm{in}}, s_t, s_t^{\mathrm{out}}, z_t^{\mathrm{su}}, z_{ts}^{\mathrm{h}}, z_t^{\mathrm{on}}, z_t^{\mathrm{off}}, z_t^{\mathrm{sb}}\}.\end{aligned} \tag{28}$$

Accordingly, in addition to $|\mathcal{T}|(4 + |\mathcal{S}|)$ number of binary variables, we have $|\mathcal{T}|(9 + |\mathcal{S}|)$ number of continuous variables.

3.2 Two-state Models

The optimal operation problem (5)-(28) of the hybrid power plant accounting for three states of the electrolyzer can be simplified if two states only are considered, either on-off states or on-standby states. Both result in MILPs.

In the latter, i.e., the MILP with on-off states, one binary variable (instead of three) per hour t is sufficient, such that it indicates whether the electrolyzer in the given hour is on or off. The resulting MILP is provided in [15]. The total number of binary variables in this MILP is $|\mathcal{T}|(2 + |\mathcal{S}|)$.

Similarly, a single binary variable per hour t is enough in the MILP with on-standby states, indicating whether the electrolyzer is online or in standby mode. Also, the start-up binary variable is not needed. The corresponding MILP is given in [15], where among three MILPs, we need the lowest number of binary variables, i.e., $|\mathcal{T}|(1 + |\mathcal{S}|)$.

4 Numerical Study

We apply the proposed MILPs of Section 3 to a case study and investigate how the optimal operation of the hybrid power and the resulting profit change by adding more operational details of the electrolyzer. All source codes and input data are publicly shared[5]. We consider several options for

[5] GitHub: `https://github.com/mtba-dtu/detailed-electrolyzer-model`

Table 1: Input data for the case study

Wind farm	Capacity	C^{w}	104.5	MW
Electrolyzer	Capacity	C^{e}	52.25	MW
	Standby load	P^{sb}	0.52	MW
	Minimum load	P^{min}	7.84	MW
	Pressure		30	bar
	Temperature		90	°C
	Max. current density		5,000	A/m^2
	Start-up cost	λ^{su}	2,612.50	€ [10]
	TSO tariff	λ^{TSO}	15.06	€/MWh
Storage	Capacity	C^{s}	22,000	kg
	Maximum output	S^{out}	912.13	kg/h
Compressor	Consumption coefficient	K^{c}	0.0012	MWh/kg
Hydrogen	Price	λ^{h}	2.10	€/kg
	Minimum demand	D_n^{min}	3,667	kg/day

the number of linearization segments, i.e., $|\mathcal{S}|$, used to approximate the hydrogen production curve of the electrolyzer, including 1, 2, 4, 8, and 12 segments. Also, we consider three options for the number of electrolyzer states: three states on-off-standby (OOS), two states on-standby (OS), and two states on-off (OO). In the rest of this section, we will refer to various models as, for example, OOS-12, implying we consider three states (OOS) with 12 segments. Finally, we conduct a sensitivity analysis to explore the impact of various input parameters, such as wind farm capacity, hydrogen demand, and hydrogen price, on the operation of the hybrid power plant.

4.1 Case Study

We consider a hybrid power plant whose structure equals the one in Fig. 2, and its input data is provided in Tab. 1. The capacity of the wind farm is 104.5 MW, corresponding to 11 V164-9.5 MW™ Vestas turbines, located in Køge Bay, Denmark. The electrolyzer capacity is set to 50% of the wind farm capacity, amounting to 52.25 MW. The modeling horizon spans one year with an hourly temporal resolution. We apply hourly electricity price data for 2019, as price data for the following years might be distorted by macroeconomic impacts, such as COVID-19. Day-ahead electricity prices for the East Denmark area (DK2) are obtained from ENTSO-e Transparency platform [20] and hourly historical wind capacity factors at the given location for 2019 are retrieved from the Renewable.ninja web platform [21]. The average yearly capacity factor for the selected location is 43.7%. The hybrid power plant is only allowed to buy power from the grid to keep the electrolyzer in standby mode, in case the wind power is insufficient. In that case, the electricity is bought at the hourly day-ahead market price plus the grid tariff of the TSO. Since the wind farm is located in DK2, the consumption tariff imposed by the Danish TSO, Energinet, is applied[6]. The minimum daily demand can be met by the full-load operation of the electrolyzer for around four hours. The hydrogen storage is scaled to store all hydrogen produced if the electrolyzer operates at full capacity for 24 consecutive hours.

[6]Source: https://energinet.dk/El/Elmarkedet/Tariffer/Aktuelle-tariffer/

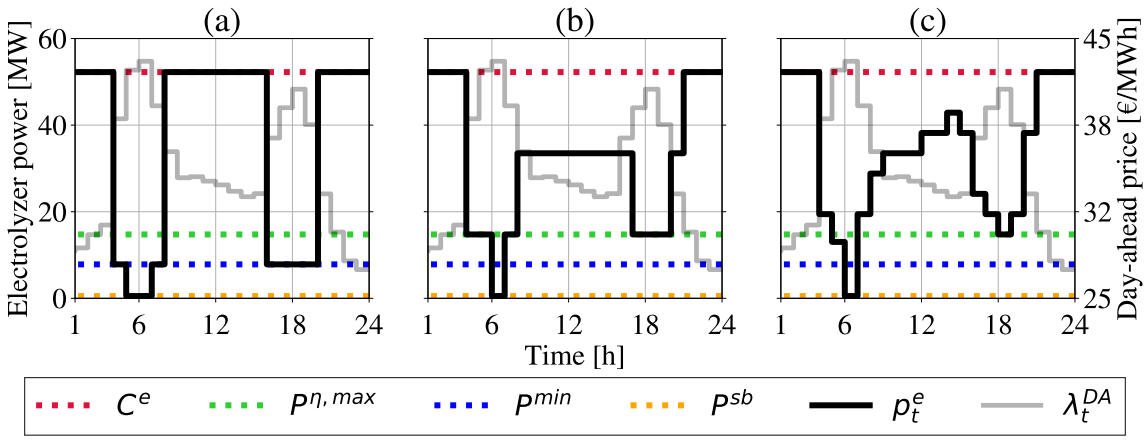

Figure 3: The power consumption schedule of the electrolyzer (p_t^e) in an example high-wind day when its hydrogen production curve is linearized by (a) 1, (b) 4, and (c) 12 segments. These three plots, from left to right, correspond to cases OOS-1, OOS-4, and OOS-12, respectively.

4.2 Impact of the Number of Segments

Let us consider the OOS case with three states, for which we solve the proposed MILP (5)-(28). We start with OOS-1, where $|\mathcal{S}| = 1$. This means the original non-linear hydrogen production curve, depicted in Fig. 1(b), is approximated by a single linear curve. Here, the minimum power consumption $P^{\min}$ and the capacity C^e of the electrolyzer are taken as two endpoints. By moving to OOS-2, where the number of segments $|\mathcal{S}|$ is 2, we consider an additional point $P^{\eta,\max}$, which refers to the power consumption level corresponding to the peak in the efficiency curve in Fig. 1(a). By increasing $|\mathcal{S}|$ to 4, and then to 8, the mean load value between existing points is added, splitting one segment into two. The same procedure but only on the right side of $P^{\eta,\max}$ is applied when we move from OOS-8 to OOS-12, as this side covers over around 70% of the feasible operating range. With the adoption of this procedure, all cases from OOS-2 to OOS-12 include the point $P^{\eta,\max}$. In addition, points are not removed when refining the discretization. By adding more segments, the hydrogen production curve and thus the electrolyzer efficiency with partial loading is more accurately represented.

The increase in the number of segments $|\mathcal{S}|$ enables the electrolyzer to consume power more flexibly, as depicted in Fig. 3, where the optimal power consumption schedule of the electrolyzer for one example day of the year is shown for three different numbers of segments (1, 4, and 12). It is observed that when the optimal power consumption of the electrolyzer is not constrained by wind production shortage, as on the chosen day, the optimal consumption level is always one of the piecewise linearization points. There are instances, e.g., hour 5 in Fig. 3, where OOS-1 goes into the standby state as the day-ahead price is too high for profitable hydrogen production. In contrast, OOS-4 and OOS-12 continue the operation in the on state, but at the power consumption level corresponding to the maximum efficiency, where hydrogen production is still profitable.

The number of segments $|\mathcal{S}|$ plays an important role in the optimal dispatch decision when the day-ahead price lies within a specific *price range*. The lower bound of this price range is the price below which, for any set of segments $\mathcal{S}$, the optimal dispatch decision is always the maximum electrolyzer consumption. The upper bound is the price after which, for any set of segments $\mathcal{S}$, the electrolyzer is in standby or off state. These bounds are calculated based on the electrolyzer

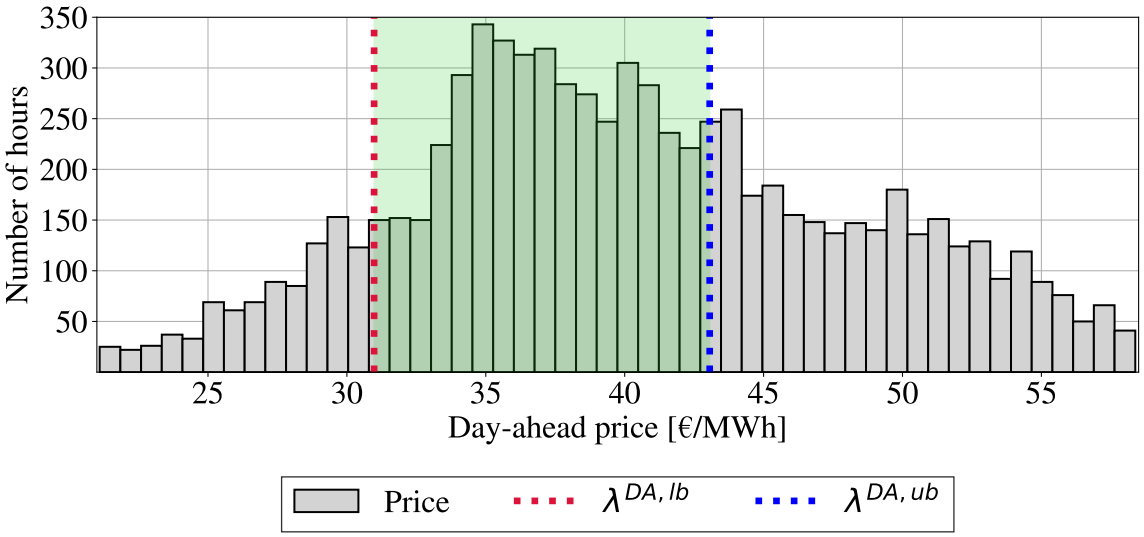

Figure 4: Histogram of day-ahead hourly electricity prices for year 2019 in DK2 (only the prices between the 5% and 95% quantiles are shown). Prices $\lambda^{\mathrm{DA,lb}}$ and $\lambda^{\mathrm{DA,ub}}$ (defined in the Appendix) are respectively the lower and upper bound of the price range (shaded green area) where different choices of linearization segments lead to different optimal dispatch decisions.

efficiency curve, standby power consumption, and hydrogen price, as explained in the Appendix. Fig. 4 shows the distribution of day-ahead hourly prices for year 2019 in DK2 with the bounds of the price range of interest marked by the red and blue dotted lines. If the day-ahead price of a given hour lies inside this price range (green shaded in Fig. 4), different dispatch decisions are taken by MILP models with different choice and number of segments. If the day-ahead price lies outside of this range, the dispatch decision for any number of segments would be the same (i.e., produce at maximum load or cease the production) and there would be no added value of a detailed production curve. This will be further investigated in Section 4.6.

4.3 Impact of the States

We consider three cases OOS, OO, and OS, each for both 1 and 12 segments. Recall that their corresponding MILPs are different[7]. Comparing the results of MILPs with the same number of segments, we observe OS and OOS perform almost equally, as observed in Fig. 5. The reason for this is the low frequency of consecutive hours of too high day-ahead prices, where a complete shut-off would be preferred over the standby state. Over 8,760 hours, OOS-1 starts up only 2 times, with a total of 286 hours offline. The difference in results obtained for OS and OOS increases if a higher standby power consumption or lower cold start-up cost for the electrolyzer is assumed, which would lead to more frequent shut-offs. On the contrary, OO earns the lowest profit, mainly due to the high start-up cost, which decreases the operational flexibility as even a short pause in production incurs a high cost.

[7]While we solve the proposed MILP (5)-(28) for OOS, the MILPs presented in [15] are solved for OO and OS, respectively.

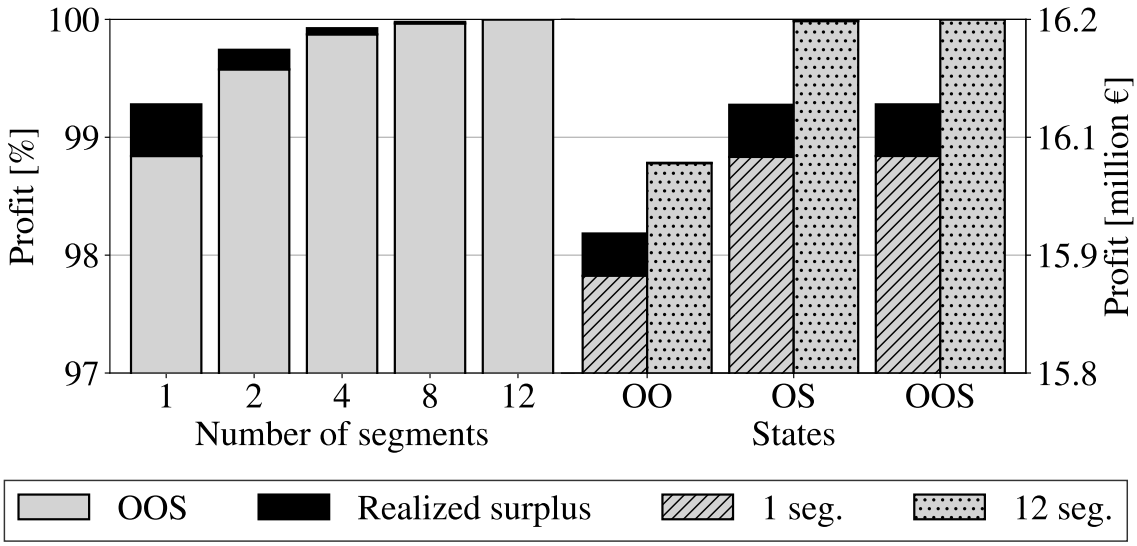

Figure 5: Estimated and realized surplus profit. The first five bars from the left correspond to OOS-1 to OOS-12. The next six bars show the results for OO-1, OO-12, OS-1, OS-12, OOS-1, and OOS-12, respectively. The right vertical axis is the profit in million €, whereas the left vertical axis is the relative profit in % in comparison to the highest profit achieved by OOS-12.

4.4 Ex-post Performance Analysis

Recall that three MILPs solve the problem based on the linearized hydrogen curve. Through the following ex-post performance analysis, it is seen that this leads to both sub-optimal dispatch decisions and an underestimation of the *true* amount of hydrogen produced. We have already observed in Fig. 1(b) that the linearized red curve is below the original black non-linear hydrogen production curve, implying that the hydrogen production might be underestimated. This means that we can expect to produce more hydrogen than what MILPs calculate. Such a difference is expected to be reduced by using more segments $|\mathcal{S}|$ to approximate the original non-linear hydrogen production curve.

Pursuing a fair comparison among models, we conduct an ex-post performance analysis. Once the MILPs are solved and the optimal power consumption $p_t^{e^*}$ of the electrolyzer obtained, we re-calculate the *true* amount of hydrogen produced based on the original non-linear hydrogen production curve. Note that we do not re-optimize the problem[8]. We refer to the amount of extra hydrogen and its corresponding profit as "realized surplus". We assume that all extra hydrogen is sold at the same constant price, i.e., €2.10/kg.

Fig. 5 provides the *estimated* and *realized surplus* profit among different cases. The estimated profit (gray area) is the optimal value obtained for the objective function of the corresponding MILP, while the realized profit (dark area), calculated ex-post, takes into account the profit of selling extra hydrogen. Similarly, Fig. 6 shows the total estimated and realized surplus hydrogen produced. Note that the compressor would need to consume more power ($\sim$ 1 MWh/ton) due to extra hydrogen.

[8]To avoid re-optimization, we assume the extra hydrogen is directly sold to the demand and is not stored in the hydrogen storage. Otherwise, one needs to re-optimize a posteriori to optimize the operation of storage and compressor.

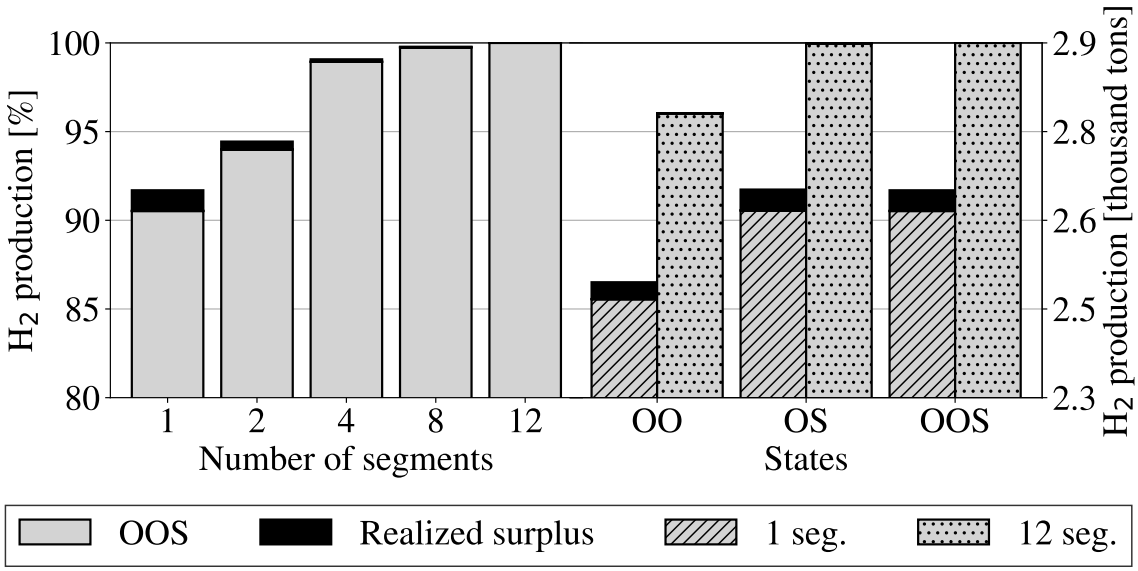

Figure 6: Estimated and realized surplus hydrogen produced. The first five bars from the left correspond to OOS-1 to OOS-12. The next six bars show the results for OO-1, OO-12, OS-1, OS-12, OOS-1, and OOS-12, respectively.

We draw two conclusions from Fig. 5 and 6:

(1) *Realized surplus*: This surplus for profit and hydrogen production is reduced by increasing the number of segments, due to the improved approximation of the original non-linear curve. The realized surplus profit decreases from €71,199 (0.44%) for OOS-1 to €602 (below 0.01%) for OOS-12. Similarly, the hydrogen production surplus is significantly decreased, yielding a realized surplus of $\sim$ 34 tons (1.27%) for OOS-1 and only 0.3 tons (0.01%) for OOS-12. By choosing a low number of segments, the hydrogen production is underestimated which may lead to logistic issues and inefficiencies in the real-life operation of the hybrid power plant.

(2) *Ex-post profit and hydrogen production*: Adding more electrolyzer details (segments or/and states) always leads to an increase in the ex-post profit. To compare various models, OOS-12 is taken as a benchmark, as it leads to the highest profit. First, the impact of the number of segments is examined, while keeping the number of states fixed and equal to 3. The ex-post profit reduction applying 1 instead of 12 segments is 0.72%, corresponding to around 117.6 k€ for the entire hybrid power plant. The ex-post hydrogen production is increased by 8.32%, corresponding to around 241 tons. This percentage deviation is notably higher in part because the increase in hydrogen profit is dampened by the reduction in electricity profit (3.86% electricity profit increase for 1 segment compared to 12 segments). For OOS-1, the profit share of selling hydrogen is much lower than the profit share of selling electricity (around 34%). By introducing more segments, the contribution of hydrogen sales is increased to 38% at the expense of electricity sales. More profit and different business models are therefore unlocked by including more electrolyzer details in the MILP formulation. Fig. 5 and 6 show that the errors are considerably reduced by implementing 4 segments instead of 1. Second, we assess the impact of the states on the ex-post profit and hydrogen production. While OS performs just as well as OOS as described in Section 4.3, OO with 12 segments results in a 1.22% lower ex-post profit, and in a 4% lower hydrogen production. For OO-1, a profit

Table 2: Computational aspects

Case	Computational time [s]	No. of binary variables
OS-1	1.4	2×8760
OS-12	12.7	13×8760
OOS-1	137.8	5×8760
OOS-2	135.8	6×8760
OOS-4	236.3	8×8760
OOS-8	350.3	12×8760
OOS-12	473.7	16×8760
OO-1	767.1	3×8760
OO-12	1,763.1	14×8760

reduction of around 1.8% and a reduced hydrogen production of 13.5% are observed, compared to the benchmark. Finally, we observe that neglecting the standby state in the model formulation leads to the worst outcome in terms of profit and hydrogen production potential.

4.5 Computational Analysis

All MILPs have been solved using the Gurobi solver in Julia on a MacBook Pro M1 2020 with 16 GB RAM. The optimality gap is fixed to 0.01% when we solve every MILP. The increase in the number of linearization segments $|\mathcal{S}|$ leads to an increase in computational time due to introducing more binary variables. For OOS, the computational time is increased from 138 seconds for 1 segment to 474 seconds for 12 segments, as reported in Fig. 2. Removing the off state significantly reduces the computational time, with OS-1 being by far the fastest MILP to be solved (1.4 seconds). The OO models require the highest computational time, although they embody fewer binary variables than their OS and OOS counterparts. We hypothesize the reason is that the start-up cost constraints with inter-temporal nature are more often active when the option of standby state is not present. Therefore, we do not recommend using OO as its corresponding profit is the lowest among all cases (Fig. 5), and it is being solved comparatively slower. Further, if computational efficiency is crucial, it may be beneficial to neglect the off state and run the OS model for improved computational performances. In general, the computational time increases with the number of segments but is deemed reasonable for the OS and OOS models, considering that our optimization problem is run over 8,760 hours. As operational problems are typically solved for a shorter time horizon, e.g., 24 hours for day-ahead scheduling, the computational cost of adding more details to the electrolyzer would be minimal.

4.6 Sensitivity Analysis with Respect to Input Data

In the previous sections, we have shown that adopting a simplified electrolyzer model can lead to an underestimation of the profit and hydrogen production for the hybrid power plant. We have also shown that the benefit of added details is case-specific, and depends on the input parameters. We now aim at assessing the impact of input parameters and system configuration on these results, through a sensitivity analysis. In particular, we will focus on wind over electrolyzer capacity ratio, hydrogen demand over electrolyzer capacity ratio, and the hydrogen price. The sensitivity analysis is performed on the OOS-1 and OOS-12 models.

Wind size

Recall from Fig. 1 that the wind farm capacity is 2 times that of the electrolyzer. To assess the impact of the wind-to-electrolyzer capacity ratio, two additional cases are considered, under which such a ratio is 1, 2 (reference), and 8. When this ratio is reduced from 2 to 1, the number of hours where the power input to the electrolyzer is limited by the wind availability is increased from 5,326 to all hours. Conversely, when the ratio is increased from 2 to 8, the number of power-limited hours is reduced to 1,236. We observe that the realized surplus for hydrogen production increases with the number of hours with limited wind power. The reason for this is that the piecewise approximation is exact only on the linearization points, and the limited wind availability forces the electrolyzer to operate out of those points. Conversely, when the number of wind power-limited hours is reduced, the electrolyzer operates more often on the linearization points, where the approximation is exact. It follows that the underestimation of hydrogen production is greater the more the electrolyzer is limited from operating at the linearization points. With a wind-to-electrolyzer ratio of 1, the difference in ex-post hydrogen production between 1 and 12 segments is 13%, which is reduced to 3% when the ratio increases to 8. Therefore, incorporating electrolyzer details is crucial for hybrid power plants where the wind-to-electrolyzer capacity ratio is small.

Hydrogen demand size

To investigate the sensitivity of optimization outcomes with respect to the hydrogen demand, the minimum daily demand is doubled, corresponding to around 8 full-load hours of hydrogen production. We observe that the impact of adding more segments to the electrolyzer production curve diminishes when the demand constraint is tighter, i.e., with a higher minimum daily demand. For the case with the reference demand, the difference between the ex-post profit for OOS-12 and OOS-1 is 8%. This difference, when the hydrogen demand is doubled, is reduced to 2%. The increase in demand forces the electrolyzer to operate more frequently at its maximum load, where both OOS-1 and OOS-12 share the same linearization point and efficiency.

Hydrogen price

To explore the impact of the hydrogen price, we increase it from €2.1/kg to €5/kg. As already discussed in Section 4.2, adding more segments impact the optimal solution and profit as long as the electricity price in the given hour is in the range $[\lambda^{\mathrm{DA,lb}}, \lambda^{\mathrm{DA,ub}}]$, shown in Fig. 4. Since $\lambda^{\mathrm{DA,lb}}$ and $\lambda^{\mathrm{DA,ub}}$ are proportional to the hydrogen price, by increasing the hydrogen price, the range is moved towards higher electricity prices, where the frequency of occurrence is reduced. When the MILP is solved with the hydrogen price of €5/kg, it is more frequently optimal to operate the electrolyzer at full load (39% of the time, compared to 11% for the case with the hydrogen price of €2.1/kg) and the linearization segments are utilized less. This also results in a significantly decreased computational time (below 20 seconds for OOS-12). The profit contribution from the hydrogen sale is increased significantly to 92%. The ex-post profit and hydrogen production difference between OOS-1 and OOS-12 are reduced to 0.01% and 0.03%, respectively (they are 0.72% and 8.32% for the €2.1/kg case).

The modeling of segments is relevant if higher hydrogen prices are coupled with also higher electricity prices. In this way, the electricity price range $[\lambda^{\mathrm{DA,lb}}, \lambda^{\mathrm{DA,ub}}]$ would still be overlapping with the majority of day-ahead price occurrences. For example, we test an artificial case where the day-ahead electricity price time series was multiplied by a constant factor to increase the mean price to around €90/MWh (similar to the mean value for 2021 in DK2). In this case, with the hydrogen price of €5/kg, similar results to the 2019 test case with the hydrogen price of €2.1/kg were obtained

in terms of the impact of the number of segments. For a given hydrogen price and efficiency curve, checking if the price range $[\lambda^{\mathrm{DA,lb}}, \lambda^{\mathrm{DA,ub}}]$ overlaps with the expected electricity price is therefore crucial to assess a priori the impact of choosing a simplified model for the production curve (e.g., 1 linearization segment only) and support the modeling choices.

5 Discussion and Conclusion

Several studies have focused on the optimal dispatch of hybrid renewable-hydrogen power plants assuming simplified models for the electrolyzer component. This paper investigates the impact of choosing different levels of operational details for the electrolyzer model on the dispatch decisions, profit, the amount of hydrogen produced, and computational time. The impact of two modeling choices is considered: the operating states (on, off, standby), and the number of segments used to linearize the hydrogen production curve. The problems are formulated as MILPs, where the number of binary variables depends on the number of states and segments.

For fixed states, adding more linearization segments for approximating the hydrogen production curve results in a higher profit, and a reduced surplus in the ex-post profit calculation, meaning that the model is able to estimate the actual cost and revenue streams more accurately. Moreover, a better estimation of the produced hydrogen is achieved. In fact, the linearization results in an underestimation of the produced hydrogen, but the underestimation is reduced by increasing the number of segments. Apart from introducing errors in the actual realized profit, thus potentially impacting the investment decisions in these types of technologies, the systematic underestimation of the hydrogen produced by the electrolyzer might introduce logistical inefficiencies, e.g., truck scheduling, and storage discharging/filling.

The impact of adding more piecewise segments to the hydrogen production curve depends on the distribution of day-ahead electricity prices in the given time horizon. The model formulations with 1 and 12 segments take significantly different dispatch decisions when the day-ahead electricity price is within a certain range, which depends on the electrolyzer efficiency (minimum and maximum) and the hydrogen price. Out of this day-ahead electricity price range, the model with 1 and 12 segments takes the same dispatch decisions. Therefore, the value of adding more details to the hydrogen production curve could differ by varying input data and case studies. It is observed that this value decreases when the electrolyzer operates less at partial loading, e.g. when the input power is less limited by available wind power or with high-demand constraints. In this paper, revenues from other than the day-ahead market are not considered but this may also impact the dispatch strategy and therefore benefit from more segments.

Choosing to represent only on and off states leads to the highest profit underestimation and worst ex-post performance while modeling only on and standby states lead to similar profit and dispatch decisions to the three-state model. This result is, however, significantly affected by the assumption made on the standby power consumption of the electrolyzer and its start-up cost. These parameters are highly uncertain due to the lack of data on large-scale electrolyzers.

In conclusion, adopting more simplified models for the electrolyzer always leads to a reduced profit and sub-optimal scheduling. However, the impact of adding more details may vary depending on the case study considered and especially the range of day-ahead electricity prices, hydrogen price, wind power production compared to the electrolyzer installed capacity, standby power consumption, and start-up cost. Among all considered models, the most complete one (three states with 12 segments) was solved for a 1-year horizon in less than 10 minutes. The increase in computational time by adding more details would be marginal if a day-ahead scheduling problem is considered instead. Moreover, reducing the three-state model to two states only is not always faster, as it

was observed that the two-state on-off model with 12 segments was the longest to solve among all the cases considered. A more detailed representation of the electrolyzers should be preferred for operational problems. For investment problems, we hypothesize that it may be adequate to adopt a more simplified model of the electrolyzer, but this should be further assessed and it was out of the scope of the current paper.

Further research should be conducted to assess the impact of modeling choices when additional revenue streams are considered, such as flexibility provisions in ancillary service markets, which may impact the dispatch decisions of the hybrid power plant.

The Value of Ancillary Services for Electolyzers

1 Introduction

Electrolyzers and in general power-to-X facilities are envisioned as key elements for green transition, as a solution to electrify hard-to-abate sectors including heavy transport and energy-intensive industry [2]. Converting power to hydrogen and then to green fuels also facilitates technically and financially the realization of ambitious projects such as two energy islands in the Baltic and North Seas, each with 3-GW offshore wind capacity in the first stage, and more in the longer run [22]. Besides, in future renewable-based power systems with flexibility scarcity, electrolyzers as flexible power loads can considerably contribute to flexibility provision. Among others, one main barrier against the rapid integration of electrolyzers is uncertainty regarding their long-term profitability [3].

Aiming to accelerate the integration of electrolyzers, this paper provides a value analysis on how much more an electrolyzer in Denmark could have earned in 2021 and 2022 by the provision of ancillary services. Among others, we consider frequency containment reserve (FCR) and manual frequency restoration reserve (mFRR) services, since there are mature markets for these services in Denmark with relatively high prices. The ability of electrolyzers to provide FCR as a fast service is investigated in [23], concluding that electrolyzers might have even faster response times than conventional generators for both upwards and downward regulation. The value analysis requires the accurate modeling of the physics of the electrolyzer as well as developing a bidding strategy model, enabling the profit-maximizing electrolyzer to optimally participate in day-ahead electricity, FCR, and mFRR markets, besides its business in the hydrogen sector. For this purpose, we develop a mixed-integer linear optimization model with a set of activation-aware constraints, which is critical in the case of an energy-intensive service such as mFRR.

The current literature on the value analysis of ancillary services for electrolyzers is limited. In the discussion paper [24] by the Danish transmission system operator (TSO), Energinet, such a value is analyzed with a simple power-to-hydrogen conversion factor, discarding physical characteristics of electrolyzers and the effect of service activation on hydrogen production. A value estimation of the FCR services for an electrolyzer in the Nordic synchronous region (DK2) is conducted in [25], where a detailed model of the electrolyzer physics is adopted, showing that FCR participation could account for 72% of the total electrolyzer revenues. However, the activation of reserves is not accounted for as no energy-intensive reserve products are considered. Similarly, [26] and [27] investigate the economic feasibility of ancillary service provision for an electrolyzer located in France and Germany, respectively, again without accounting for activation. Finally, [28] conducts an economic evaluation of an electrolyzer which enforces through chance constraints that the activated reserve will not

exceed the capacity with a high probability. However, it allows the electrolyzer to overbid reserves, relying on the assumption of having an accurate probabilistic forecasting of the reserve activation. This paper proposes a *pragmatic* activation-aware approach for the participation of electrolyzers in ancillary service markets.

The rest of the paper is structured as follows: Section 2 describes the physics of electrolyzers and explains the target markets. Section 3 provides the bidding strategy model. Section 4 presents the numerical results. Finally, Section 5 concludes the paper.

2 Preliminaries

We describe the electrolyzer physics and target markets.

2.1 Electrolyzers

Electrolyzers are electrochemical assets that consume power and water, splitting the water molecules into oxygen and hydrogen. We limit our focus on conventional electrolysis technologies such as alkaline and polymer electrolyte membrane In reality, the electrolyzer efficiency is a non-linear function of the consumed power, with a peak efficiency at around 30% nominal loading. To avoid a non-linear model while accurately representing the physics of the electrolyzer, we apply an electrolyzer model as proposed by [29], where the hydrogen production curve is approximated by a *piece-wise linear function*, at the cost of adding a set of binary variables.

Furthermore, electrolyzers are subject to three separate *operational states*, namely online, standby, and off. In the online state, the electrolyzer produces hydrogen and consumes electricity. Due to safety concerns, this state has a minimum loading of around 10%. In the standby state, the electrolyzer is not producing hydrogen, but consuming a small amount of electrical energy to maintain the ability to resume hydrogen production and transition into the online state within seconds or minutes. Finally, in the off state, the system is shut off completely, no longer consuming electricity nor producing hydrogen. Once the electrolyzer enters this state, it requires up to a couple of hours to transition to the online state.

2.2 Bilateral Contracts and Target Markets

The produced hydrogen is assumed to be sold through bilateral hydrogen purchase agreements (HPAs) at a fixed hydrogen price, as no market for hydrogen currently exists. In our formulation, the hydrogen demand is represented through a set of tube-trailers that arrive on-site and depart at a given daily schedule. When a tube-trailer has arrived on-site, it functions as a gas storage, with a storage capacity that must be respected. Further, if no tube-trailer is present on-site, or any present tube-trailer is full, the system cannot produce hydrogen as there is no off-take possibility. Another important aspect of the HPA is the possibility of a minimum demand requirement over a given time period, for example daily. This requirement provides certainty for the off-taker but may add operational challenges to the producer, obliging them to produce under unprofitable price conditions.

As reported in the Energinet report [24], electrolyzers are expected to operate in multiple frequency-supporting ancillary service markets, bringing an opportunity for additional revenue streams[9]. In addition, electrolyzers must participate in the day-ahead electricity market to procure electricity,

[9]The automatic FRR (aFRR) market is disregarded as its procurement in Denmark follows a pay-as-bid scheme with monthly auctions [30].

if not being (sufficiently) supplied by co-located wind or solar units. Note that the recent renewable fuels of non-biological origin (RFNBO) delegated act by the European Commission [31] defines certain operational conditions under which electrolyzers producing green hydrogen are allowed to directly buy power from the grid. This paper considers a single electrolyzer only, without being combined with wind turbines or other renewable assets. Therefore, the electrolyzer buys all power it requires from the grid, discarding RFNBO conditions. Now, we briefly describe target markets for electrolyzers in chronological order of market closure time in Denmark.

FCR market: In the Continental Europe synchronous area including the Danish bidding zone DK1, FCR, also known as primary reserve, is the fastest frequency service — note that it is not the case in the Nordic synchronous area, including the other Danish bidding zone, i.e., DK2. The FCR capacity market is a mechanism used to stabilize the electricity grid by providing a reserve of power that can be automatically activated within seconds in response to changes in frequency. The product is symmetric, meaning that a placed bid is identical both for upward and downward regulation. In DK1, the FCR market closes at 8 AM the day before delivery, and bids can be placed for every 4-hour blocks. The market is operated with uniform pricing. In all target markets, it is assumed that the electrolyzer is price-taker. Therefore, the electrolyzer forecasts the FCR price and decides to bid a reserve quantity accordingly. By this, the decision variable is the quantity bid. The forecasted price together with the quantity bid form the final bid of the electrolyzer to be placed.

mFRR market: The product being traded in this market is the reserved capacity for manual frequency services, also known as tertiary reserve. The mFRR market is a mechanism used to ensure sufficient capacities to balance electricity supply and demand in real time. It is a reserve that can be activated within 15 minutes in response to imbalances in the system. The market is split into two separate auctions for the procurement of the reserve capacity and the energy activation of the reserve. First, the mFRR market is closed at 9:30 AM the day before delivery. Bids placed consist of quantity in terms of reserved capacity for every 1-hour interval, and a price per MW per hour. The market is settled with uniform pricing. Once a reserve bid is accepted, the electrolyzer is obliged to submit a corresponding regulation bid (a price) for the energy activation of the reserve into the balancing market. Whenever needed, bids are activated following the merit order curve, and activation is remunerated with the uniform balancing price.

Day-ahead electricity market: The electrolyzer places bids for quantity and price to procure electricity for the following day. A separate bid consisting of the forecasted day-ahead price and a quantity can be placed for each hour. In Denmark, the day-ahead market gate closure is at noon the day before delivery, and is settled with uniform pricing. The day-ahead bid should respect the reserve bids placed in the FCR and mFRR markets. We assume that there is no information gain between the different gate closure times, and therefore that all bids can be placed simultaneously.

3 Model Formulation

Notational remark: Hereafter, lower-case symbols are variables, whereas upper-case and Greek symbols are parameters. In addition, symbol z is used for various binary variables.

3.1 Electrolyzer Profit

This section presents a deterministic mixed-integer linear programming (MILP) problem, maximizing the total profit of an electrolyzer operating in the day-ahead, FCR, and mFRR markets, while selling hydrogen at a fixed price with a minimum production requirement. The profit-maximizing

objective function reads as

$$\max_{\mathcal{X}} \sum_{t\in\mathcal{T}} \left(h_t^{\mathrm{e}} \lambda_t^{\mathrm{h}} + p_t^{\mathrm{m}\uparrow} \lambda_t^{\mathrm{m}\uparrow} + p_t^{\mathrm{m}\downarrow} \lambda_t^{\mathrm{m}\downarrow} - p_t^{\mathrm{DA}} \lambda_t^{\mathrm{DA}} \right) + \sum_{i\in\mathcal{I}} p_i^{\mathrm{F}} \lambda_i^{\mathrm{F}} \Delta T^{\mathrm{F}}, \tag{29}$$

where $\mathcal{X}$ is the set of variables, and will be defined later at the end of this section. While index $t \in \mathcal{T}$ represents 1-hour time intervals, $i \in \mathcal{I}$ denotes 4-hour periods. Both these indexes are needed to model the FCR market. The first term in (29) is the revenue of selling hydrogen, which is the product of hydrogen production h_t^{e} and the fixed hydrogen price λ^{h}. The mFRR capacity bids (second and third terms) are split into that of the upward $p_t^{\mathrm{m}\uparrow}$ and downward $p_t^{\mathrm{m}\downarrow}$ reserves to be sold at forecasted prices $\lambda_t^{\mathrm{m}\uparrow}$ and $\lambda_t^{\mathrm{m}\downarrow}$, respectively. The fourth term represents the cost of procuring power from the day-ahead market, including the quantity bid p_t^{DA} and forecasted price λ_t^{DA}. Finally, the last term corresponds to the profit of selling FCR capacity, where the quantity p_i^{F} is placed for a 4-hour interval i at forecasted price λ_i^{F}, where $\Delta T^{\mathrm{F}} = 4$. At the time of the bidding decisions, it is complicated to provide accurate forecasts for hourly balancing prices of the day of delivery. Therefore, we neglect the potential revenues/costs from activation in real time, and maximize the total profit to be earned in the day-ahead stage only.

We can categorize constraints in the three strands of electrolyzer, bidding, and activation constraints, which will be given in the next three subsections.

3.2 Electrolyzer Constraints

The electrolyzer is modeled with a varying efficiency level, depending on the operational point, via a piece-wise formulation of the hydrogen production curve. We also model its three operational states, as already explained in Section 2.1.

Piece-wise hydrogen production curve: Each segment s on the production curve is defined within a range of electrolyzer consumption power, i.e., $\underline{P}_s$ and $\overline{P}_s$. These segments are activated based on the scheduled electrolyzer power consumption $p_{t,s}^{\mathrm{e}}$, if no reserves are activated:

$$\underline{P}_s z_{t,s}^{\mathrm{e}} \le p_{t,s}^{\mathrm{e}} \le \overline{P}_s z_{t,s}^{\mathrm{e}} \qquad \forall t \in \mathcal{T}, s \in \mathcal{S}, \tag{30a}$$

where $z_{t,s}^{\mathrm{e}}$ is a binary variable for the segment selection. The rationale of using these binary variables is that the concave relaxation is no longer tight due to the presence of reserve revenues in the objective function. Further, we should ensure that at most one segment can be active at any time, i.e.,

$$\sum_{s\in\mathcal{S}} z_{t,s}^{\mathrm{e}} \le 1 \qquad \forall t \in \mathcal{T}. \tag{30b}$$

The hydrogen production h_t^{e} is defined as a linear function of the electrolyzer power consumption $p_{t,s}^{\mathrm{e}}$, with a slope A_s and intercept B_s depending on the active segment, i.e.,

$$h_t^{\mathrm{e}} = \sum_{s\in\mathcal{S}} \left(A_s p_{t,s}^{\mathrm{e}} + B_s z_{t,s}^{\mathrm{e}} \right) \Delta_{\mathrm{T}} \qquad \forall t \in \mathcal{T}, \tag{30c}$$

where $\Delta_{\mathrm{T}} = 1$. For a coherent formulation, an auxiliary variable p_t^{tot} is defined, representing the total power consumption across segments at any time period t:

$$p_t^{\mathrm{tot}} = \sum_{s\in\mathcal{S}} p_{t,s}^{\mathrm{e}} \qquad \forall t \in \mathcal{T}. \tag{30d}$$

Operating states: The three operating states of the electrolyzer are defined by one binary variable each, i.e., z_t^{on}, z_t^{sb}, and z_t^{off}. The online state z_t^{on} is defined so that hydrogen production occurs in the online state only:

$$z_t^{\text{on}} = \sum_{s \in \mathcal{S}} z_{t,s}^{\text{e}} \qquad \forall t \in \mathcal{T}. \tag{30e}$$

It is also possible to define the online state as the sum of all segment selection variables without defining a new binary variable, but it is here defined for clarity. The standby state z_t^{sb} is defined as

$$p_t^{\text{sb}} = z_t^{\text{sb}} P^{\text{sb}} \qquad \forall t \in \mathcal{T}, \tag{30f}$$

stating that there is no hydrogen production, but the electrolyzer is still consuming power p_t^{sb} to keep the system pressurized and heated for quick start-up of the production. The power consumption is assumed constant at P^{sb}. In case of a complete shut down of the electrolyzer and surrounding system z_t^{off}, there is a minimum down-time required due to the time it takes to re-heat and pressurize the system. The down time is defined by the t-dependent set $\mathcal{N}_t$ as

$$z_t^{\text{off}} - z_{t-1}^{\text{off}} \leq z_n^{\text{off}} \qquad \forall t \in \mathcal{T} \setminus \{1\}, n \in \mathcal{N}_t, \tag{30g}$$

where $\mathcal{N}_t$ is defined as the N^{down} next periods from t. Finally, the electrolyzer must only be in one state at any time, i.e.,

$$z_t^{\text{on}} + z_t^{\text{sb}} + z_t^{\text{off}} = 1 \qquad \forall t \in \mathcal{T}. \tag{30h}$$

3.3 Bidding Constraints

The bids into the day-ahead, FCR, and mFRR capacity markets are all limited by the scheduled electrolyzer consumption and power capacity.

Day-ahead quantity bids: It is defined as the total scheduled consumption of the electrolyzer, including the stand-by consumption:

$$p_t^{\text{DA}} = p_t^{\text{tot}} + p_t^{\text{sb}} \qquad \forall t \in \mathcal{T}. \tag{31a}$$

Note that the power consumption of the compressor is assumed to be embodied within the production curve of the electrolyzer, therefore it is not explicitly indicated in (31a).

Reserve quantity bids: As the FCR market is symmetric, i.e., the identical capacity p_i^{F} is reserved for activation in both directions, it must be limited both by the ability to up regulate and down regulate the power consumption of the electrolyzer. The mFRR reserve is, however, split between the upwards and downwards reserve, hence each reserve bid $p_t^{\text{m}\downarrow}$ and $p_t^{\text{m}\uparrow}$ is limited in its respective direction only. As the electrolyzer can participate in both markets simultaneously, it is the sum of reserves in each direction that is constrained. For the downward reserve, this is simply limited by the difference between the electrolyzer capacity C^{e} and the scheduled power consumption p_t^{tot}. Further, as the electrolyzer has a cold start time of up to 2 hours, the reserve cannot be provided if the electrolyzer is shut off. For the downward reserve we enforce

$$p_i^{\text{F}} + p_t^{\text{m}\downarrow} \leq C^{\text{e}}\left(1 - z_t^{\text{off}}\right) - p_t^{\text{tot}} \qquad \forall t \in \mathcal{T}_i, i \in \mathcal{I}, \tag{31b}$$

where $\mathcal{T}_i$ is the set of hours t within the 4-hour interval i. For the upward reserve, the total bids are limited by the difference in the scheduled power consumption and the minimum allowed electrolyzer power $\underline{E}$, i.e.,

$$p_i^{\text{F}} + p_t^{\text{m}\uparrow} \leq p_t^{\text{tot}} - \underline{E}\left(1 - z_t^{\text{off}}\right) \qquad \forall t \in \mathcal{T}_i, i \in \mathcal{I}, \tag{31c}$$

where the off-state binary variable is included to avoid infeasibility in the case of no consumption.

Minimum and maximum bid sizes: Both FCR and mFRR capacity markets operate with minimum and maximum allowed bid sizes. These limits are enforced by the following constraints, with the binary variable z_i^{F} enabling a FCR bid in the range of $\underline{P}^{\mathrm{F}}$ and $\overline{P}^{\mathrm{F}}$. The binary variables $z_t^{\mathrm{m}\uparrow}$ and $z_t^{\mathrm{m}\downarrow}$ serve similarly for the mFRR bids:

$$\underline{P}^{\mathrm{F}} z_i^{\mathrm{F}} \leq p_i^{\mathrm{F}} \leq \overline{P}^{\mathrm{F}} z_i^{\mathrm{F}} \qquad \forall i \in \mathcal{I} \tag{31d}$$

$$\underline{P}^{\mathrm{m}} z_t^{\mathrm{m}\downarrow} \leq p_t^{\mathrm{m}\downarrow} \leq \overline{P}^{\mathrm{m}} z_t^{\mathrm{m}\downarrow} \qquad \forall t \in \mathcal{T} \tag{31e}$$

$$\underline{P}^{\mathrm{m}} z_t^{\mathrm{m}\uparrow} \leq p_t^{\mathrm{m}\uparrow} \leq \overline{P}^{\mathrm{m}} z_t^{\mathrm{m}\uparrow} \qquad \forall t \in \mathcal{T}. \tag{31f}$$

3.4 Activation Constraints

The capacity reserved in ancillary service markets can be activated upon deviations of the grid frequency. This causes deviations in the hydrogen production, which might be infeasible in a system where there are upper and lower limits to the possible hydrogen off-take. For the FCR bids, it is assumed that the activation is symmetric in both directions, so that the total difference from the scheduled hydrogen production due to activation is negligible. For the mFRR bids, however, the activation could be energy-intensive, and a large deviation in the scheduled production could yield full tube-trailers or unmet minimum demand requirements. Assuming an expected upward mFRR activation $\alpha_t^{\mathrm{act}\uparrow}$ or a downward mFRR activation $\alpha_t^{\mathrm{act}\downarrow}$ at time period t, a set of constraints is defined to ensure that the capacity bids are feasible in terms of deviations in hydrogen production. Note that $\alpha_t^{\mathrm{act}(.)} = 1$ refers to the full capacity activation for one hour.

Upward mFRR activation: In this case, the actual power consumption $\sum_s p_{t,s}^{\mathrm{act}\uparrow}$ of the electrolyzer is defined as

$$\sum_{s \in \mathcal{S}} p_{t,s}^{\mathrm{act}\uparrow} = p_t^{\mathrm{tot}} - p_t^{\mathrm{m}\uparrow} \alpha_t^{\mathrm{act}\uparrow} \qquad \forall t \in \mathcal{T}. \tag{32a}$$

Let the binary variable $z_{t,s}^{\mathrm{act}\uparrow}$ define the range for where a segment on the production curve is active based on the activated power consumption. By this, we restrict $p_{t,s}^{\mathrm{act}\uparrow}$ by

$$\underline{P}_s z_{t,s}^{\mathrm{act}\uparrow} \leq p_{t,s}^{\mathrm{act}\uparrow} \leq \overline{P}_s z_{t,s}^{\mathrm{act}\uparrow} \qquad \forall t \in \mathcal{T}, s \in \mathcal{S}, \tag{32b}$$

while only one segment is allowed to be active:

$$\sum_{s \in \mathcal{S}} z_{t,s}^{\mathrm{act}\uparrow} \leq 1 \qquad \forall t \in \mathcal{T}. \tag{32c}$$

The actual hydrogen production following an upward activation can then be calculated based on the power consumption and corresponding segment on the production curve, i.e.,

$$h_t^{\mathrm{act}\uparrow} = \sum_{s \in \mathcal{S}} \left(A_s p_{t,s}^{\mathrm{act}\uparrow} + B_s z_{t,s}^{\mathrm{act}\uparrow} \right) \Delta_{\mathrm{T}} \qquad \forall t \in \mathcal{T}. \tag{32d}$$

Even if the full activation of mFRR occurs, the hydrogen production is still constrained by the minimum hydrogen demand $\underline{H}$ over time period $\mathcal{T}$, i.e.,

$$\sum_{t \in \mathcal{T}} h_t^{\mathrm{act}\uparrow} \geq \underline{H}. \qquad . \tag{32e}$$

Downward mFRR activation: In this case, the actual power consumption $\sum_s p_{t,s}^{\text{act}\downarrow}$ of the electrolyzer is defied as

$$\sum_{s\in\mathcal{S}} p_{t,s}^{\text{act}\downarrow} = p_t^{\text{tot}} + p_t^{\text{m}\downarrow}\alpha_t^{\text{act}\downarrow} \qquad \forall t \in \mathcal{T}. \tag{32f}$$

We define the binary variable $z_{t,s}^{\text{act}\downarrow}$ to indicate the corresponding production curve segment. Similar to the upward activation constraints, we enforce

$$\underline{P}_s z_{t,s}^{\text{act}\downarrow} \le p_{t,s}^{\text{act}\downarrow} \le \overline{P}_s z_{t,s}^{\text{act}\downarrow} \qquad \forall t \in \mathcal{T}, s \in \mathcal{S} \tag{32g}$$

$$\sum_{s\in\mathcal{S}} z_{t,s}^{\text{act}\downarrow} \le 1 \qquad \forall t \in \mathcal{T}. \tag{32h}$$

The actual hydrogen production following a downward activation can then be calculated as

$$h_t^{\text{act}\downarrow} = \sum_{s\in\mathcal{S}} (A_s p_{t,s}^{\text{act}\downarrow} + B_s z_{t,s}^{\text{act}\downarrow})\Delta_{\text{T}} \qquad \forall t \in \mathcal{T}. \tag{32i}$$

In this case, the additional hydrogen production should respect the upper limit of available capacity of tube-trailers on site. Let $d \in \mathcal{D}$ a set of tube-trailers. A set of auxiliary variables is defined tracking the dispensed hydrogen $h_{t,d}^{\text{d}}$ and state of tube-trailers for the activated hydrogen flow $s_{t,d}^{\text{d}}$. These flows are then constrained by the dispenser capacity C^{d}, the tube-trailer availability indicated by the binary parameter $Z_{t,d}$, and their capacity S^{d}:

$$h_t^{\text{act}\downarrow} = \sum_{d\in\mathcal{D}} h_{t,d}^{\text{d}} \qquad \forall t \in \mathcal{T} \tag{32j}$$

$$h_{t,d}^{\text{d}} \le C^{\text{d}} Z_{t,d} \qquad \forall t \in \mathcal{T}, d \in \mathcal{D} \tag{32k}$$

$$s_{t,d}^{\text{d}} = h_{t,d}^{\text{d}} \qquad \forall t = 1, d \in \mathcal{D} \tag{32l}$$

$$s_{t,d}^{\text{d}} = s_{t-1,d}^{\text{d}} + h_{t,d}^{\text{d}} \qquad \forall t \in \mathcal{T}\setminus\{1\}, d \in \mathcal{D} \tag{32m}$$

$$s_{t,d}^{\text{d}} \le S^{\text{d}} \qquad \forall t \in \mathcal{T}, d \in \mathcal{D}. \tag{32n}$$

With separate sets of constraints for upward and downward activated hydrogen flows, it is ensured that all market bids are feasible for any assumed expected activation. This is intrinsically a conservative approach, as activation in one direction can be fully or partially cancelled out by activation in the other, which is not accounted for in this formulation. However, accounting for this effect requires information regarding the timing and frequency of activation, as the number of *consecutive* hours of activation in one direction is of significance when constrained by tube trailer capacity and minimum demand requirements. An alternative approach is to only apply the activation constraints on the *net* activation. In the proposed formulation, the risk can be adjusted through the selection of expected activation, $\alpha_t^{\text{act}\uparrow}$ and $\alpha_t^{\text{act}\downarrow}$. If set to zero, the model does not take activation into account at all. If set to one, the bids are robust in terms of activation in any direction.

Now, we list variables as $\mathcal{X} = \{h_t^{\text{act}\uparrow}, h_t^{\text{act}\downarrow}, h_{t,d}^{\text{d}}, h_t^{\text{e}}, p_{t,s}^{\text{act}\uparrow}, p_{t,s}^{\text{act}\downarrow}, p_t^{\text{DA}}, p_{t,s}^{\text{e}}, p_i^{\text{F}}, p_t^{\text{m}\uparrow}, p_t^{\text{m}\downarrow}, p_t^{\text{sb}}, p_t^{\text{tot}}, s_{t,d}^{\text{d}}, z_{t,s}^{\text{act}\uparrow}, z_{t,s}^{\text{act}\downarrow}, z_{t,s}^{\text{e}}, z_i^{\text{F}}, z_t^{\text{m}\uparrow}, z_t^{\text{m}\downarrow}, z_t^{\text{off}}, z_t^{\text{on}}, z_t^{\text{sb}}\}$, where $\boldsymbol{z}$ is the set of binary variables, and the rest are non-negative continuous variables.

4 Numerical Study

We first explain our case studies and then provide numerical results. All input data and source codes are shared in [32].

Table 3: Price inputs for three case studies

	$\boldsymbol{\lambda^{h}}$ [EUR/kg]	**Other prices** $\boldsymbol{\lambda}$ [33, 34]
DK1 2021	10	Historical prices from DK1 in 2021
DK1 2022	10	Historical prices from DK1 in 2022
DK2 2022	10	Historical prices from DK2 in 2022

4.1 Description of Case Studies and Ex-post Analysis

We consider an electrolyzer of 10 MW, as this is the maximum bid size for the FCR and mFRR services in the Danish bidding zone DK1. For the purpose of the value analysis, it is assumed that all tube-trailers are exchanged at midnight, and are available all day. Further, we assume a daily demand of 2000 kg H_2, corresponding to approximately 50% of the daily production capacity of the electrolyzer.

Case studies: The MILP model (29)-(32) is applied to three different case studies, built upon historical prices in DK1 and DK2 in 2021 and 2022, summarized in Table 3. The first two case studies, namely DK1 2021 and DK1 2022, explore how offering ancillary services to the TSO changes the total profit of an electrolyzer operating in the DK1 zone. The reason for including the third case study, i.e., DK2 2022, is that the upward mFRR prices were relatively low in DK1 in the years 2021 and 2022, so we are interested in exploring DK2 with comparatively higher mFRR prices. Note that the Danish TSO, Energinet, has recently implemented a joint reserve market for DK1 and DK2. As further integration between the Nordic ancillary service markets is planned as part of the Nordic Balancing Model [30], it is deemed a reasonable assumption that mFRR prices will increase in DK1. Fig. 7 depicts the distribution of day-ahead, FCR[10] , and upward mFRR prices[11] in DK1 and DK2, corresponding to our three case studies. Four different model variations are applied to three case studies:

1. **No AS:** It stands for no ancillary services. This variation serves as a benchmark, wherein the electrolyzer only participates in the day-ahead market as a power consumer and sells hydrogen.

2. **Oracle:** This model serves as an *ideal* benchmark, where the electrolyzer participates in ancillary service markets with perfect foresight on the reserve activation. Hence, at the time of solving the MILP model (29)-(32), the electrolyzer perfectly knows the values of $\alpha_t^{\text{act}\uparrow}$ in (32a) and $\alpha_t^{\text{act}\downarrow}$ in (32f) for every hour t. This variation provides insight into the maximum potential profit (upper-bound) that the electrolyzer could have earned.

3. $\boldsymbol{\alpha = 0}$**:** In this variation we enforce $\alpha_t^{\text{act}\uparrow}$ in (32a) and $\alpha_t^{\text{act}\downarrow}$ in (32f) to be zero in the day-ahead stage. Here, the electrolyzer will still always respect the total capacity limits of the reserve, but assumes that there will be no change in the scheduled hydrogen production due to placed reserves. Therefore, any activation may challenge the hydrogen production plan and lead to infeasibility in the downstream processes. This could be a severe case if upward mFRR is significantly activated, requiring the electrolyzer to remarkably reduce the power consumption, thereby the risk of not fulfilling the minimum daily hydrogen production requirement. One may see this model variation pragmatic (not assuming any future knowledge of activation) but optimistic (assuming that the hydrogen schedule will not be compromised).

[10] For the DK2 case study, FCR-N prices are applied.
[11] The Danish TSO is currently not procuring downward mFRR capacities.

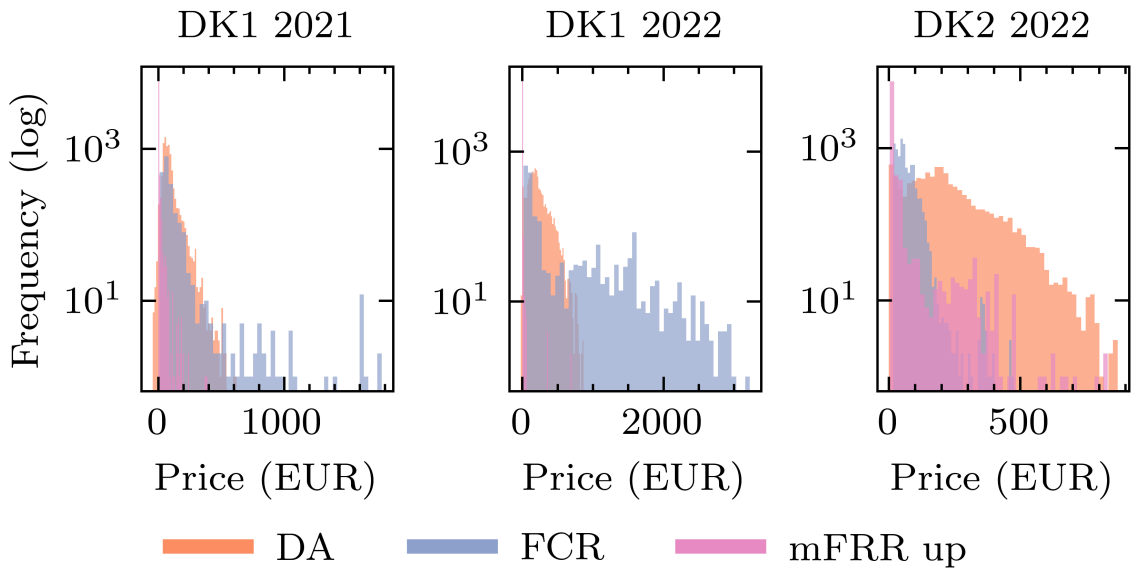

Figure 7: Distribution of day-ahead, FCR, and upward mFRR prices in DK1 and DK2 in 2021 and 2022.

4. $\boldsymbol{\alpha = 1}$**:** On the contrary, the electrolyzer here assumes the full mFRR activation will happen at every hour t. This variation is again pragmatic, but conservative.

Ex-post analysis: Three case studies and four model variations are compared ex-post, where the *true* realization of the reserve activation and balancing prices are revealed. See Fig. 8 for an overview of the ex-post analysis. Once the MILP model (29)-(32) is solved, we fix the mFRR and FCR capacity reservations and day-ahead schedules. The final profit of the electrolyzer in every day is calculated based on the *true* activation and the balancing prices realized. Recall that the true hydrogen production in model variations $\boldsymbol{\alpha = 0}$ and $\boldsymbol{\alpha = 1}$ might vary from their day-ahead schedule when we account for the true activation. We do not assume a penalty for any unmet hydrogen demand.

As explained in Section 2.2, after the mFRR capacity bids are accepted, the mFRR capacity providers are obliged to submit an activation price, the so-called regulation bid. The TSO activates mFRR reserves in the balancing stage according to the merit order principles, i.e., starting from cheapest regulation bids. Hence, for our ex-pots analysis, it can be assumed that if the electrolyzer places a regulation bid that is lower than the realized balancing price λ_t^{B}, the reserved capacity would have been activated. Further, it is assumed that the electrolyzer is price-taker and would place a regulation bid that is equal to the opportunity cost in the case of upward activation, i.e., the lost revenue from selling hydrogen. Assuming a constant efficiency $\bar{\eta}$ for the electrolyzer, this opportunity cost, and thereby the regulation bid, can be computed as $\bar{\eta}\lambda^{\mathrm{h}}$. We consider the same regulation bid for upward and downward activation. Finally, the activation would only occur if the power system experiences an imbalance. While the real activation of mFRR reserves occurs per 15-minute interval, the relevant historical data found is only given in hourly resolution [33]. It is therefore assumed that a capacity reserve is fully activated for a whole hour if the described conditions are fulfilled. The Danish TSO is currently procuring upwards mFRR reserves only, i.e. reserves for the case of a supply deficit in the system. Let $I_t < 0$ note a negative system imbalance.

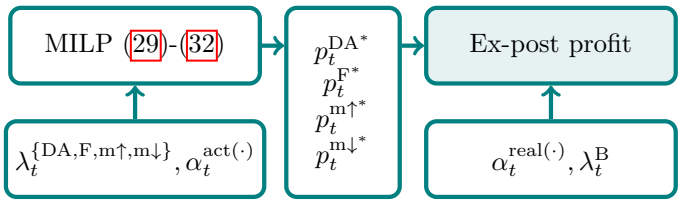

Figure 8: Overview of the ex-post analysis. Superscript * denotes the optimal day-ahead schedules.

The assumed *realized* upwards activation for every time period t is then

$$\alpha_t^{\mathrm{real}\uparrow} = \begin{cases} 1, & \text{if } \bar{\eta}\lambda^{\mathrm{h}} \leq \lambda_t^{\mathrm{B}} \text{ and } I_t < 0 \\ 0, & \text{otherwise.} \end{cases}$$

4.2 Results and Discussion

For the case studies DK1 2021 and DK2 2022, Fig. 9 shows the ex-post annual profit of the electrolyzer, whereas Fig. 10 depicts the cumulative FCR and upward mFRR capacities that the electrolyzer offers over a year. In both cases, particularly in DK2 2022, the participation of the electrolyzer in ancillary service markets could yield a manyfold in profits, largely due to very high FCR prices, peaking at around 3,000 EUR/MW in 2022 (see Fig. 7).

For DK1 2021, the profit in the oracle (upper bound) is around 57% higher than that in the case with no ancillary services. The interesting observation is that the profit in the pragmatic variations, i.e., $\boldsymbol{\alpha} = \mathbf{1}$ and $\boldsymbol{\alpha} = \mathbf{0}$, is not significantly lower than that in the oracle, as the main increase in profit arises form the FCR market. Further, it is seen that for the oracle and $\boldsymbol{\alpha} = \mathbf{0}$ variations, the electrolyzer offers services in both FCR and mFRR markets, whereas it only provides FCR in $\boldsymbol{\alpha} = \mathbf{1}$. This implies that the mFRR market is not attractive for the electrolyzer when considering activation. Fig. 10 shows that the $\boldsymbol{\alpha} = \mathbf{0}$ variation places more bids in the mFRR up reserve over the year 2021 than the FCR market. This is, however, largely driven by the electrolyzer "leftover" capacity when, e.g., operating at full load due to low day-ahead prices, rather than the profitability of the reserve itself.

For DK1 2022, we observe an extreme case. When not providing ancillary services, the profit is almost zero due to very high day-ahead prices, making the hydrogen generation financially unattractive. However, owed to very high FCR prices, the estimated profit is around EUR 30 million in the oracle, while it is around EUR 19 million in two pragmatic variations. The electrolyzer mostly offers FCR, although mFRR services have also been offered to some extent. This raises the question of why the model is still placing bids in the mFRR market when FCR prices are several times higher.

There are two aspects of the FCR market design that makes it in some cases less advantageous for the electrolyzer than the upward mFRR market, even with the higher prices. The first reason is the symmetric nature of the FCR service. While it is obvious that this limits the electrolyzer to offering at maximum half of its available capacity, it is also important to note that it limits the electrolyzer from operating at full load when providing FCR. This is disadvantageous due to the fact that the electrolyzer is exposed to the day-ahead prices. In low-price hours, it might therefore be beneficial to rather utilize those hours for hydrogen production than for FCR services, especially considering the minimum daily hydrogen production requirement. Second, the FCR service must

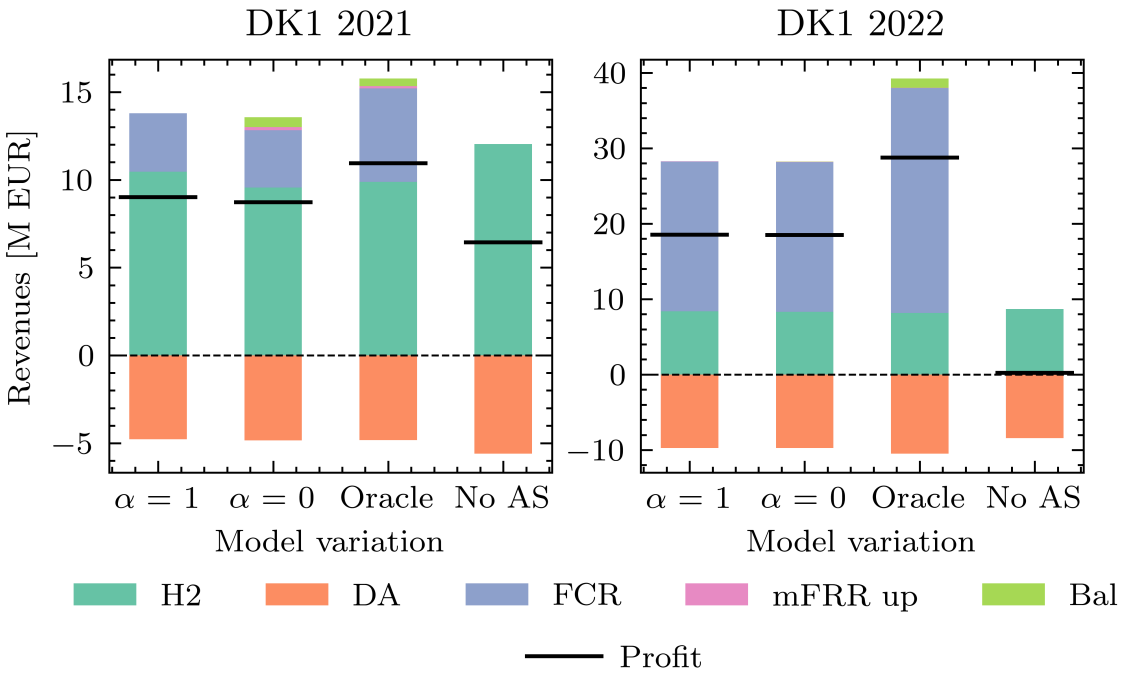

Figure 9: Ex-post annual profit in DK1 2021 and DK1 2022.

be provided in time blocks of four hours. Thus, the electrolyzer is either not able to utilize low day-ahead prices fully, or forced to produce during high prices while providing FCR.

We now explore the effect of activation on profits. As historical DK1 prices for mFRR are relatively low, we consider the DK2 2022 case to investigate the effect of upward mFRR activation. Fig. 11 shows the cumulative ex-post profit development when the electrolyzer, in addition to hydrogen production, participates in: (*i*) the mFRR market only, (*ii*) both mFRR and FCR markets, and (*iii*) the FCR market only. In all cases, we also plot the profit evolution in the oracle and when no ancillary services are offered, indicating upper and lower bounds, respectively. It is clear from all three plots in this figure that the participation in ancillary service markets significantly increases the total profit. While $\boldsymbol{\alpha = 0}$ yields a higher profit compared to $\boldsymbol{\alpha = 1}$, it may also lead to unmet hydrogen demand. In total, 82 tonnes of hydrogen demand was not met for the electrolyzer participating in the mFRR market only, not meeting the daily minimum hydrogen production requirement in 192 days throughout the year 2022. This may cause issues for the electrolyzer as per existing bilateral contracts. However, with a robust (pessimistic) approach to activation, i.e., $\boldsymbol{\alpha = 1}$, the profit has still increased from 0.9 to 2.5 million euro when the electrolyzer participates in both ancillary service markets. Note that the mFRR activation approach is not relevant to the case with the FCR market participation only (right plot).

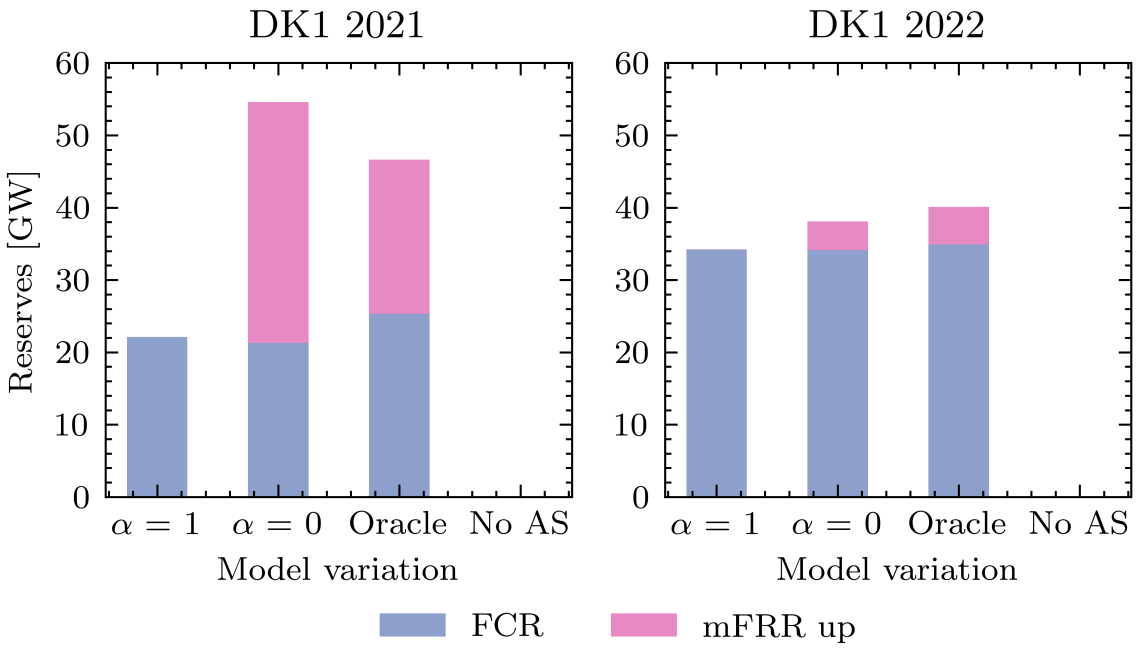

Figure 10: Cumulative reserve capacities the electrolyzer provided over a year for cases DK1 2021 and DK1 2022.

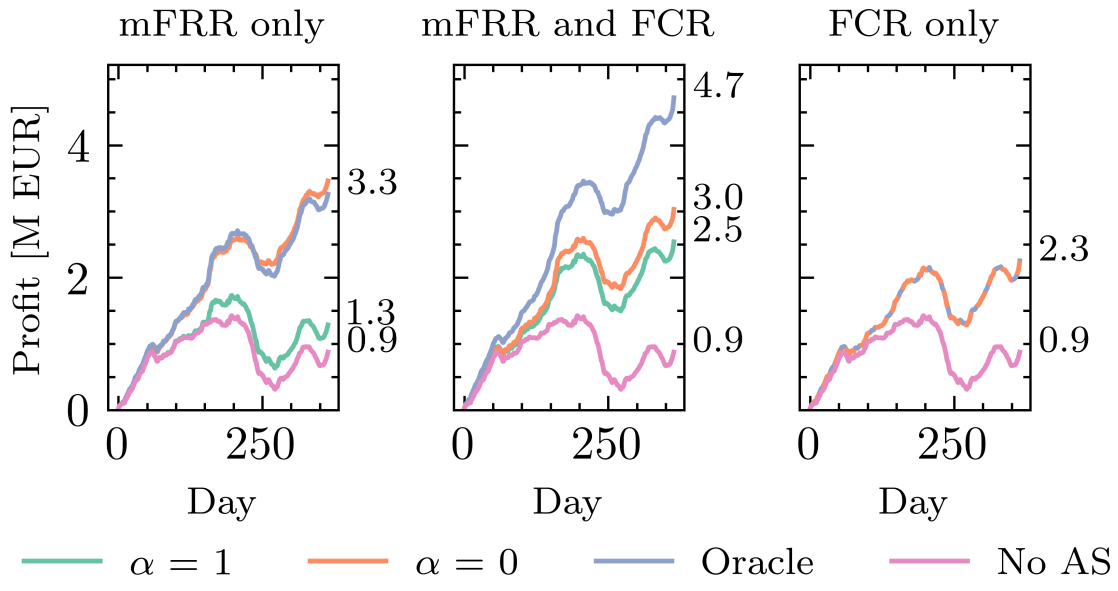

Figure 11: Cumulative ex-post profit in the DK2 2022 case.

Stochastic Model for Trading Wind Power and Hydrogen

1 Introduction

Hybrid power plants, comprising an electrolyzer and wind turbines, are expected to be largely installed in many countries, such as Denmark [4]. The plant operator, aiming to maximize their profit, can either allocate the entire generated wind power for hydrogen production, sell the whole or part of generated wind power to the grid, or buy power from the grid to produce more hydrogen. The plant operator should make informed decisions for trading power and hydrogen in a forward stage, when neither day-ahead and balancing prices nor the true wind power generation are realized. This requires developing a trading strategy, which is the focus of this paper.

There are many papers in the literature that develop trading strategies for wind power producers (wind power as the sole product) under price and wind uncertainty using stochastic optimization methods. Among others, [35] solves a newsvendor problem, [36] develops a two-stage stochastic programming, [37] devises a range of robust optimization models, and finally [38] develops a distributionally robust model. In addition, various data-driven approaches have been proposed that take advantage of contextual information to train a probabilistic forecast model and use its outcomes to solve a stochastic optimization problem, as summarized in [39]. These approaches include sequential training and optimization methods, in which the probabilistic forecast model is trained independently of the optimization task [40], and integrated training and optimization methods, in which the forecast model is trained in order to minimize the losses in a specific optimization task [41]. While all these methods outperform the deterministic counterpart, they require (*i*) knowledge of probabilistic forecasting, (*ii*) generating a set of scenarios, an uncertainty set, or a family of probability distributions, and then (*iii*) developing a stochastic optimization model to be solved in the decision-making stage. The trading problem is even more challenging for hybrid power plants, where hydrogen is also a product in addition to wind power. Although one may expect large companies to have great expertise in making trading decisions under uncertainty, it might be more challenging for a small-scale hybrid power plant operator. Therefore, the aim of this paper is to develop a *pragmatic* trading approach, which outperforms the deterministic model by enabling the hybrid power plant to learn from historical data, without the need for the plant to use probabilistic forecasting and complex stochastic solutions.

The first contribution of this paper is to propose a novel application of a prescriptive analytics framework based on decision rules, inspired by [42], to the multi-market bidding problem of hybrid power plants. In this data-driven approach, we exploit contextual information, so-called *features*, such as historical (deterministic) forecasts of wind power and directly map them to an optimal

action. In the *training stage*, the hybrid power plant operator learns feature-driven *policies* based on historical features and uncertainty realizations. In the *decision-making stage*, the learned policies are applied to new available features, leading to trading decisions without the need to solve a complex optimization problem. A few papers in the literature, e.g., [43], [44] and [45], develop feature-driven trading models for renewable power producers. To the best of our knowledge, this is the first paper that develops such a model for hybrid power plants trading both wind power and hydrogen, which is a more complicated problem. The second contribution of this paper is to extend these previous works by investigating various model architectures, in particular price- and time-dependent policies, and feature vectors, including an improved forecast feature vector. Finally, the third contribution of this paper is to develop a pragmatic rule-based adjustment strategy for real-time hydrogen production. Using an out-of-sample simulation, we show how the resulting profit from feature-driven trading in the day-ahead stage and the adjustment strategy in real time is very close to that in an ideal benchmark (oracle).

The rest of the paper is organized as follows. Section 2 explains the decision-making framework. Section 2 details the feature-driven trading strategy model in the day-ahead stage. Section 4 presents the proposed real-time adjustment strategy. Section 5 provides numerical results. Finally, Section 6 concludes the paper.

2 Decision-Making Framework

We consider a hybrid power plant comprising an electrolyzer and a wind turbine, behind the meter. The wind power generation can be exported to the grid or directed to the electrolyzer to produce hydrogen with a constant efficiency coefficient[12]. The electrolyzer has also the possibility to buy power directly from the grid[13]. The produced hydrogen is sold through a bilateral contract at a fixed hydrogen price. As part of the contract, there is a minimum amount of hydrogen that should be produced in a daily basis. In practice, this minimum daily requirement is fulfilled by filling tube trailers that are collected daily by the hydrogen off-taker. However, the proposed models could be generalized straightforwardly to other off-take structures, such as injection of hydrogen in gas pipelines. The hydrogen production thus needs to be scheduled for the whole day in order to ensure fulfilling this minimum production requirement. Any real-time adjustment should likewise account for the imposed hydrogen production quota. The power production capacity of the wind farm is assumed to be identical to the power consumption capacity of the electrolyzer.

The hybrid power plant aims to maximize the total profit from electricity trading and hydrogen sales. This leads to two stages for decision making:

Day-ahead decision making: Given the available (deterministic) wind power forecast, the hybrid power plant must decide how much electricity to trade (buy or sell) in the day-ahead market and how to schedule the operation of the electrolyzer for each hour of the following day, depending on hourly day-ahead market prices and the fixed hydrogen price. Recall the minimum daily hydrogen production requirement needs to be accounted for. In Nord Pool, all these decisions for every hour $t \in \mathcal{T}$ of day D should be made before noon of day D-1.

Real-time decision making: The hybrid power plant must settle imbalances arising from deviations in wind power production (compared to the day-ahead schedule) in the balancing market.

[12] The efficiency of electrolyzers in practice is variant, depending on their power consumption level following a non-linear curve. We refer the interested reader to [46] for alternative convexified solutions.

[13] According to the "Renewable Fuels of Non-Biological Origin (RFNBO)" Delegated Act of the European Commission published in 2023 [47], the produced hydrogen in this case will not be seen green except for certain operational conditions. We do not consider this legislation in our paper.

Therefore, at the time of delivery, i.e., in every hour t of day D, the plant must decide how to adjust the schedule of the electrolyzer based on the realized wind power production and electricity balancing prices, while ensuring the minimum daily hydrogen production requirement is fulfilled.

3 Day-Ahead Bidding

We first define a feature-driven model for making power and hydrogen trading decisions in the day-ahead stage. Next, we explain feature vectors, and then elaborate on architecture of linear policies. We eventually provide an optimization model for training the proposed feature-driven model.

3.1 Model Definition

The main challenge for the hybrid power plant in the day-ahead stage is to account for uncertainty on day-ahead and balancing electricity prices and wind power production.

Aiming to develop a feature-driven trading strategy in the day-ahead stage, we first define the vector of available features with N elements corresponding to hour t as

$$\mathbf{X}_t = \left[X_t^1, ..., X_t^N\right] \quad \forall t \in \mathcal{T}. \tag{33}$$

The features should be those contextual information for hour t of the following day that the plant has access to when making day-ahead decisions. Examples of available features for the hybrid power plant at the day-stage stage are (i) deterministic forecasts of wind power generation of the underlying farm at different points before the day-ahead market gate closure at the noon of day D-1, (ii) aggregate wind power forecast in the area (or bidding zone) where the farm is located, (iii) aggregate wind power forecast in the neighboring areas, (iv) realized wind power production in day D-1.

Let variable p_t^{DA} denote the electricity traded (bought or sold) in the day-ahead market for hour t of the next day. In addition, variable p_t^{H} is the electricity consumption schedule of the electrolyzer for the same hour. We exploit linear decision rules [48], so called *linear policies*, to define p_t^{DA} and p_t^{H} as a function of features $\mathbf{X}_t$, such that

$$p_t^{\mathrm{DA}} = \mathbf{q}^{\mathrm{DA}}\ \mathbf{X}_t^\top \qquad \forall t \in \mathcal{T} \tag{34a}$$

$$p_t^{\mathrm{H}} = \mathbf{q}^{\mathrm{H}}\ \mathbf{X}_t^\top \qquad \forall t \in \mathcal{T}, \tag{34b}$$

where $(.)^\top$ is the transpose operator. Vectors $\mathbf{q}^{\mathrm{DA}} \in \mathbb{R}^N$ and $\mathbf{q}^{\mathrm{H}} \in \mathbb{R}^N$ are the policies, so called $\mathbf{q}$-policies, to be learned from historical data in the training stage.

If the model is designed and trained appropriately, $\mathbf{q}^{\mathrm{DA}}$ and $\mathbf{q}^{\mathrm{H}}$ will reflect relations between the input features and the decision variables p_t^{DA} and p_t^{H} that persist into the future, such that the model will produce well-performing trading decisions for new feature vectors.

Feature Vectors: The day-ahead market allows for simultaneously placing multiple independent price-quantity bids $\{\lambda_b, p_b\}_{b=1,...,B}$ for each hour of the following day. Therefore, we can model the electricity traded in the day-ahead market p_t^{DA} as a function of the day-ahead price at hour t. This is achieved by introducing an unknown price variable $\lambda \in \mathbb{R}$ in the feature vector $\mathbf{X}_t$. Since all other values in the feature vector are known at the time of decisions, this results in p_t^{DA} being a linear function of this unknown variable λ. In practice, the day-ahead price-quantity bids are then derived by discretizing this linear function and approximating it as a stepwise function with arbitrary step

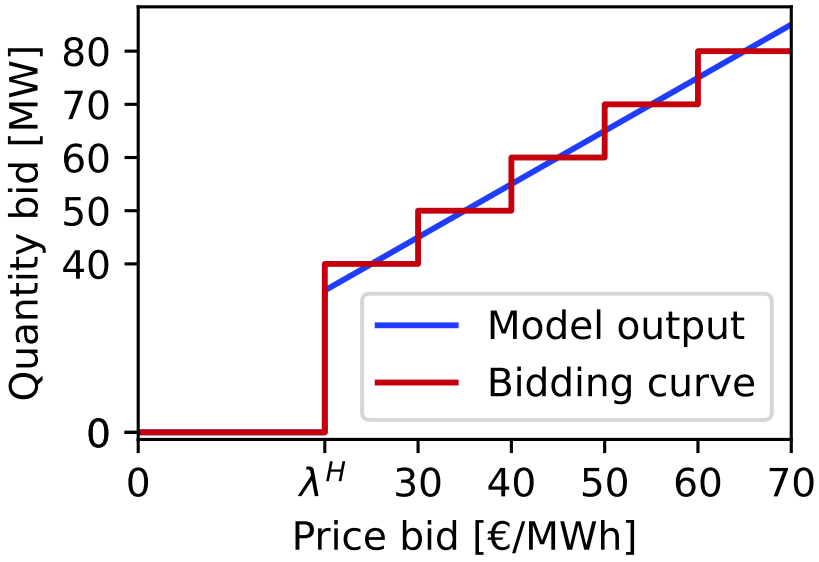

Figure 12: The discretization of $p_t^{\mathrm{DA}} = \mathbf{q}^{\mathrm{DA}}\mathbf{X}_t^\top$ to create piece-wise price-quantity bids $\{\lambda_b, p_b\}_{b=1,\dots,B}$.

size, as illustrated in Fig. 12. Each step b of the resulting stepwise function will represent one pair of price-quantity bids $\{\lambda_b, p_b\}_{b=1,\dots,B}$. Since the electricity traded in the day-ahead market and the power consumption p_t^{H} of the electrolyzer are interdependent, p_t^{H} is also expressed as a linear function of the day-ahead electricity price at hour t.

All feature vectors investigated in this paper will have the form $\mathbf{X}_t = \left[\tilde{\mathbf{X}}_t, \lambda, 1\right]$, where the constant feature 1 provides an intercept and $\tilde{\mathbf{X}}_t \in \mathbb{R}^{N-2}$ is the vector of remaining features. The remaining features can include any relevant data that are expected to be related with the uncertain parameters including the wind power production (e.g., wind power forecasts) and the day-ahead and balancing prices (e.g., electricity price and demand forecasts and imbalance forecasts). Note that the plant has usually access to an extensive database, including *historical* values of these features and corresponding *realized* values of the uncertain parameters.

Architecture of Linear Policies: Several approaches can be used regarding the architecture of the $\mathbf{q}$-policies. The simplest but restrictive architecture, so-called *general architecture*, considers *constant* policies $\mathbf{q}^{\mathrm{DA}} \in \mathbb{R}^N$ and $\mathbf{q}^{\mathrm{H}} \in \mathbb{R}^N$ for every hour t.

It is widely acknowledged that daily patterns exist in the day-ahead prices. Accounting for these patterns could remarkably increase the performance of the model. This can be achieved by introducing an *hourly architecture*, where the $\mathbf{q}$-policies in (34) are specific to the hour of the day and denoted as $\mathbf{q}_{h_t}^{\mathrm{DA}} \in \mathbb{R}^N$ and $\mathbf{q}_{h_t}^{\mathrm{H}} \in \mathbb{R}^N$ for $h_t = t \mod 24$, with mod representing the modulo operator. This hourly architecture allows the model to learn daily patterns. However, it results in 24 times as many $\mathbf{q}$-policies to train as in the general architecture, and thus requires a larger training dataset. The trade-off between these factors will be empirically studied later in our case study.

Besides, in order to capture more complex and non-linear dependencies between the features $\mathbf{X}_t$ and decision variables p_t^{DA} and p_t^{H}, multiple sets of model parameters can be introduced, each covering one domain of the features. In particular, we introduce M price domains $\mathcal{D} = \{\mathcal{D}_1, ..., \mathcal{D}_M\}$,

each defined as a range of prices $\mathcal{D}_i = [\lambda_{i-1}, \lambda_i]$ with $\lambda_{i-1} < \lambda_i$ for all $i \in \{1, ..., M\}$. Over each price domain, we define $\mathbf{q}$-policies as $\mathbf{q}_i^{\mathrm{DA}}$ and $\mathbf{q}_i^{\mathrm{H}}$. As a result, the decision variables p_t^{DA} and p_t^{H} are expressed as piece-wise linear functions of the day-ahead prices, such that

$$p_t^{\mathrm{DA}} = \mathbf{q}_i^{\mathrm{DA}}\ \mathbf{X}_t^{\top} \qquad \text{if } \lambda \in \mathcal{D}_i, \qquad \forall t \in \mathcal{T} \tag{35a}$$

$$p_t^{\mathrm{H}} = \mathbf{q}_i^{\mathrm{H}}\ \mathbf{X}_t^{\top} \qquad \text{if } \lambda \in \mathcal{D}_i, \qquad \forall t \in \mathcal{T}. \tag{35b}$$

Note that a trade-off between complexity and flexibility can be achieved, if optimal domains can be chosen based on statistical characteristics of the data. For example, a natural threshold where it might be beneficial to divide the model into different trading strategies is when the day-ahead electricity price is equal to the hydrogen price λ^{H}.

3.2 Optimization Model for Training Stage

In the training stage we determine the adequate values of the $\mathbf{q}$-policies using a batch learning mechanism. The training of the $\mathbf{q}$-policies can be represented as an optimization problem, in which the profit of the plant is maximized over a *historical* dataset, containing values of the feature vectors along with corresponding realizations of the uncertain parameters, e.g., market prices, for all $t \in \mathcal{T}^{\mathrm{hist}}$. This optimization problem, formulated as a mixed-integer linear program (MILP), reads as

$$\max_{\Omega} \sum_{t \in \mathcal{T}^{\mathrm{hist}}} \left[\lambda_t^{\mathrm{DA}} \mathbf{q}^{\mathrm{DA}} \mathbf{X}_t^{\top} + \lambda^{\mathrm{H}} \rho^{\mathrm{H}} \mathbf{q}^{\mathrm{H}} \mathbf{X}_t^{\top} + \lambda_t^{\mathrm{UP}} o_t - \lambda_t^{\mathrm{DW}} u_t \right] \tag{36a}$$

$$\text{s.t.} \quad o_t - u_t = P_t^{\mathrm{W}} - \mathbf{q}^{\mathrm{DA}} \mathbf{X}_t^{\top} - \mathbf{q}^{\mathrm{H}} \mathbf{X}_t^{\top} \qquad \forall t \in \mathcal{T}^{\mathrm{hist}} \tag{36b}$$

$$0 \le o_t \le M(1 - b_t) \qquad \forall t \in \mathcal{T}^{\mathrm{hist}} \tag{36c}$$

$$0 \le u_t \le M b_t \qquad \forall t \in \mathcal{T}^{\mathrm{hist}} \tag{36d}$$

$$0 \le \mathbf{q}^{\mathrm{H}} \mathbf{X}_t^{\top} \le \overline{P}^{\mathrm{H}} \qquad \forall t \in \mathcal{T}^{\mathrm{hist}} \tag{36e}$$

$$-\overline{P}^{\mathrm{H}} \le \mathbf{q}^{\mathrm{DA}} \mathbf{X}_t^{\top} \le \overline{P}^{\mathrm{W}} \qquad \forall t \in \mathcal{T}^{\mathrm{hist}} \tag{36f}$$

$$\sum_{t=24(d-1)+1}^{24d} \rho^{\mathrm{H}} \mathbf{q}^{\mathrm{H}} \mathbf{X}_t^{\top} \ge \underline{H} \qquad \forall d \in D^{\mathrm{hist}}, \tag{36g}$$

where the set of variables $\Omega = \{\mathbf{q}^{\mathrm{DA}},\ \mathbf{q}^{\mathrm{H}},\ o_t,\ u_t,\ b_t\}\ \forall t \in \mathcal{T}^{\mathrm{hist}}$ includes the $\mathbf{q}$-policies $\mathbf{q}^{\mathrm{DA}}$ and $\mathbf{q}^{\mathrm{H}}$, as well as the real-time decisions, including the over-production o_t and under-production u_t settled in real time, and the auxiliary binary variable $b_t \in \{0, 1\}$ indicating the state of over- or under-production. Note that the $\mathbf{q}$-policies in (36) can take index h_t and/or index i as discussed in Section 3.1.

The objective function (36a) maximizes the total profit of the hybrid power plant over the historical dataset, including four terms. The first term $\lambda_t^{\mathrm{DA}} \mathbf{q}^{\mathrm{DA}} \mathbf{X}_t^{\top}$ corresponds to the revenue/cost from electricity trading in the day-ahead market, where $\lambda_t^{\mathrm{DA}} \in \mathbb{R}$ is the historical day-ahead price reported by the market operator. Note that $\mathbf{q}^{\mathrm{DA}} \mathbf{X}_t^{\top}$, reflecting the power quantity, could be positive or negative, indicating whether the plant sells or buys power. The second term $\lambda^{\mathrm{H}} \rho^{\mathrm{H}} \mathbf{q}^{\mathrm{H}} \mathbf{X}_t^{\top}$ is the revenue from hydrogen sales, where $\lambda^{\mathrm{H}} \in \mathbb{R}_+$, in €/Kg, is the fixed hydrogen price. In addition, $\rho^{\mathrm{H}} \in \mathbb{R}_+$, in Kg/MWh, is the constant power-to-hydrogen efficiency of the electrolyzer, whereas $\mathbf{q}^{\mathrm{H}} \mathbf{X}_t^{\top}$ reflects the power consumed by the electrolyzer. Finally, the third and fourth terms in (36a) refer to the settlement of over- and under-production, respectively, in the balancing market with a

dual-price imbalance settlement scheme. Note that $\lambda_t^{\mathrm{UP}} \in \mathbb{R}$ is the upward regulation price, which is lower than or equal to the day-ahead price λ_t^{DA}, reflecting a lost opportunity cost for over-production. In addition, $\lambda_t^{\mathrm{DW}} \in \mathbb{R}$ is the downward regulation price, which is higher than or equal to the day-ahead price λ_t^{DA}, reflecting a penalty cost for under-production. By this, it is always costly for the hybrid power plant to create any imbalance either over- or under-production.

Constraint (36b) defines the power imbalance $o_t - u_t$ to be settled in real time as the difference between the realized wind power generation P_t^{W} and the power scheduled in the day-ahead stage. The set of disjunctive constraints (36c)-(36d), with M a large enough positive constant, enforces over- and under-production to not happen simultaneously at each hour t. If $b_t = 1$, then (36c) enforces the over-production o_t to be zero. On the other hand, if $b_t = 0$, then (36d) sets the under-production u_t to zero. Constraint (36e) enforces the power consumption of the electrolyzer to lie within zero and its capacity $\overline{P}^{\mathrm{H}}$. Note that the lower bound being set to zero means that the electrolyzer cannot operate as a fuel cell, converting the hydrogen back to electricity. In order to avoid imbalance settlement costs, the power traded in the day-ahead market is restricted by (36f) to lie within the minus consumption capacity of the electrolyzer and the nominal capacity of the wind turbine $\overline{P}^{\mathrm{W}}$. Finally, the minimum daily hydrogen production requirement $\underline{H}$ is enforced by (36g) for each day $d \in D^{\mathrm{hist}}$ in the historical dataset. This requirement could be alternatively implemented using a slack variable penalized in the objective function. However, a value for such a penalty is unknown. One may assume the penalty would always be higher than the revenue that could be generated by not meeting the requirement.

3.3 Decision-Making Stage and Retraining

For each day of the testing period, the trained $\mathbf{q}$-policies are applied to a new feature vector $\tilde{\mathbf{X}}_t$ for each hour t of the following day, to compute the linear functions representing the electricity traded in the day-ahead market and consumed by the electrolyzer as functions of the future day-ahead prices. These functions are then discretized, and stepwise price-quantity bids are placed in the day-ahead market. The realized day-ahead price will then determine the electricity traded in the day-ahead market and consumed by the electrolyzer. For the sake of simplicity, we assume none of the technical constraints of the hybrid power plant is violated in the testing period. This is in practice likely as long as the testing data does not differ significantly from the training one. If it is the case, one should restore feasibility of those constraints by adjusting trading decisions at the minimum cost, or projecting the decisions onto the feasible space.

Once the uncertain parameters, i.e., day-ahead prices, balancing prices, and wind power production, are realized, the new feature vector and the associated realizations are added to the historical dataset. Retraining the model considering more recent historical data points is thus performed at regular intervals. One can use a sliding window approach in order to keep the length of the training dataset constant, as illustrated in Fig. 13. Note that, at each retraining interval, the blue part of the window represents the previous testing data points recently added to the training dataset. The length of this window is a hyperparameter of the model that should be selected appropriately, as further discussed in our numerical analysis.

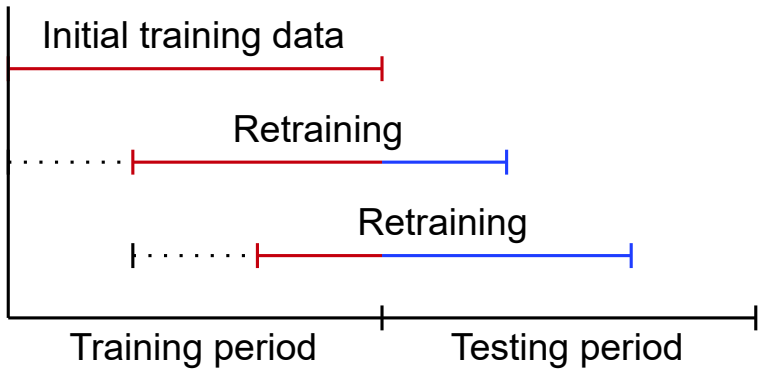

Figure 13: Illustration of sliding window approach to determine training data in each retraining interval.

4 Real-Time Adjustments

We assume the electrolyzer is subject to negligible ramping constraints. Therefore, the hybrid power plant is able to adjust the hydrogen production schedule in real time based on the realized wind power production and balancing prices. This section introduces a rule-based adjustment algorithm for the real-time operation of the electrolyzer that accounts for the minimum daily hydrogen production requirement.

4.1 Decision Rule for a Single Hour

In each hour, the decision rule is dependent on whether balancing prices are higher or lower than the hydrogen price. Hereafter, to make electricity and hydrogen prices comparable in terms of €/MWh, we refer to $\rho^{\mathrm{H}}\lambda^{\mathrm{H}}$ as the hydrogen price. Balancing prices are unknown until after the balancing settlements, however it is assumed that they can be approximated to a sufficient degree for the current hour by predicting the system status [49] and observing the intraday market. This will be explained in further detail after the introduction of the algorithm and required parameters.

As mentioned earlier, we assume that the balancing market follows a dual-pricing mechanism, implying that $\lambda_t^{\mathrm{UP}} \leq \lambda_t^{\mathrm{DA}} \leq \lambda_t^{\mathrm{DW}}$ for each hour $t \in \mathcal{T}$. The following three situations can thus occur regarding the relation between the hydrogen price and balancing prices: (i) $\rho^{\mathrm{H}}\lambda^{\mathrm{H}} \leq \lambda_t^{\mathrm{UP}} \leq \lambda_t^{\mathrm{DW}}$; (ii) $\lambda_t^{\mathrm{UP}} \leq \lambda_t^{\mathrm{DW}} \leq \rho^{\mathrm{H}}\lambda^{\mathrm{H}}$; and (iii) $\lambda_t^{\mathrm{UP}} \leq \rho^{\mathrm{H}}\lambda^{\mathrm{H}} \leq \lambda_t^{\mathrm{DW}}$. In the first situation where both up and down balancing prices are higher than the hydrogen price, producing hydrogen would result in less revenue than what is compensated for over-production in the balancing market. This means that the producer would benefit from adjusting the electrolyzer's consumption down and exporting as much electricity to the grid as possible. In the second situation where both balancing prices are lower than the hydrogen price, producing hydrogen results in higher revenue than the cost incurred from under-production in the balancing market. This means that the hybrid power plant would benefit from adjusting the electrolyzer's consumption up and importing as much electricity from the grid as possible. In the final situation, over-production results in lower revenues than hydrogen production, and under-production results in higher costs than revenues from hydrogen production. In this situation, the electrolyzer should be adjusted in order to minimize any deviation from the day-ahead market bid. This decision rule that maximizes the profit for a single hour can be formulated

as a piece-wise linear function $\Pi(.)$ that returns the adjusted electricity consumption level of the electrolyzer, such that

$$\Pi\left(\delta_t, \lambda^{\mathrm{H}}, \lambda_t^{\mathrm{UP}}, \lambda_t^{\mathrm{DW}}\right) = \begin{cases} 0 & \text{if } \lambda_t^{\mathrm{UP}} > \rho^{\mathrm{H}}\lambda^{\mathrm{H}} \\ \overline{P}^{\mathrm{H}} & \text{if } \lambda_t^{\mathrm{DW}} < \rho^{\mathrm{H}}\lambda^{\mathrm{H}} \\ \alpha^{\mathrm{H}}[\delta_t] & \text{otherwise,} \end{cases} \tag{37}$$

where $\delta_t = P_t^{\mathrm{W}} - p_t^{\mathrm{DA}}$ is the surplus/deficit of wind power production compared to the day-ahead market bid, and $\alpha^{\mathrm{H}}[\cdot]$ ensures that the electrolyzer production is feasible:

$$\alpha^{\mathrm{H}}\left[\delta_t\right] = \begin{cases} 0 & \text{if } \delta_t < 0 \\ \overline{P}^{\mathrm{H}} & \text{if } \delta_t > \overline{P}^{\mathrm{H}} \\ \delta_t & \text{otherwise.} \end{cases} \tag{38}$$

Adjusting the electricity consumption of the electrolyzer according to the decision rule (37) will maximize the generated revenues for a single hour, when the estimated balancing price is the only source of uncertainty. Note that (37) does not require an accurate estimation of balancing prices, but only whether balancing prices will be higher or lower than the hydrogen price, which is a more straightforward task. Whether the balancing price will be higher or lower than the known day-ahead price will depend on the system status (surplus or deficit energy in the system).

4.2 Real-time Adjustment Algorithm

Implementing the hourly decision rule (37) independently for each single hour of the optimization period would not guarantee that the minimum daily hydrogen production requirement $\underline{H}$ is satisfied. Instead, we introduce an algorithm which only adjusts the electrolyzer's schedule according to the hourly decision rule in a given hour t if this requirement can still be met during the day. Therefore, the electrolyzer's consumption can always be adjusted upward from the day-ahead schedule at any given hour. However, in order to perform a downward adjustment in a given hour t of the day d, the adjusted hydrogen production in this hour $\rho^{\mathrm{H}} p_t^{\mathrm{adj}}$, plus the cumulative realized production in previous hours $\rho^{\mathrm{H}} p_t^{\mathrm{real}} = \sum_{i=24(d-1)+1}^{t-1} \rho^{\mathrm{H}} p_i^{\mathrm{adj}}$, plus the cumulative production schedule for the remaining hours of the day $\sum_{i=t+1}^{24d} \rho^{\mathrm{H}} p_i^{\mathrm{H}}$ must be higher than the minimum daily hydrogen production requirement $\underline{H}$. For example, let us consider a hybrid power plant with a certain minimum daily hydrogen production requirement, equivalent to the consumption of 15 MWh. If the realized cumulative hydrogen production at hour 15 is equal to 10 MWh and the cumulative planned hydrogen production from hour 15 to 23 is equal to 7 MWh, then the electrolyzer has a scheduled hydrogen surplus of 2 MWh, which can be adjusted down at hour 15. If the hourly decision rule (37) outputs a lower set-point for the electrolyzer than its schedule for this hour, the electrolyzer can then be turned down as much as the surplus allows. On the contrary, if the realized cumulative hydrogen production is only equal to 8 MWh, then the electrolyzer has no scheduled hydrogen surplus and cannot be adjusted down in this hour, regardless of the outputs of the hourly decision rule (37). The size of the production requirement compared to the production capacity of both the wind farm and the electrolyzer thus directly affects the possible space of adjustments, with a higher requirement reducing the amount of adjustment possible. The complete adjustment algorithm is provided in Algorithm 1.

Algorithm 1 Real-time upward and downward adjustment

for each day d **do**
  Initialize $p^{\text{real}}_{24(d-1)+1} = 0$
  for each hour $t \in [24(d-1)+1, 24d]$ **do**
    Receive model output: p^{DA}_t, $\mathbf{p}^{\text{H}}$
    Receive balancing price forecasts: λ^{UP}_t, λ^{DW}_t
    Realize production: P^{W}_t
    Compute real-time deviation $\delta_t = P^{\text{W}}_t - p^{\text{DA}}_t$
    Compute $p^{\text{H}*}_t = \Pi\big(\delta_t, \lambda^{\text{UP}}_t, \lambda^{\text{DW}}_t\big)$
    if $p^{\text{H}*}_t > p^{\text{H}}_t$ **then**
      $p^{\text{adj}}_t = p^{\text{H}*}_t$
    else
      $p^{\text{adj}}_t = \max\left(p^{\text{H}*}_t, \frac{H}{\rho^{\text{H}}} - \left(p^{\text{real}}_t + \sum_{i=t+1}^{24d} p^{\text{H}}_i\right)\right)$
    end if
    Receive revenue from allocations $\left(p^{\text{DA}}_t, p^{\text{adj}}_t\right)$
    $p^{\text{real}}_{t+1} = p^{\text{real}}_t + p^{\text{adj}}_t$
  end for
end for

5 Numerical Analysis

This section provides a numerical analysis of the proposed feature-driven day-ahead trading strategy and rule-based real-time adjustment.

5.1 Case Study Data

We use historical data for the year 2019 for training, and the year 2020 for testing, ensuring that the models are evaluated through all seasonal variations. It is essential to evaluate the models with out-of-sample testing in this way, using more recent data for testing than was used for training, to ensure the performance of the models is due to them generalizing observed patterns in the features and not overfitting the training data. All price data is publicly available on ENTSO-e [50], along with production data for specific wind farms, and aggregated forecasts of offshore/onshore wind production in the Danish bidding zones DK1 and DK2. The production from the wind farm in Roedsand, Denmark is used to model the realized wind production of the hybrid power plant.

Realistic forecasts of day-ahead price and wind power production have been provided by Siemens Gamesa Renewable Energy for five consecutive months. Two years of synthetic forecasts are created for both price and wind production, by fitting the statistical characteristics of the forecast error of Siemens Gamesa forecasts to a theoretical distribution, and then sampling from this distribution to generate new forecast errors with the same characteristics. Fig. 14 provides a histogram of both original and generated forecast errors for both day-ahead market price and wind production forecasts.

Forecasts are produced by sampling forecast error values from the fitted distributions, and then adding these errors to the realized production data to create a forecast. The entire training and testing datasets thus consist of realized day-ahead prices, upward and downward balancing prices, and production for the wind farm in Roedsand, and forecasts for day-ahead prices and wind production, for 2019 and 2020.

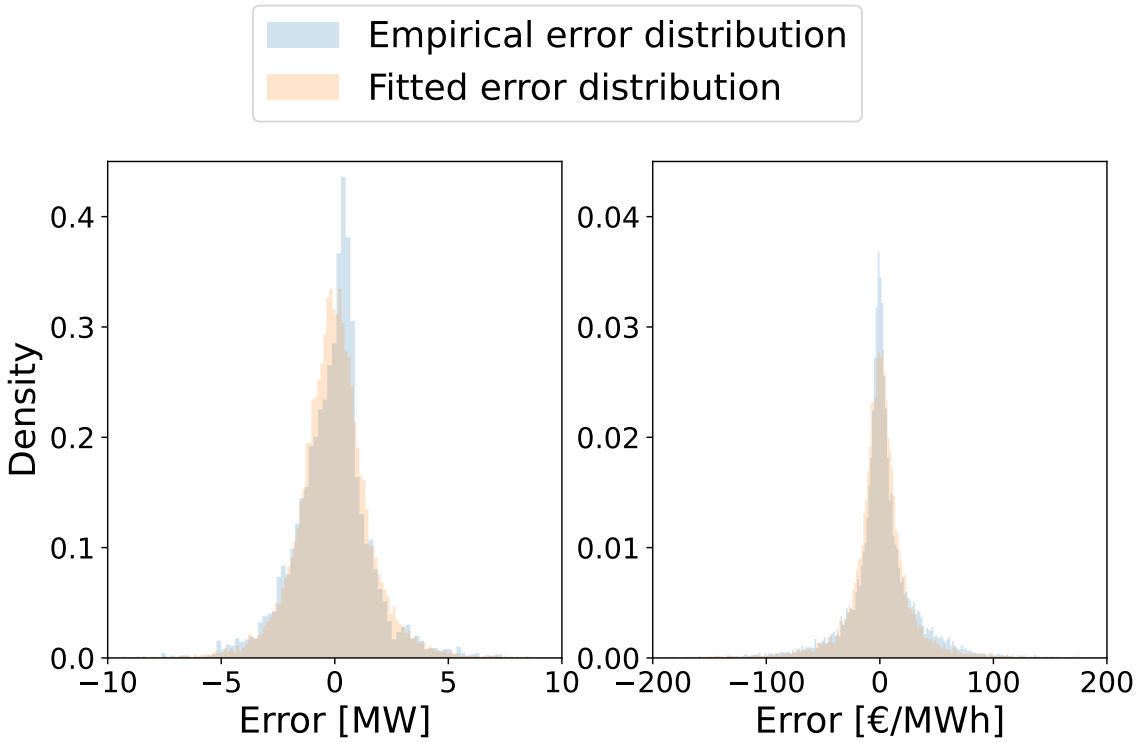

Figure 14: Distribution of day-ahead market price **(right)** and wind power generation **(left)** forecast errors.

5.2 Models to be Compared

This numerical analysis compares several trained models with various combinations of (i) linear policies architecture as introduced in Section 3.1 and (ii) feature vectors. These trained models are compared to a deterministic (**Det.**) optimization approach as a base-case, and a benchmark with perfect information (**Hindsight**). In addition, we explore the impact of the length of the training period, ranging between 1 and 12 months, on the outcomes of different models.

We first compare models with **General Architecture (GA)** and **Hourly Architecture (HA)** for **q**-policies. Recall that **q**-policies take index t in the **HA** model, which is not the case in the **GA** model. Next, we compare the **GA** and **HA** in the cases where a single set of policies is defined over all values of prices, and a case where the policies are split into multiple **Price Domains (PD)**. When considering multiple price domains, we refer to models as **GA+PD** and **HA+PD**. Three price domains are chosen: one below the hydrogen price $\rho^{\mathrm{H}}\lambda^{\mathrm{H}}$, one above the 90% percentile of realized day-ahead prices in the training data, and one in between. The hydrogen price is a natural threshold to separate the trading decisions because producing hydrogen is necessarily more profitable than selling power for day-ahead prices below the hydrogen price. The 90% percentile is chosen to reduce the influence of extreme outliers on the **q**-policies.

Additionally, we investigate three different types of feature vectors $\mathbf{X}_t$. Firstly, the simplest **Reduced Feature (RF)** vector contains only the deterministic wind production forecast $\hat{P}_t^{\mathrm{W}}$, such that $\mathbf{X}_t^{\mathrm{RF}} = \left[\hat{P}_t^{\mathrm{W}}, \lambda, 1\right]$. Secondly, the **Augmented Feature (AF)** vector includes additional

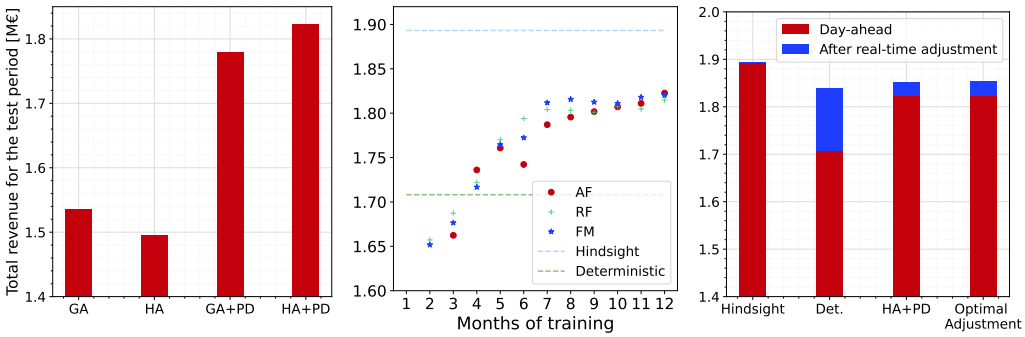

(a) (b) (c)

Figure 15: Ex-post profit of the hybrid power plant with (a) four policy architectures (**GA**, **HA**, **GA+PD**, **HA+PD**); (b) the **HA+PD** model for various training dataset lengths and available feature vectors (**AF**, **RF**, **FM**), compared to the **Deterministic** and **Hindsight** models; and (c) the **HA+PD** model before and after the real-time adjustment, compared to the deterministic (**Det.**) and **Hindsight** model, and the **Optimal Adjustment** strategy.

features, namely the aggregated onshore/offshore wind production forecasts in the two bidding zones DK1 and DK2, released by the Danish transmission system operator, Energinet, before the time of bidding, such that $\mathbf{X}_t^{\mathrm{AF}} = \left[\tilde{\mathbf{X}}_t^{\mathrm{AF}}, \lambda, 1\right]$ with $\tilde{\mathbf{X}}_t^{\mathrm{AF}} = \left[\hat{P}_t^{\mathrm{W}}, \hat{P}_t^{\mathrm{on,DK1}}, \hat{P}_t^{\mathrm{on,DK2}}, \hat{P}_t^{\mathrm{off,DK1}}, \hat{P}_t^{\mathrm{off,DK2}}\right]$. This augmented feature vector may capture additional information related to the uncertainty sources at the cost of training additional **q**-policies and requiring a larger amount of training data. Increasing the length of the historical dataset raises issues of stationarity of the environment, in particular of electricity prices. Therefore, a so-called **Forecast Model (FM)** feature vector is introduced, that accounts for the same additional features $\tilde{\mathbf{X}}_t^{\mathrm{AF}}$, while minimizing the added complexity of the model. This is achieved by first training a separate feature-driven forecast model that provides a single improved wind power generation forecast feature $\tilde{X}_t^{\mathrm{FM}} = \tilde{\mathbf{q}}^{\mathrm{FM}}\left[\tilde{\mathbf{X}}_t^{\mathrm{AF}}, 1\right]^\top \in \mathbb{R}$, where $\tilde{\mathbf{q}}^{\mathrm{FM}}$ represents a vector of policies that is trained using a historical dataset. As the environment related to wind power generation is expected to be stationary, to a large extent, this feature-driven forecast model can be trained on a longer historical dataset. Then, the **FM** feature vector is defined as $\mathbf{X}_t^{\mathrm{FM}} = \left[\tilde{X}_t^{\mathrm{FM}}, \lambda, 1\right]$.

5.3 Results

The results presented are the profits generated by each model from electricity trades in the day-ahead market, hydrogen production, and settlements in real time, evaluated ex-post for the entire year 2020.

Fig. 15a illustrates the comparison between the different policy architectures, showing the best performing feature vector and training period for each architecture. This plot shows that introducing multiple price domains increases the performance radically for both types of architectures, resulting in the **HA+PD** model outperforming the **GA+PD** model with price domains included. Additionally, we note that the training period yielding the best results for the **GA** model is 5 months, and the model performed within 99% of this performance after only 3 months. With a training period of 3 months, the **GA** model generates around 5% higher revenues than the **HA** model. This indicates

that for time periods with a more non-stationary environment than the one used in the study, or with limited available historical data, the **GA** model might be a more appealing choice. Since Fig. 15a shows that **HA+PD** is the model that outperforms others, we further analyze this model in the rest of this section.

Fig. 15b depicts the performances of **HA+PD** for different feature vectors and varying lengths of the training dataset, from one to 12 months. First, we observe that the improvement of the model by having access to a training dataset longer than 7 months is limited, irrespective of the feature vectors chosen. For example, the profit when models trained on a 12-month dataset is only 1-2% higher than when trained on a 7-month dataset. The second observation is that the model with the **FM** feature vector setting usually exhibits a better performance than the ones with the **AF** and **RF** feature vector settings, especially when the length of the training dataset is lower than 12 months. However, these three models show a similar performance when the plant uses a dataset of 12 months. The third observation is the performance of our models in comparison to the deterministic model, where the hybrid power plant makes day-ahead bidding decisions by using deterministic forecasts only. We notice that, by using a training dataset of at least 4 months, our model outperforms the deterministic model. For example, when using the 12-month dataset, the plant makes around 5.9% more profit by using the **HA+PD** model with either of three feature vector settings. The final observation corresponds to the comparison of the **HA+PD** model with respect to the hindsight model, in which the plant has perfect information on the prices and wind generation. We observe that the profit earned by our proposed **HA+PD** model is only 3.7% lower than the profit in hindsight, whereas it is 9.8% for the deterministic model. For the rest of this section, we further analyze the best-performing model, i.e., the **HA+PD** model with a 12-month training dataset and (**AF**) feature vector setting.

Fig. 15c depicts the profit across various models before and after real-time adjustments. Obviously, the hindsight model does not need any real-time adjustment. The *final* profit, i.e., after in the day-ahead stage plus real time, earned by the deterministic (**Det.**) and the proposed **HA+PD** model is computed using the rule-based adjustment strategy proposed in Section 4.2. This profit is compared to the final profit obtained by the HA+PD model with an *optimal adjustment*, implemented as an optimization problem over 24 hours with perfect foresight, which provides an upper bound on the benefits of any adjustment policy. We observe that the the proposed real-time adjustment strategy achieves a higher increase in the profit of the deterministic model compared to that of the **HA+PD** model. Indeed, due to a less efficient day-ahead scheduling, the deterministic model has more potential for improvement in the real-time stage than the **HA+PD** model. However, the final profit of the deterministic model is still slightly lower than that of the proposed **HA+PD** model. Yet, it is important to note that its result relies on having access to accurate upward and downward balancing price forecasts for the the real-time adjustment strategy, which is not a straightforward task. As the final profits of the deterministic model are highly dependent on the performance of the real-time adjustment policy, in the absence of accurate price forecasts, the deterministic model risks achieving significantly lower final profits than the **HA+PD** model. Additionally, we observe that the proposed rule-base adjustment strategy achieves almost as much profit as the optimal adjustment one, under the assumption of accurate price forecasts. This shows that, owed to the proposed real-time adjustment strategy, the final profit of the **HA+PD** model gets even closer to the profit in hindsight, making it an even more attractive model.

Finally, Fig. (16) provides two examples of feature-driven bidding strategies in the day-ahead market, obtained by the **HA+PD** model. The left plot shows the bidding strategy in a representative hour during which the hybrid power plant sells power to the grid. In this hour, the plant sells the first 10 MW at price $\rho^{\mathrm{H}}\lambda^{\mathrm{H}}$ and the rest at the 90% percentile of the realized day-ahead prices in the training data ($\lambda^{90\%}$). The right plot shows a representative hour during which the hybrid

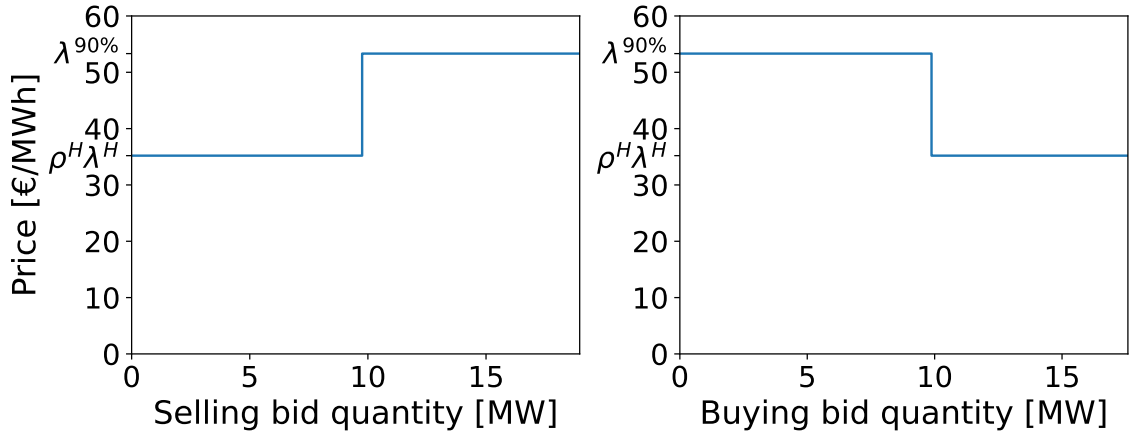

Figure 16: Example of resulting price-quantity bidding curves in the day-ahead market, when the hybrid power plant buys **(right)** and sells **(left)** electricity. Recall $\rho^{\mathrm{H}}\lambda^{\mathrm{H}}$ is the hydrogen price, and $\lambda^{90\%}$ is the 90% percentile of realized day-ahead prices in the training data.

power plant buys power from the grid. The first 10 MW is bought at price $\lambda^{90\%}$ and the rest at price $\rho^{\mathrm{H}}\lambda^{\mathrm{H}}$.

We applied a retraining procedure to all models with a monthly retraining schedule. This retaining procedure is expected to improve the performance of the algorithm over time, for instance, adapting to seasonal wind patterns and changes in electricity prices distribution. However, over the testing period considered, retraining provided minimal improvements, and is therefore not considered adequately to draw any conclusions about its impact.

6 Conclusion

This paper explains how hybrid power plants with co-located wind turbines and an electrolyzer can implement efficient feature-driven models to learn from historical data and make informed day-ahead trading decisions. The proposed feature-driven model derive trading (selling or buying) decisions in the day-ahead electricity market, as well as a hydrogen production schedule for the next day, fulfilling the minimum daily hydrogen quota. This is a pragmatic solution, which properly accounts for wind power and price uncertainty without the need to generate probabilistic forecasts or solve complex stochastic optimization problems. Our numerical analysis shows that the proposed feature-driven models outperform the deterministic model, and require less adjustment in real time. In addition, they result in a final profit which is close to that in hindsight.

For future work, it is of interest to explore the performance of the model in a non-stationary environment. This could be tackled by developing online decision-making methods, similar to the one proposed in [51] for wind power trading only. Another valuable potential of implementing an online decision-making method is an expansion of the adjustment model to account for the uncertainty in the prediction of the balancing price and thereby improve the value of real-time adjustment. It is also interesting to include more complex physical characteristics of the electrolyzer, such as non-linear efficiency and degradation curves, and add more relevant assets to the hybrid power plant, such as battery and hydrogen storage.

19

Bibliography

[1] European Commission, "A European green deal," 2019. https://commission.europa.eu/strategy-and-policy/priorities-2019-2024/european-green-deal_en.

[2] European Comission, "A hydrogen strategy for a climate-neutral Europe," 2020. https://energy.ec.europa.eu/system/files/2020-07/hydrogen_strategy_0.pdf.

[3] International Energy Agency, "Global hydrogen review," 2022. https://iea.blob.core.windows.net/assets/c5bc75b1-9e4d-460d-9056-6e8e626a11c4/GlobalHydrogenReview2022.pdf.

[4] Danish Ministry of Climate, Energy and Utilities, "The goverment's strategy for power-to-x," 2021. https://ens.dk/sites/ens.dk/files/ptx/strategy_ptx.pdf.

[5] K. Raj, P. Lakhina, and C. Stranger, "Harnessing green hydrogen opportunities for deep decarbonisation in India," 2022. https://www.niti.gov.in/sites/default/files/2022-06/Harnessing_Green_Hydrogen_V21_DIGITAL_29062022.pdf.

[6] S. Clegg and P. Mancarella, "Integrated modeling and assessment of the operational impact of power-to-gas (P2G) on electrical and gas transmission networks," *IEEE Trans. Sustain. Energy*, vol. 6, no. 4, pp. 1234–1244, 2015.

[7] G. Matute, J. Yusta, and L. Correas, "Techno-economic modelling of water electrolysers in the range of several MW to provide grid services while generating hydrogen for different applications," *Int. J. Hydrog. Energy*, vol. 44, no. 33, pp. 17431–17442, 2019.

[8] G. Matute, J. Yusta, J. Beyza, and L. Correas, "Multi-state techno-economic model for optimal dispatch of grid connected hydrogen electrolysis systems operating under dynamic conditions," *Int. J. Hydrog. Energy*, vol. 46, no. 2, pp. 1449–1460, 2021.

[9] M. Roach and L. Meeus, "The welfare and price effects of sector coupling with power-to-gas," *Energy Econ.*, vol. 86, p. 104708, 2020.

[10] C. Varela, M. Mostafa, and E. Zondervan, "Modeling alkaline water electrolysis for power-to-x applications: A scheduling approach," *Int. J. Hydrog. Energy*, vol. 46, no. 14, pp. 9303–9313, 2021.

[11] I. Pavić, N. Čović, and H. Pandžić, "PV-battery-hydrogen plant: Cutting green hydrogen costs through multi-market positioning," *Appl. Energy*, vol. 328, p. 120103, 2022.

[12] S. S. Beerbühl *et al.*, "Combined scheduling and capacity planning of electricity-based ammonia production to integrate renewable energies," *Eur. J. Oper. Res.*, vol. 241, no. 3, pp. 851–862, 2015.

[13] Y. Zheng *et al.*, "Optimal day-ahead dispatch of an alkaline electrolyser system concerning thermal–electric properties and state-transitional dynamics," *Appl. Energy*, vol. 307, p. 118091, 2022.

[14] M. Götz *et al.*, "Renewable power-to-gas: A technological and economic review," *Renew. Energy*, vol. 85, pp. 1371–1390, 2016.

[15] M. T. Baumhof, E. Raheli, A. G. Johnsen, and J. Kazempour, "Online Companion: Optimization of hybrid power plants: When is a detailed electrolyzer model necessary?," 2023. https://github.com/mtba-dtu/detailed-electrolyzer-model/blob/main/Online_Companion.pdf.

[16] A. Ursúa *et al.*, "Integration of commercial alkaline water electrolysers with renewable energies: Limitations and improvements," *Int. J. Hydrog. Energy*, vol. 41, no. 30, pp. 12852–12861, 2016.

[17] M. Sánchez *et al.*, "Aspen plus model of an alkaline electrolysis system for hydrogen production," *Int. J. Hydrog. Energy*, vol. 45, no. 7, pp. 3916–3929, 2020.

[18] O. Ulleberg, "Modeling of advanced alkaline electrolyzers: A system simulation approach," *Int. J. Hydrog. Energy*, vol. 28, no. 1, 2003.

[19] M. Sanchez *et al.*, "Semi-empirical model and experimental validation for the performance evaluation of a 15 kW alkaline water electrolyzer," *Int. J. Hydrog. Energy*, vol. 43, no. 45, pp. 20332–20345, 2018.

[20] ENTSO-e, "Transparency platform, day-ahead prices," 2022. https://transparency.entsoe.eu/dashboard/show.

[21] I. Staffell and S. Pfenninger, "Using bias-corrected reanalysis to simulate current and future wind power output," *Energy*, vol. 114, 2016.

[22] Energinet, "Energy islands in Denmark," 2023. https://en.energinet.dk/infrastructure-projects/energy-islands/.

[23] B. Tuinema, E. Adabi, P. Ayivor, *et al.*, "Modelling of large-sized electrolysers for real-time simulation and study of the possibility of frequency support by electrolysers," *IET Gener. Transm. Distrib*, vol. 14, no. 10, pp. 1985–1992, 2020.

[24] T. Dalgas Fechtenburg, "The value of flexibility for electrolyzers," 2022. https://energinet.dk/media/bonk4x1i/the-value-of-flexibility-for-electrolyzers-thomas-dalgas-fechtenburg-energinet.pdf.

[25] M. Saretta, E. Raheli, and J. Kazempour, "Electrolyzer scheduling for Nordic FCR services," in *IEEE SmartGridComm*, pp. 1–6, 2023.

[26] B. Guinot, F. Montignac, B. Champel, and D. Vannucci, "Profitability of an electrolysis based hydrogen production plant providing grid balancing services," *Int. J. Hydrog. Energy*, vol. 40, no. 29, pp. 8778–8787, 2015.

[27] M. Scolaro and N. Kittner, "Optimizing hybrid offshore wind farms for cost-competitive hydrogen production in Germany," *Int. J. Hydrog. Energy*, vol. 47, no. 10, pp. 6478–6493, 2022.

[28] Y. Zheng, C. Huang, S. You, and Y. Zong, "Economic evaluation of a power-to-hydrogen system providing frequency regulation reserves: a case study of Denmark," *Int. J. Hydrog. Energy*, vol. 48, no. 67, pp. 26046–26057, 2023.

[29] M. T. Baumhof, E. Raheli, A. Gloppen Johnsen, and J. Kazempour, "Optimization of hybrid power plants: When is a detailed electrolyzer model necessary?," in *2023 IEEE Belgrade PowerTech*, pp. 1–10, 2023.

[30] Nordic Balancing Model, 2023. https://nordicbalancingmodel.net.

[31] European Commision, "Delegated act on renewable fuels of non-biological origin," 2023. https://energy.ec.europa.eu/system/files/2023-02/C_2023_1087_1_EN_ACT_part1_v8.pdf.

[32] A. G. Johnsen, L. Mitidatri, D. Zarrilli, and J. Kazempour, "Online Companion: The Value of Ancillary Services for Electrolyzers," 2023. https://github.com/andreagloppen/Value_of_AS_ELY.

[33] Energinet, "Energi data service electricity." https://www.energidataservice.dk/groups/electricity, 2023. Accessed: 2023-09-30.

[34] Regelleistung, "Datacenter FCR/aFRR/mFRR." https://www.regelleistung.net/apps/datacenter/tenders/?productTypes=PRL&markets=BALANCING_CAPACITY,BALANCING_ENERGY&date=2022-05-09&tenderTab=PRL$CAPACITY$1, 2023. Accessed: 2023-09-30.

[35] P. Pinson, C. Chevallier, and G. N. Kariniotakis, "Trading wind generation from short-term probabilistic forecasts of wind power," *IEEE Transactions on Power Systems*, vol. 22, no. 3, pp. 1148–1156, 2007.

[36] J. Morales, A. Conejo, and J. Pérez-Ruiz, "Short-term trading for a wind power producer," *IEEE Transactions on Power Systems*, vol. 25, no. 1, pp. 554–564, 2010.

[37] A. Sun and A. J. Conejo, *Robust Optimization in Short-Term Power System Operations*. Springer, 2021.

[38] P. Pinson, "Distributionally robust trading strategies for renewable energy producers," *IEEE Transactions on Energy Markets, Policy and Regulation*, vol. 1, no. 1, pp. 37–47, 2023.

[39] U. Sadana, A. Chenreddy, E. Delage, A. Forel, E. Frejinger, and T. Vidal, "A survey of contextual optimization methods for decision making under uncertainty," *arXiv preprint arXiv:2306.10374*, 2023.

[40] D. Bertsimas and N. Kallus, "From predictive to prescriptive analytics," *Management Science*, vol. 66, no. 3, pp. 1025–1044, 2019.

[41] A. N. Elmachtoub and P. Grigas, "Smart "predict, then optimize"," *Management Science*, vol. 68, no. 1, pp. 9–26, 2022.

[42] L. H. Liyanage and J. G. Shanthikumar, "A practical inventory control policy using operational statistics," *Operations Research Letters*, vol. 33, no. 4, pp. 341–348, 2005.

[43] M. Muñoz, J. M. Morales, and S. Pineda, "Feature-driven improvement of renewable energy forecasting and trading," *IEEE Transactions on Power Systems*, vol. 35, no. 5, pp. 3753–3763, 2020.

[44] A. Stratigakos, S. Camal, A. Michiorri, and G. Kariniotakis, "Prescriptive trees for integrated forecasting and optimization applied in trading of renewable energy," *IEEE Transactions on Power Systems,*, vol. 37, no. 6, pp. 4696–4708, 2022.

[45] K. Parginos, R. Bessa, S. Camal, and G. Kariniotakis, "Interpretable data-driven solar power plant trading strategies," in *2022 IEEE PES Innovative Smart Grid Technologies Conference Europe (ISGT-Europe)*, pp. 1–5, 2022.

[46] E. Raheli, Y. Werner, and J. Kazempour, "A conic model for electrolyzer scheduling," *Computers & Chemical Engineering*, vol. 179, p. 108450, 2023.

[47] European Commission, "Delegated act on renewable fuels of non-biological origin," 2023. https://energy.ec.europa.eu/system/files/2020-07/hydrogen_strategy_0.pdf.

[48] A. Georghiou, D. Kuhn, and W. Wiesemann, "The decision rule approach to optimization under uncertainty: Methodology and applications," *Computational Management Science*, vol. 16, no. 4, pp. 545–576, 2019.

[49] A. Skajaa, K. Edlund, and J. M. Morales, "Intraday trading of wind energy," *IEEE Transactions on Power Systems*, vol. 30, no. 6, pp. 3181–3189, 2015.

[50] "ENTSO-e transparency platform," 2023.

[51] M. A. Muñoz, P. Pinson, and J. Kazempour, "Online decision making for trading wind energy," *Computational Management Science*, vol. 20, pp. 1–31, 2023.

8.3 RHYPE solution

8.3.1 System setup

The RHYPE solution allows planning (establishing optimised market bids) and optimized operation (intra-day adjustments considering deviation of available wind and realized market prices) and comprises a windfarm with connected battery storage system and electrolyser. For the demonstrator, the following ancillary services were implemented:

- FCR from wind-power and the battery storage system, and
- mFRR provided by the electrolyser.

This setup for ancillary services was chosen due to the required symmetry (up- and downward) for FCR, and non-symmetric mFRR in DK1 market zone, in which the Flø site is located. The advantage is, that electrolysers can be operated most of the time and the setpoint must not be lowered to accommodate for downward reserve.

8.3.2 Detailed results from analysis at SGRE's Flø test site

The test operation and evaluation with data from SGRE's Flø test site in Denmark was analysed with regards to Commercial KPIs, Technical KPIs and an Environmental KPI. Those are summarized in tables Table 4, Table 5, Table 6.

Table 4 Commercial KPIs within test period (not extrapolated to one year, use factor 1.977)

Model	KPI	
	Site income	**Δ to Base**
Base	551413.49 €	
Deterministic	611566.84 €	60153.35 € (10.91%)
Stochastic	605227.54 €	53814.05 € (9.76%)
	Site revenue	**Δ to Base**
Base	697369.44 €	
Deterministic	818361.47 €	120992.03 € (17.35%)
802725.50 €	802725.50 €	105356.06 € (15.11%)
	Imbalance cost (day ahead)	**Imbalance cost (ancillary)**
Base	146724.96 €	0.00 €
Deterministic	141649.76 €	67965.91 €
802725.50 €	139911.64 €	58598.22 €

Table 5 Technical KPIs within test period (not extrapolated to one year, use factor 1.977)

Model	KPI	
	Electricity export	**Electricity import**
Deterministic	11242.61 MWh	1.83 MWh
Stochastic	11248.32 MWh	10.17 MWh
	Site flexibility increase	
Deterministic	1.62 MW	
Stochastic	1.38 MW	
	Unbalance (DA) shortfall	**Unbalance (DA) surplus**
Base	1801.84 MWh	7.95 MWh
Deterministic	1734.68 MWh	23.15 MWh
Stochastic	1704.91 MWh	10.44 MWh

	Unbalance (ANC) shortfall	Unbalance (ANC) surplus
Deterministic	389.64 MWh	0.00 MWh
Stochastic	341.82 MWh	0.00 MWh
	Renewable curtailment	**Δ to Base**
Base	6151.82 MWh	
Deterministic	6025.75 MWh	-126.07 MWh
Stochastic	6075.72 MWh	-76.1 MWh
	Grid dependency	
Base	0.05 MWh/kg	
Deterministic	0.00 MWh/kg	
Stochastic	0.00 MWh/kg	
	H2 product. cost	
importing all electricity	4.23 €/kg	
Deterministic	3.60 €/kg	
Stochastic	3.61 €/kg	

Table 6 Environmental KPIs within test period (not extrapolated to one year, use factor 1.977)

Model	KPI
	CO2 emissions
non-green H2	169.35 T
Deterministic	0.00 T
Stochastic	0.00 T
	H2 production
Deterministic	24298.32 kg
802725.50 €	23622.75 kg

In the following figures (Figure 7 – Figure 10), the optimizations for day-ahead (top-sub-figure) and ancillary (bottom-sub-figure) market are illustrated for months with overall rather low wind speeds, as well as higher wind speeds. Further, differences between the optimized Portfolio Management and the realized operating condition is shown. That is, the dashed lines in light colours mark the planned bid into the different markets, while solid lines or bars are the final setpoint under the current condition. The setpoint is to be understood as the final command for the power plant controller and being the best outcome given the bid to be fulfilled and the unavoidable imbalance to a market.

June 2023 was a month with rather low wind speeds, while October 2023 shows mainly higher wind speeds. Especially for June with low wind speeds, the deterministic model is too optimistic with bids into the ancillary service market, which also may not be fulfilled as planned. The stochastic model would aim at placing fewer bids to avoid too much risk. The difference is not as significant when looking at the day-ahead market. This shortcome is significantly less in “high wind” seasons, such as the shown October. The issue can very likely be mitigated with a different method for determining and predicting the forecast uncertainty, especially for wind forecasts. Various improved methods are already in discussion. One would be the use of probabilistic forecast, which provides already a bandwidth usable as potential errors, which in turn can be sampled to establish a sample space for each time.

It is important to note, that there is strong indication, that the method for evaluation of forecast uncertainty plays a crucial role for the risk-affinity of the stochastic model. That is, how risky or conservative a bid is planned with respect to forecast uncertainty. Model parameters such as the Wasserstein distance are used as given during the RHYPE evaluation period, due to the thorough analysis and parameter study conducted by DTU. However, forecast uncertainty can be estimated in different ways and for the evaluation and tests the prediction of forecast errors was simplified. This allowed for reduced computational effort. The method used

in RHYPE was to fixed time-blocks of e.g., 3 hours. These blocks of forecast data for the past 6 weeks as well as next 2 days into the future were categorised regarding their statistical distribution. Knowing the error (forecast versus measured/realized values) for each category, those errors are used for the respective “categories” of the future data. This method is very basic and does not account e.g., for the bimodal property of day-ahead market prices, nor the occurrence of wind front with a change from lower wind speeds to larger wind speeds (different from general variation of wind speeds). More effort should be spent to improve RHYPE in this regard.

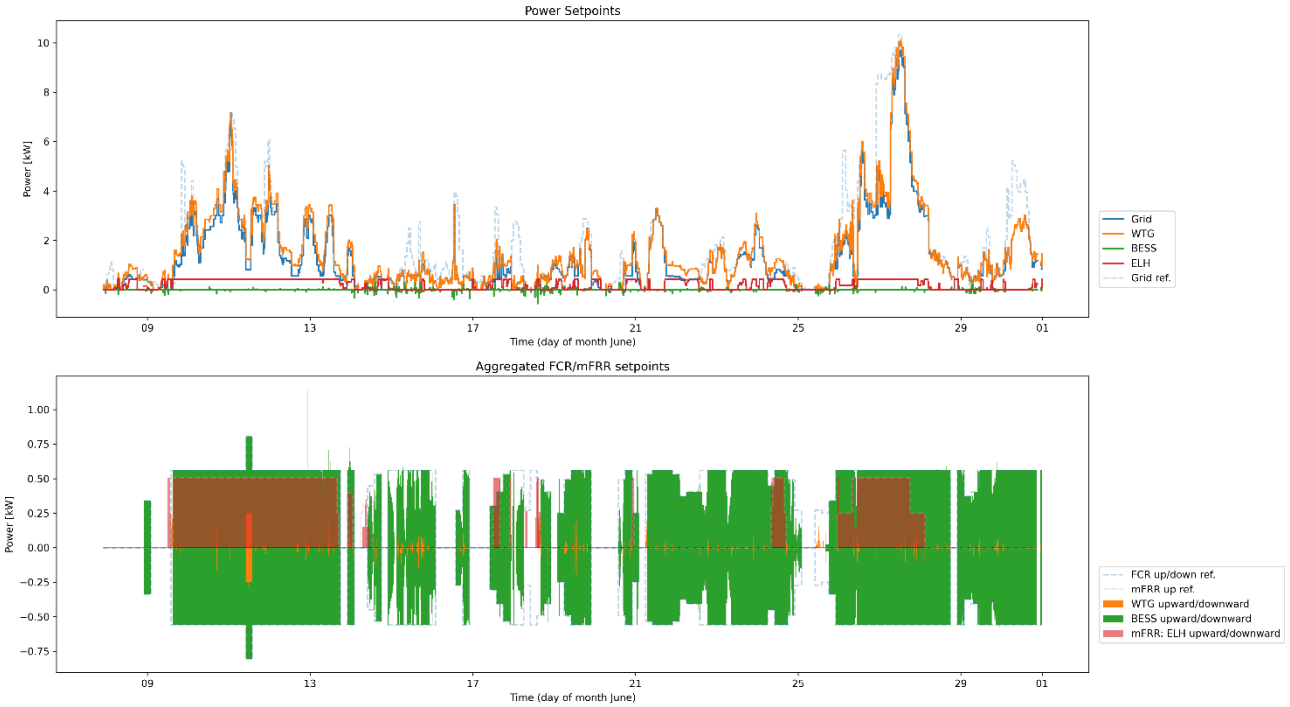

Figure 7 Deterministic model, June 2023

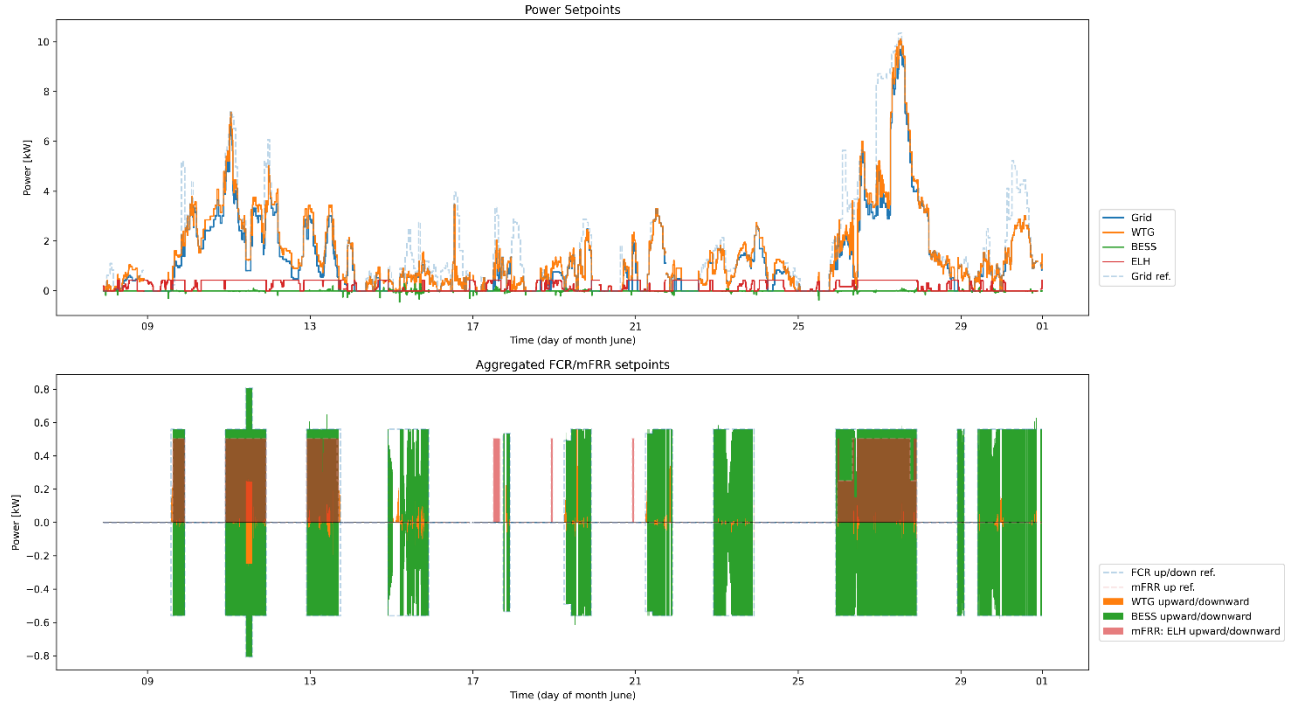

Figure 8 Stochastic model, June 2023

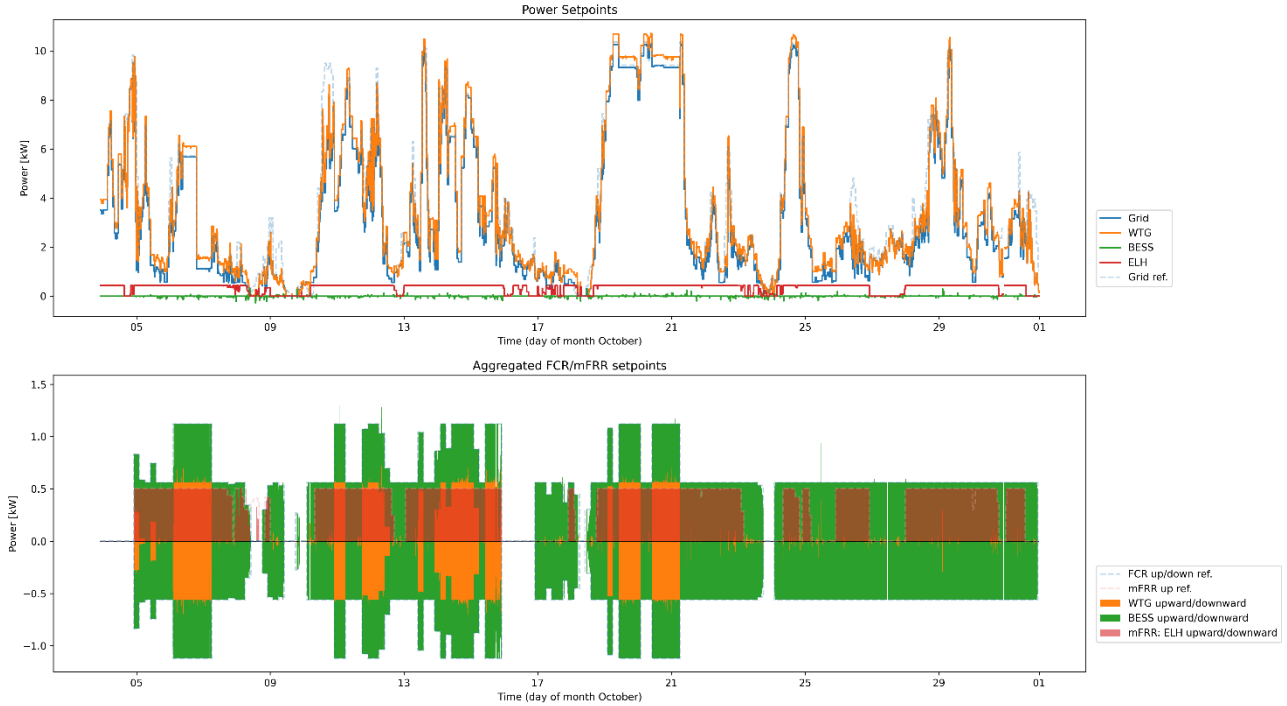

Figure 9 Deterministic model, October 2023

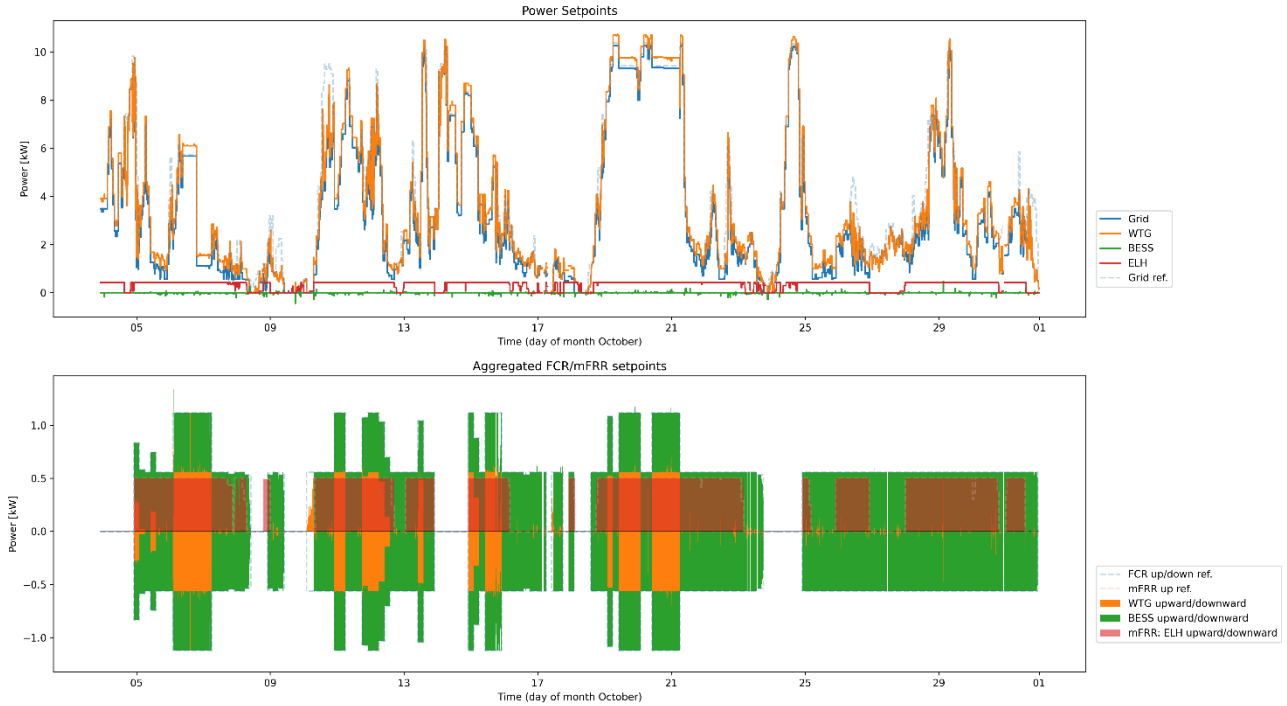

Figure 10 Stochastic model, October 2023

8.4 Project webpage

A dedicated section to the company Hydrogen web-page has been created (Green Hydrogen Unlocked: The Brande Hydrogen Project (siemensgamesa.com).

8.5 Summary per work package

8.5.1 End 2022 report

WP1: Project baselines (i.e., time, scope, cost, and risk) are thoughtfully managed, and progress and risks tracked and reported periodically. Efficient communication has been established between SGRE and DTU, including a mix of online (bi-weekly) and in person meetings. No major unexpected changes occurred, and no major risks identified so far. Project reached its planned deliverables and milestones for the considered reporting period.

WP2: The modified WP2 “System modelling and portfolio management optimization development” is currently in due progress. The first activity T2.1 regarding development of a deterministic model without ancillary services has been completed. This was achieved through research on operational model for electrolyzers, after which several model formulations were developed and evaluated, and feedback was given by the SGRE team, in particular by the lead engineer of Power-to-X at SGRE. Additionally, a visit to the pilot site Brande was arranged. Further, work on the addition of ancillary services and stochastic input to the model has been initiated.

WP3: The software architecture for the energy management system was successfully designed (T3.1) and the prototype code deployed (T3.2) on a demonstration site to manage and accommodate for the new additional features needed by hybrid-site energy managers such as energy bidding under uncertainty. Back/front-end software development will be completed by the end of February. Features of the current SW application as follows:

- The application can run both as service at site and be run in Docker containers (tested via Continuous Deployment strategies), allowing also centralized operation in the cloud.

- The optimization unit is designed for easy integration of new mathematical problem formulations, whose model are mainly developed by the DTU. The design allows for flexible, easy, and modular model integration for new assets or different model types and select between those. As a result, the integration of new models can be achieved with minimum efforts.

- Data Management is collecting data from field measurements as well as forecast data. Interpolation (arbitrary temporal sample size) and aggregation methods (mean, maximum, minimum) were implemented for forecast data and the planned schedule. Communication with the field devices is achieved through the implementation of the Modbus protocol. In progress, is the introduction of methods to select arbitrary forecast providers. While two fixed providers are already implemented for this task (in-house WEF for wind forecast, external energy market price forecast by Volue-Insight), more flexibility is anticipated without the need of using predefined providers. The latter is expected to conclude by February 2023.

- Regarding the User Interface (UI), Grafana is adopted. Grafana allows easy connection to any database and is customizable. The current implementation of the dashboard shows the status, planned schedules and current operation state for all assets as well as market participation (FCR).

- Last but not least, the Orchestrator Module coordinates and automates all facets of energy management, from the forecast data collection to the optimization results exposure. This was achieved by using the Python package "apscheduler". Each operation is defined as a schedule with periodic timing.

WP4: To start in M13.

WP5: SGRE planned to add a dedicated section to the company Hydrogen webpage. Both content and back-end for the website are finalized. Project web presence will be live from January 2023 (D5.1).

Project results will be made public through the project webpage and disseminated though exhibition events over the course of final project year (M13-M24), subject to successful acceptance by EUDP committee. Conferences, fairs, and similar exhibition will be identified by mid of 2023.

8.5.2 First year report

WP1: Project baselines (i.e., time, scope, cost and risk) are thoughtfully managed, and progress and risks tracked and reported periodically. Efficient communication has been established between SGRE and DTU, including a mix of online (bi-weekly) and in person meetings. No major unexpected changes occurred, and no major risks identified so far. Project reached its planned deliverables and milestones for the considered reporting period.

WP2: The **developments of the deterministic** portfolio management problem both **without** (T2.1) and **with** (T2.2) **ancillary services** have been completed and are ready for integration and testing in the operational environment. The focus of the work has been on **approximating non-linearities of the electrolyzer for integration in a linear program**, and on the implications of an electrolyzer delivering ancillary services on the upstream components. Further, the potential benefit of applying ambiguity-aware Distributionally Robust Optimization (DRO) compared "conventional" uncertainty-aware methods such as stochastic optimization was identified (T2.3). This has further led to the **development of a DRO model** (T2.4), which shows **promising preliminary results** when back tested on data provided by SGRE.

WP3: The **software architecture** for the energy management system was **successfully designed** (T3.1), back/front-end software development completed, and the code deployed (T3.2) on the Floe (outside Brande, DK) demonstration site to manage and accommodate for the new additional features needed by hybrid-site energy managers, such as energy bidding under uncertainty. Integration of RHYPE deterministic model with software architecture (T.3.3) is ongoing and will be concluded by end of June (1-month late with regard to original plan). This will neither cause any major issue, nor impact on the test campaign.

WP4: We have already started some activities (2 months before original plan) at the test site to compensate for the 1-month delay of the T.3.3. Main activities focus on designing effective test plan to prove the reliability and effectiveness of the devised operation and control strategies as well as identifying necessary signals (actual measurements) from deployed assets to be read by the EMS to improve the simulation accuracy.

WP5: A dedicated **section to the company Hydrogen web-page** has been **created** (Green Hydrogen Unlocked: The Brande Hydrogen Project (siemensgamesa.com). Both content and back-end for the website are finalized and project web presence is live from January 2023 (D5.1). Project results will be made public through the project webpage and disseminated though exhibition events over the course of final project year (M13-M24), subject to successful acceptance by EUDP committee.

We are currently planning to participate in the PSCC conference (PSCC2024 – Power Systems Computation Conference) to be held in Paris, June 4-7, 2024, as well as to organize a workshop at DTU to present our results through live-demo event. Additional events like fairs are also on the radar, but no concrete plan yet.

8.5.3 End 2023 report

WP1: Project baselines (i.e., time, scope, cost, and risk) continue to be thoughtfully managed, and progress and risks tracked and reported periodically. No major unexpected changes occurred, and no major risks have been identified so far. Project reached its planned deliverables and milestones for the considered reporting period.
Michael Revesz takes over as the technical project lead, since Donato Zarrilli left the company (SGRE) with 1. December 2023.

WP2: The development and first application of Distributionally Robust Optimization (DRO) model, which considers uncertainty of the wind-forecast and spot-market prices, is completed (T2.4). This model was further extended to include ancillary services (T2.5), building on the developments from (T2.2) and (T2.4). The DRO model is ready for integration in the RHYPE software architecture.

WP3: Integration of RHYPE deterministic model with software architecture (T.3.3) was concluded by end of June (1-month late with regard to original plan) and is running at the test site. The integration of the RHYPE stochastic model (T3.4) was started in November and expected to be concluded within M20. A required software module for the evaluation of historic errors (needed for T3.4) as part of the stochastic model is currently under development for RHYPE stochastic model.

WP4: A detailed and effective test plan was developed to facilitate activities in (T4.2) and (T4.3): while the RHYPE deterministic model is being tested, historic measured data as well as forecast data is being collected since June 2023 for testing and analyzing results and the performance for both models as part of (T4.2) and (T4.3). The tools required for assessing the operation and control strategies, including evaluation of KPIs, (T4.4) are in preparation and 60% concluded.

WP5: A paper based on the developments of (T2.2), regarding an electrolyzer operating in ancillary service markets, has been submitted to the PSCC conference (PSCC2024 – Power Systems Computation Conference) to be held in Paris, June 4-7, 2024. Further, work related to (T2.4), a DRO model, was presented at the INFORMS Annual Meeting held in Phoenix, Arizona in October 2023.

8.5.4 Final report

WP4: RHYPE is tested within (T4.2) and (T4.3) with the real site data at Flø. The operational site data is used to test both the deterministic and stochastic model, as well as simulate the BaU model (base). Overall, there is data from June 2023 until January 2024 available and used for the tests and evaluation. All KPIs relevant and estimated for the beginning of the project are evaluated (T4.4). The evaluation was conducted in alignment with the proposal to conduct a fair and valuable comparison between pre-project estimate and findings after development of RHYPE.

WP5: The potential and value of RHYPE was analyzed (T5.4).